1967

# A Pharmacological Analysis of the Ionic Channels of Nerve

Bertil Hille

# A PHARMACOLOGICAL ANALYSIS OF THE IONIC CHANNELS OF NERVE

A thesis submitted to the Faculty of The Rockefeller University

in partial fulfillment of the requirements

for the degree of Doctor of Philosophy

by

Bertil Hille, B. S.

Approved for publication

Clarence M. Connelly

Associate Professor at The Rockefeller University

and

Associate Professor

22 February 1967

The Rockefeller University

New York, New York

## Preface

I would like to express the gratitude of a student, first, to all the students and faculty who together enabled me to enjoy a wide range of intellectual pursuits and, more specifically, to Dr. Detlev W. Bronk who gave me the opportunity to engage in an extraordinary experience in graduate study at The Rockefeller University.

I am happy to acknowledge several rewarding years of study with my advisors, Dr. Clarence M. Connelly and Dr. Alexander Mauro. I thank them and the other members of Dr. Frank Brink's laboratory for their warm friendship.

My deepest personal thanks go to Dr. Frederick A. Dodge, who started these experiments. Without his energetic enthusiasm for the initiation and perfection of experimental design and execution I would not have been able to undertake this work.

I am grateful to many others for their help: to Dr. H. K. Hartline for letting me use his computer for hundreds of hours and to the members of his laboratory who helped me to learn programming and who built special devices to join my experiment to the computer; to Mr. John Hervey for much advice on electronic circuit design; to Dr. John W. Moore for suggestions on the interpretation of some of my records and on a method of improving the potential measurement; to many people for generously supplying various drugs and chemicals; to Miss Florence Ling for typing several drafts of this thesis; and to Miss Ruth Mandlebaum and the Illustrations Service for their artistry in producing the figures.

## Summary

The effects of various drugs on single myelinated nerve fibers from Rana pipiens were studied with the voltage clamp technique of Frankenhaeuser and Dodge. The observed currents were analysed by a computer in terms of the mathematical model of Hodgkin and Huxley. The sodium, the potassium, and the leakage current components and the time constants associated with their changes were calculated.

Tetrodotoxin abolished the sodium currents selectively, and tetraethylammonium ion abolished the potassium currents selectively. Neither of these drugs affected the time constants associated with any of the current components. The curves relating the kinetic parameters of the sodium currents to the voltage were displaced along the voltage axis by calcium concentration changes. The three agents mentioned acted rapidly (within one second) and reversibly and probably bind to specific receptors on the extracellular side of the nodal membrane. Other drugs including local anesthetics, some general anesthetics, and veratrine alkaloids exerted moderately specific effects on the components of current. The anesthetics abolished sodium currents and the veratrine alkaloids enhanced sodium currents and prolonged their time courses. None of the agents tested affected the leakage current.

The demonstrated pharmacological independence of the three components of current suggests that the ion fluxes are handled by independent permeability systems, the sodium channels, the potassium channels, and the leakage channels. Some of the properties of these channels are described.

Table of Contents

# Chapter I

## AN HISTORICAL INTRODUCTION TO THE MEMBRANE THEORY

The key to the current understanding of the excitation and propagation of action potentials in nerve and muscle is the "ionic hypothesis" or "membrane theory". The theory supposes that electrical potentials in cells are ionic diffusion potentials arising solely across the unit membrane of the cells. The potentials depend on the ionic concentration differences across the membranes and on the selective permeability of the membranes. This thesis is about the inhibition by some drugs of the changes of permeability to ions that underlie the excitation and propagation of action potentials. The goal of this study is to provide more clues to the understanding of the mechanisms of ionic permeation through cell membranes. Although the experiments are exclusively devoted to a particular type of myelinated nerve fiber from the frog Rana pipiens, the conclusions could be useful for all excitable tissues.

From 1939 to 1952 the membrane theory received so much experimental confirmation that it can be considered one of the established facts of neurophysiology. One might imagine that the idea is a relatively new one since it was only recently proven, but this is not so. It was formulated as soon as the words in it received scientific meaning. Indeed the development of the whole theory of nerve and muscle action has been characterized by bursts of ideas and rapid advances, following quickly on the heels of some fundamental or technical discovery in physics, and periods of waiting from which new ideas were absent. I should like to trace the history of some of the ideas to show that many basic principles were formulated long ago, before it was possible to consider proving them.[1]

[1] See bibliographical note at the end of this section for sources quoted or used in preparing this essay.

Galvani's experiments between 1780 and 1795 mark the beginning of experimental electrophysiology. He investigated in great detail the excitation of twitching in frog's legs by static electric machines, by metallic arcs applied at two points, and even by the severed muscles of other frog legs. He felt he had discovered an animal electricity and concentrated on showing "how many qualities the animal electricity we have discovered has in common with ordinary electricity." Although subsequent developments showed that some of his interpretations were poorly founded, Galvani's (1791) conclusions are extraordinarily like our current views:

> It seems to be established from these experiments that both artificial and atmospheric [e.g. lightning] electricity exert far greater force upon muscles and nerves than hitherto was known; and that they exercise so great a power on animal electricity to be able to incite this same animal electricity to movement. . . . Two facts are particularly evident, namely that a two-fold electricity is present in these bodily parts, one positive, the other negative and that each is completely separated from the other by nature: otherwise if there were a state of equilibrium, no movement, no flow of electricity, and no phenomenon of muscular contration would take place. . . . The hypothesis is not absurd . . . which compares a muscle fiber to something like a small Leyden jar or to some other similar electrical body . . . . In this way one likens the whole muscle, as it were, to a group of Leyden jars . . . . A muscle fiber, although simple at first sight is composed of solid as well as fluid parts (substances which produce in it no slight diversity) . . . . a condition which could not exist without different little hollows and surfaces in the substances of the muscle [to separate the hypothetical positive and negative electricities].

On writing of nerve conduction Galvani postulates that

> nerves are so constituted that they are hollow internally, or . . . . composed of some material adapted to carrying

> electric fluid, and that externally they are oily, or have some other similar substance which prohibits the dissipation and effusion of this fluid flowing through the nerve.

At this point we diverge from his view, for he goes on to claim that the electric fluid flows from the brain through the inside of the nerve and into the muscle. To him the nerve is like, to use a modern analogy, an insulated wire. We can forgive his inaccuracies in language, however, if we realize that most of his research was completed before Ohm was born.

Galvani's experiments were important not only because they initiated the development of electrophysiology but also because they led to fundamental discoveries in physics without which electrophysiology would not have been able to advance. In a few years Volta (1800) had developed his pile as a direct result of his experiments with Galvani's phenomenon. Volta's battery, the only known source of moderate currents at moderate voltages, enabled Davy (1807) to discover electrolysis and Faraday (1834) to prove his law of equivalent weights. These were the beginnings of electrochemistry. Surprisingly, still fifty more years had to pass before it was determined that salts are normally dissociated into ions in solution.

Again, currents from the battery flowing around a loop of wire turned Oersted's compass (1819) and led Ampere to the beginnings of electromagnetic theory. This discovery of a force between currents and magnets introduced a new, sensitive instrument that was to serve neurophysiologists for over a century, the galvanometer.

Combining the galvanometer, the battery, and a slide wire the neurophysiologists were able to make new progress. Matteucci (1838) described the demarcation potential of injured muscle and saw that it disappeared in strychnine tetanus. By 1849 Du Bois-Reymond had shown that cut muscles and nerves were negative at the injury. During tetanic electrical stimulation there was also an increased negativity in the living parts of the nerve. The magnitude of the change was

independent of the distance from the stimulus or of whether the stimulus was applied at the central or the peripheral end. He thought that he could explain what he had seen through the orientation of a set of dipolar "electromotor molecules". Bernstein (1866) devised an ingenious mechanical device, the differential rheotome, to close the measuring circuit of his potentiometer for an extremely short period at known times after the stimulus. The slow galvanometer became a rapid instrument. He found a negativity about equal to the injury potential travelling rapidly away from the stimulus and lasting less than a millisecond in any place.

Pflüger (1859) observed that the electrotonus of nerves differed from action potentials especially in its decrement. He proposed that during the propagation of action potentials changes in each nerve element released an independent elastic force in the neighboring element, thus keeping the response at full amplitude as it travelled. The analogy between a burning fuse and propagation was developed, immediately raising the question why the nerve did not release all its energy in the first impulse. At this time another observation was made that played an important part in later theories. While stimulation normally took place at the cathode (depolarization), the response of the nerve could be enhanced by a preceeding maintained anelectrotonus (hyperpolarization) or diminished by a maintained catelectrotonus (depolarization). Various theories were proposed with elastic forces and molecular restraints acting on the dipolar "electromotor molecules". The restraints kept the nerve from releasing all its energy and the elastic forces were weakened and strengthened by depolarization and hyperpolarization, respectively, in order to enhance or diminish the response.

By the time that Hermann's "Handbuch der Physiologie" (1879) appeared, electrophysiology had lost its momentum. Hermann's book was remarkable in one sense, however: it contained one of the first complete statements of what we call local circuit theory. Calling

the fiber a polarizable core conductor, he discussed the electric currents circulating from the active part of the nerve to the resting parts saying that the outward current through the "resting substance" must of necessity stimulate that region. He wrote that this fact is the "germ of a future definitive theory of nerve function". Indeed it was, although it took sixty more years to demonstrate.

A new era began in the 1880's when Ringer and de Vries developed physiological solutions. Ringer found that it was the cationic components of his solution, sodium, potassium, and calcium, that made the difference, but his observation could not be understood until Arrhenius (1887) showed that salts were largely dissociated in aqueous solution and that each ion was free to exert its effects independently. One of the observations contributing to Arrhenius's conclusion was the difference between the concentrations of salt and sugar solutions that de Vries found to be isotonic with plant cells. With this major hurdle passed, Nernst and Planck (1888-1892) gave their definitive analysis of electrode and diffusion potentials, and Ostwald (1890) discussed the potentials across semipermeable membranes. Ostwald said that the potentials of muscle, nerves, and electric fish would be explained by semipermeable membranes. Now all the electrochemical ground work for the membrane theory of the neurophysiologists had been laid.

In a celebrated paper entitled "Investigation of the thermodynamics of bioelectric currents" Bernstein (1902) coined the phrase "membrane theory" and offered the first serious attempt to account for biological potentials in terms of ions moving through semipermeable membrane. He suggested that the cell membranes of muscle and nerve might be more permeable to cations than to anions and that the permeability to anions might increase temporarily during action potentials. He was able to account for the negative internal potential of the resting cell by the erroneous assumption (valid for plants) that all ions were in greater concentration inside than outside. Surprisingly, Bernstein chose to test his theory by measuring the

temperature dependence of the resting potential. Soon Höber (1904) produced more information on the effects of various ions, so that in his "Elektrobiologie" Bernstein (1912) could say with more assurance that the potassium ion permeability dominated the resting state and that all ions permeated during the action potential. For thirty more years it was assumed that at the peak of the action potential there was an indiscriminate breakdown of the membrane permeability barriers causing the membrane potential to fall to close to zero potential.

Just before Bernstein's membrane theory was proposed, a prophetic paper appeared with the solution to the inaccuracies. Showing that sodium or lithium ions were essential for muscle function, Overton (1902) wrote

> One could easily postulate that . . . . a change of the surface of the sarcoplasm occurs such that during a definite (probably extremely short) time the fiber becomes permeable to sodium and potassium ions . . . . Through an exchange of one or the other of these ion species [sodium and lithium] with potassium ions the muscle fiber could easily release an electric potential, that possibly represents one of the sources of the action current.

He pointed out, however, that if an exchange really occurs one has difficulty explaining how the heart can contract $24 \times 10^8$ times in a lifetime without equalizing its internal sodium and potassium concentrations. After this time, experiments with ions were continued by Höber, Loeb, Lillie, Osterhout and many others but the important role of sodium was rarely noted. It took fifty years to combine Overton's observations with the membrane theory.

Few improvements were made on Bernstein's picture for a long time, for the great physiologists interested themselves mainly in other things. Their instruments were improving - vacuum tubes and oscilloscopes - and there were many nerve "circuits" to trace. Gotch, Lucas, and Adrian determined the varieties of electric stimuli that were sufficient to elicit the impulse in order to test a

quantitative theory of excitation proposed by Nernst (1899) and refined by Hill (1910). The theory supposed that the ions dragged by the stimulating current piled up at a membrane. When a certain concentration was reached the excitation occurred. To account for the depressing effects of long depolarizations and enhancing effects of long hyperpolarizations, an additional chemical reaction was postulated that depended on the concentration of the accumulating ions and that opposed the excitatory effect. As it turned out, this theory, so reminiscent of the earlier electromotor molecules, was not to lead to the answer.

The break came when Young (1936) found the giant axon of the squid. Here at last was a cell big enough for a complete electrical investigation. Bernstein's conclusion could be studied with electrodes inserted inside the cell. Cole, Curtis, Hodgkin, and Huxley (1938-1942) soon found the expected increase in permeability during excitation and verified the postulated potassium dependence of the resting potential. They were completely surprised, however, to find that the inside of the axon became many millivolts positive at the peak of the action potential. As late as 1945 Hodgkin and Huxley tried to explain this reversal by an extra inductance or capacitance in the membrane, by a specific increase in permeability to some intracellular anion not found in seawater, or even by a turning of dipoles like those of Du Bois-Reymond's molecular theory of 1849. In 1949 Hodgkin and Katz found the answer. They rediscovered the indispensibility of sodium and demonstrated that the action potential was produced by a large specific increase of sodium permeability.

The crowning achievement came when the quantitative details of the permeability changes were worked out. Marmont (1949) introduced a conducting wire down the length of the axon so that the whole interior of the cell was isopotential. As we say now the axon was "space clamped". Then Cole, Marmont, Hodgkin, Huxley and Katz applied electronic feedback techniques, perfected only a few years

earlier for radar design, to keep the potential on the wire constant at any desired level. The axon was "voltage clamped." During the voltage clamp one could directly measure the ionic currents and the electromotive forces and permeabilities that underlie them. Hodgkin and Huxley (1952) showed the electromotive forces were constant and the permeabilities time- and voltage-dependent. As had been hoped the dominant electromotive forces were readily identified with the sodium and potassium concentration differences across the membrane. All of the observed currents could be described by a few empirical equations. When the mathematical description of ionic currents was combined with the "cable equation" of the leaky core conductor model, a propagating action potential could be calculated that agreed in a most remarkable manner with the details of experimentally observed action potentials. It was clear from this work that the membrane theory or ionic hypothesis could account for the potentials that had been measured in cells.

## BIBLIOGRAPHY FOR CHAPTER I

In addition to the research papers of Hodgkin, Cole, and their collaborators, the following sources were used in preparing this chapter.


Arrhenius, S. (1910). Lehrbuch der Elektrochemie. Leipzig, Verlag von Barth.

Bayliss, W. M. (1924). Principles of general physiology, 4th ed. London, Longmans, Green, and Co.

Bernstein, J. (1902). Untersuchungen zur Thermodynamik der bioelektrischen Stöme. Arch. ges. Physiol. 92, 521-562.

Bernstein, J. (1912). Elektrobiologie. Braunschweig, F. Vieweg und Sohn.

Cranefield, P. (1957). The organic physics of 1847 and the biophysics of today. J. Hist. Med. and Allied Sci., 12, 407-423.

Galvani, L. (1791). De viribus electricitatis in moto musculari commentarius (Commentary on the effects of electricity on muscular motion). Translation by M. G. Foley. Burndy Library, 1953, Norwalk.

Hermann, L. (1879). Handbuch der Physiologie v. 2, Leipzig, F. C. W. Vogel.

Höber, R. (1945). Physical chemistry of cells and tissues. Philadelphia, The Blakiston Company.

Hodgkin, A.L. (1957). The Croonian Lecture - Ionic movements and electrical activity in giant nerve fibers. Proc. Roy. Soc. B., 148, 1-37.

Katz, B. (1939). Electric excitation of nerve. London, Oxford University Press.

Lucas, K. (1912). Croonian Lecture - The process of excitation in nerve and muscle. Proc. Roy. Soc. B., 85, 495-524.

Overton, E. (1902). Beiträge zur allgemeinen Muskel und Nervenphysiologie. II. Ueber die Unentbehrlichkeit von Natrium - (oder Lithium) - Ionen für den Contractionsact des Muskels. Arch. ges. Physiol., 92, 346-386.

Pupilli, G. C. and Fadiga, E. (1963). The origins of electrophysiology. J. World Hist., 7, 547-589.

# Chapter II

## THE QUANTITATIVE DESCRIPTION OF THE PERMEABILITY CHANGES OF NERVES

A mathematical model of the currents, voltages, and permeabilities of a frog nerve forms the background of the experimental approach used in this thesis. In this chapter the outlines of the theory are sketched in with only as much detail as will be needed for my experiments. Other refinements and clues to the underlying mechanisms will be considered in Capter V.

### Conceptual Background

Let us imagine a semipermeable membrane separating two different electrolyte solutions. A pair of reversible electrodes is immersed in the solutions so that an electric current can be made to flow across the membrane. In general an electrical potential difference will develop across the membrane as ions begin to move across it. The potential difference will depend on the relative permeability of the membrane to the different ions, on the concentrations of the ions, and on the applied electric current. The symbol $\Psi$ will be used for the electrical potential. In practice the potential difference, symbolized by E, is the more useful quantity, and it is convenient to use the word potential to refer to E as well as to $\Psi$. An example is the phrase "membrane potential" that is an abbreviation for the "potential difference across the membrane."

Suppose for example that the membrane is in reality a rigid matrix perforated by two types of holes. One kind of hole, called the K-hole, permits the passage of potassium ions exclusively, and the other kind, called the Na-hole permits the passage of sodium ions exclusively. If, for a moment, all the Na-holes are covered in some fashion and no electric current is applied, the the diffusion of potassium ions will establish a potential difference between the electrolyte solutions 1 and 2 given by the Nernst

equation

$$E_K = \Psi_2 - \Psi_1 = \frac{RT}{F} \ln \frac{[K]_1}{[K]_2} \qquad (2.1)$$

where R, T, and F have their usual meaning. Here and elsewhere in this thesis I have ignored the difference between activities and concentrations. In expression 2.1 the quantities "[K]" may be considered to represent concentrations although they are more properly activities. The potential $E_K$ defined by 2.1 is called "the potassium equilibrium potential." It is important to realize that, so long as no external electric current is applied, the potential $E_K$ will appear across any membrane exclusively permeable to potassium, regardless of the microscopic structure of the membrane or regions through which the potassium permeates (including fixed charges whether symmetrical or asymmetrical) and regardless of the concentration of other ions. Similarly if in our example the Na-holes are opened and the K-holes are closed, the membrane potential will shift to the sodium equilibrium potential ($E_{Na}$).

The description of what happens to the membrane potential when both the Na-holes and the K-holes are open, is more complex. In any event, in the absence of applied current a potential intermediate between $E_{Na}$ and $E_K$ will appear, with the net diffusion of sodium and potassium never stopping. At this potential the diffusional flux of sodium is equal and opposite to the flux of potassium, and it is legitimated to speak of circulating electric currents (carried by the ions) in the membrane although no external electric current is applied. Unfortunately the potential for this case cannot be calculated from basic principles without knowledge of the molecular and the electrical structure of the membrane. Intuitively it is clear, however, that the membrane potential will move closer to $E_{Na}$ if more Na-holes are added to the membrane or if the concentration of potassium in the system is reduced to very small values. This membrane with two types of holes will be seen to resemble the nerve membrane in several respects.

Faced with the difficulties of discussing unknown structures of great complexity the neurophysiologist resorts to the use of electrical analogs called "equivalent circuits" to describe nerve membrane properties. The equivalent circuit approach removes the discussion at once from the realm of theoretical electrochemistry and molecular structure to the realm of the electrical observables that neurophysiologists commonly measure. Representing the membrane by an equivalent circuit can be justified from the theory of diffusion potentials. By suitable rearrangement of the terms of the Nernst-Planck flux equation the following transformations can be deduced for any diffusion regime (Finkelstein and Mauro, 1963). The ionic fluxes are replaced by electric currents, the diffusion forces by electromotive forces, and the permeabilities by conductances (reciprocal resistances, symbolized by g). These quantities are integrated through the membrance to yield integral electromotive forces and integral conductances. A physically accurate representation is obtained if this integration is carried out separately for each of the kinds of holes or diffusion channels in the membrane. The Nernst-Planck flux equations are then replaced by a form of Ohm's law, which in the simplest case with no electromotive force would be:

$$I = g\,E \qquad (2.2)$$

where E is the membrane potential, arising in this case because of an imposed current I. If there is an electromotive force it should be subtracted from the membrane potential to obtain the driving force, so for the potassium component of current, for example, one can write:

$$I_K = g_K\,(E - E_K) \qquad (2.3)$$

Like the net diffusional fluxes this current ceases to flow when the membrane potential equals $E_K$. As indicated, statements like 2.3 are most meaningful if the potassium ions actually move through diffusion channels that they do not share with other ions. If several ions share the same channel they will of necessity interact through their contributions to the local electric field and therefore, in general,

the integral conductances (e.g., $g_K$) will depend on the mobilities and concentrations of all the permeant ions (see Finkelstein and Mauro, 1963). Nerve membrances seem to have individual ionic conductances ($g_{Na}$ or $g_K$) that depend only on the concentration of the individual ion ([Na] or [K]) and, as this thesis shows, seem also to have specific diffusion channels that, like the Na- and K-holes of the membrane previously discussed, are reserved for individual ions.

It should be noted parenthetically that the conductance, defined by 2.2 or 2.3 is called a chord conductance to distinguish it from the slope conductance defined by

$$g_{slope} = \frac{\partial I}{\partial E} \qquad (2.4)$$

Slope conductance will not be used in this thesis. Before leaving the diffusional picture of ionic fluxes, we should note that the chord conductances are physically meaningful. They are directly proportional to the area available for diffusion or to the number of holes and are also dependent (not necessarily in a simple manner) on the concentrations of the ions and on the ionic mobilities in the holes. These properties could in principle be derived by integrating through the membrane the basic flux equation of Nernst and Planck for the potassium ion.

$$Flux_K = -A\, u_K\, [K]\, \frac{\partial}{\partial x} (F\psi + RT \ln [K]) \qquad (2.5)$$

Here A is the area and $u_K$ is the mobility of the potassium ion. It is this integration that cannot be done without knowledge of the structure of the membrane. Furthermore, it seems likely that the diffusion paths are themselves only of molecular dimensions and therefore equation 2.5 containing macroscopic variables would have to be replaced by some microscopic flux equations.

When Hodgkin, Huxley, and Katz studied the squid axon with the voltage clamp technique, they expressed their results in the language of equivalent circuits. In a voltage clamp measurement the membrane potential of the nerve is suddenly displaced from one steady value to another, and the current necessary to do this is measured. The

fundamental observation is that the total current can be resolved into four mathematically and electrically independent components whose sum equals the total current. The operational procedures for separating the components of current in experimental records of the total current will be discussed in Chapter III. This result may be expressed by the equivalent circuit of Fig. 1 consisting of three batteries, two variable resistances, a constant resistance, and a capacitor. The four branches of the circuit carry the four components of the current: the sodium, the potassium, the leakage, and the capacity current. As their names imply two of the components are identified with flow of known ions: the sodium and the potassium current. One component, the leakage current or the "leak", is ionic but has been studied so little that the ions are not identified. The last component, the capacity current, is not considered to be an ionic current through the membrane. It reflects the arrival and departure of ions from the double layer region at the interfaces between the electrolyte solutions and the thin dielectric nerve membrane.

The equivalent circuit can be regarded as an analog of a slightly more complex version of the membrane (with K-holes and Na-holes) introduced at the beginning of this section. In similar fashion the potential across the indicated terminals of this circuit can be made to vary between $E_K$ and $E_{Na}$ by changing the variable conductances $g_K$ and $g_{Na}$. This is indeed the explanation of the action potential given by Hodgkin, Huxley, and Katz. Fig. 2 shows a propagating action potential calculated by Hodgkin and Huxley (1952d) using the equivalent circuit of Fig. 1 (as it is incorporated in the cable equation). The calculation was a numerical solution of empirical kinetic equations describing the conductances. These equations will be called the squid axon model hereafter. The calculation is an accurate picture of real action potentials and shows how $g_K$ and $g_{Na}$ vary during the impulse. The rest of this chapter will be discussion of nerve models of this kind.

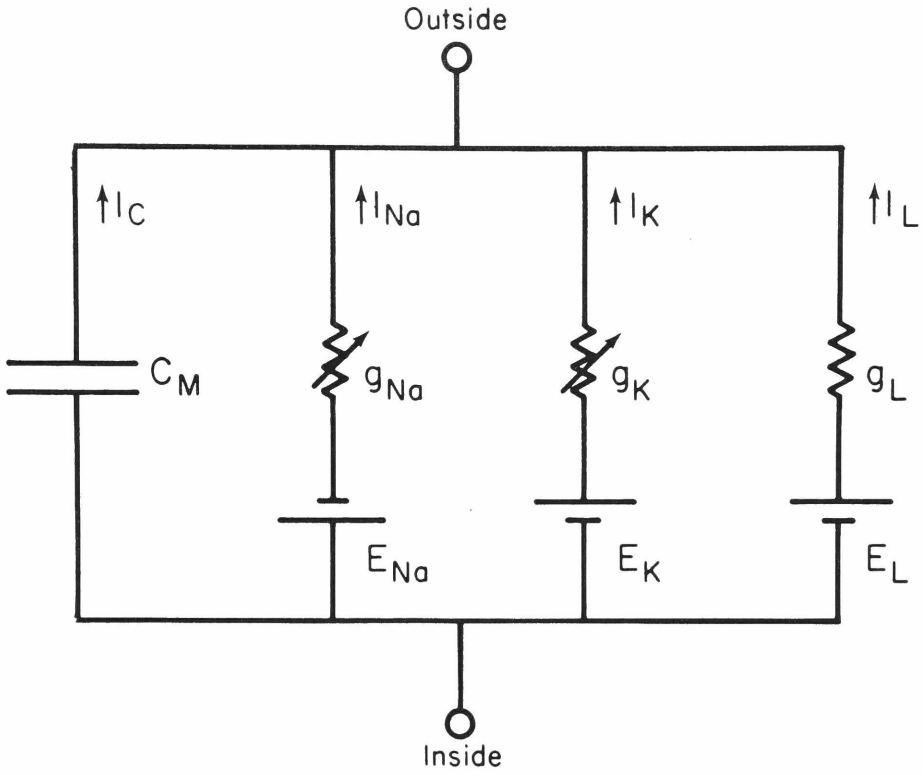


Figure 1. Equivalent circuit of the squid axon. Hodgkin and Huxley's (1952d) representation of the electrical properties of a patch of excitable membrane including a branch for each component of the total membrane current: the sodium, potassium, leakage, and capacity currents.

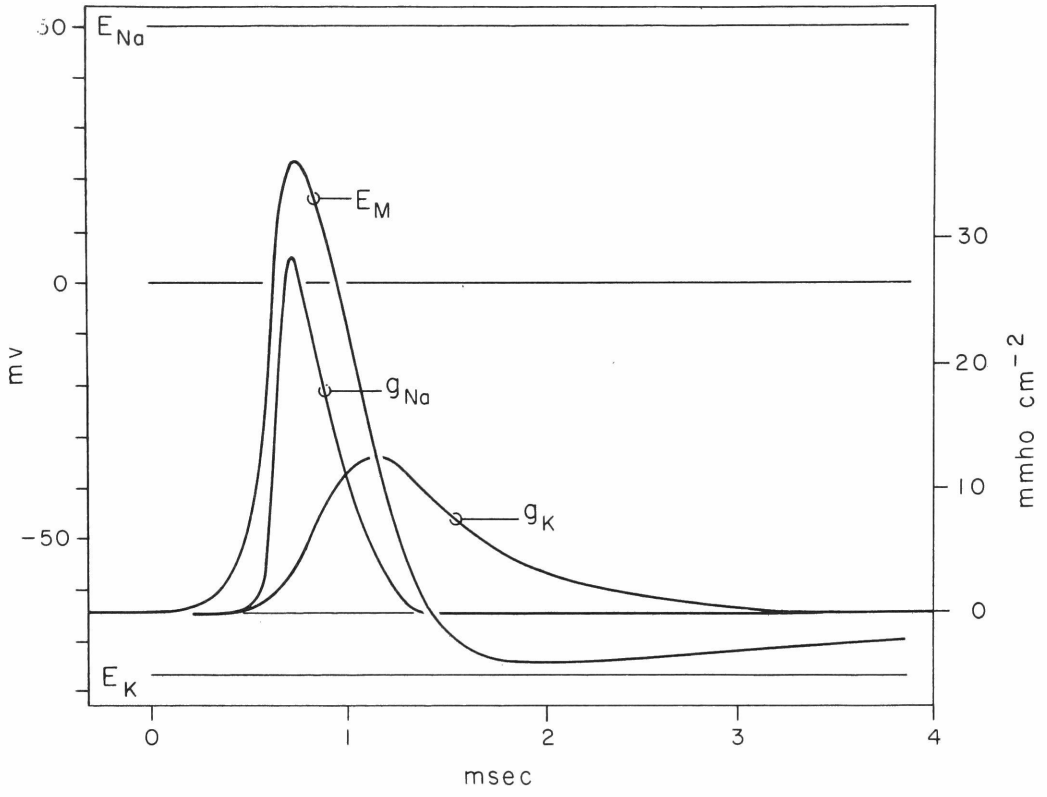


Figure 2. Action potential of the squid model. The propagating action potential ($E_M$) and the ionic conductances ($g_{Na}$ and $g_K$) calculated from the mathematical model of the squid axon. Adapted from Hodgkin and Huxley (1952d) with the assumption that the resting potential is equal to -63 mv. The values of the sodium and potassium equilibrium potentials are indicated by horizontal lines. The calculation agrees very dosely with the experimentally measured propagating action potential of the squid giant axon. T = 18.5° C.

## The Generality of the Hodgkin-Huxley Model

At present there exist three complete quantitative descriptions of the permeability changes of nerves. The original model was formulated by Hodgkin, Huxley, and Katz (1952) and Hodgkin and Huxley (1952 a,b,c,d) from voltage clamp measurements on the giant axon of the squid Loligo forbesi. Discussions of the methods used and of the manner in which the theory describes normal action potentials can be found in the original papers and in many subsequent review articles and textbooks of physiology (e.g. Hodgkin, 1957; Bard, 1961). The other two descriptions were also derived from voltage clamp experiments but on large single myelinated nerve fibers from the sciatic nerve of Xenopus laevis (Frankenhaeuser, 1960; Frankenhaeuser, 1963) and Rana pipiens (Dodge, 1963). As it turned out, the basis of the action potentials of the giant axon and of the myelinated fibers is the same, consisting of an initial large increase of permeability to sodium ions that depolarizes the fibers, followed by both a decrease of the sodium ion permeability and an increase of the potassium ion permeability that, in concert, repolarize the fiber. Therefore, the conceptual approach and method of formulation for the squid axon could be followed closely in describing the myelinated fibers, although the electronic techniques were different (described in Dodge and Frankenhaeuser, 1958).

Considered from the point of view of evolution the electrical behavior of Xenopus and Rana nodes is extraordinarily similar, even in fine details, to that of the squid axon, suggesting that the molecular mechanisms of excitation and propagation developed by the common ancestor of vertebrates and mollusks are hard to improve upon. Giant axons of one other phylum, the arthropods, have been studied successfully by voltage clamp techniques (Julian, Moore, and Goldman, 1958). These results with giant circumesophagal axons of the lobster, Homarus americanus, suggest that here again is a system like the squid's. Unfortunately no one has undertaken the mathematical analysis of the currents measured in this preparation so that the

degree of quantitative similarity between the lobster axon and the well studied nerves remains unknown. Although no other nerves have been studied as thoroughly as those of squid, frog, toad, and lobster, it has been shown that the basic principle of transient sodium permeability followed by increased potassium permeability accounts for the action potentials of most, but not all, nerves. On the other hand, muscles and electric organs exhibit such a diversity in their electrical behavior that it is certain that for each kind of cell some significant modification in the number or specificity of the permeability changes in the squid model would be needed to account for those observations that have been made. For example, specific chloride and calcium ion permeability changes are important for the normal activity of many cells. Some of the phenomena seen in muscles and electric organs will be considered in more detail in Chapter V.

## The Mathematical Model

This section deals specifically with Dodge's (1963) mathematical description of permeability changes of nodes of Ranvier in *Rana pipiens*. The *Rana* model is treated here because it is the basis of the experiments to be presented later, but it should be remembered that the equivalent circuit and the equations are, in fact, nearly the same as those for the squid. Primarily the empirical values of the coefficients are different. The model will first be developed in general and then for a particular case (Fig. 3 and Table I).

The total ionic current is the sum of the three components:

$$I_i = I_L + I_{Na} + I_K$$

$$= g_L (E-E_L) + g_{Na} (E-E_{Na}) + g_K (E-E_K) \qquad (2.6)$$

In standard electrophysiological usage the potentials are defined as the inside potential minus the outside potential. Currents, therefore, are positive when they are outward. Equation 2.6 embodies those features of the model that are most relevant to the experiments in

this thesis. As will be shown it is possible to find different drugs that will eliminate all or, at lower concentrations, a fraction of either the sodium currents or the potassium currents seen in voltage clamp measurements. The experiments show that the drugs act by selectively reducing either $g_{Na}$ or $g_K$ and indicate that the molecular mechanisms underlying these conductances may, in fact, be independent, as the formal expression 2.6 and the equivalent circuit (Fig. 1) suggest they might be.

The remaining features of the mathematical model are an empirical description of how the conductances $g_L$, $g_{Na}$, and $g_K$ depend on those parameters that can be varied experimentally. In general, they vary with potential, time, and the ionic composition of the medium, and their time dependence varies with the temperature. They are not dependent on either the total ionic current or on any component of it. In the steady state the leakage conductance is the predominant conductance of the nodal membrane at -75 mv and at all more negative potentials. In any voltage displacement in the depolarizing direction, the sodium conductance increases transiently and the potassium conductance increases more slowly to a steady level. The leakage conductance is the same at all times and at all voltages. A convenient representation of these time-dependent processes is achieved by the following equations:

$$g_L = \bar{g}_L \tag{2.7}$$

$$g_{Na} = m^3 h \bar{g}_{Na} \tag{2.8}$$

$$g_K = n^4 \bar{g}_K \tag{2.9}$$

where the $\bar{g}$'s are constants called the maximum conductances and the coefficients m,h, and n are continuous functions of time and voltage. The coefficients are dimensionless parameters that vary from zero to one with first order kinetics and rate constants that depend on the potential. They are raised to certain powers to achieve a simple expression that approximates the observed changes. The parameter m represents a "sodium activation" process that increases the sodium conductance on depolarization, and h represents a "sodium inactivation"

process that decreases the sodium permeability on depolarization. Together they give rise to the transient sodium conductance change on depolarization. It is the sodium inactivation process that accounts for the classical observation of enhancement or depression of the action potential by maintained hyperpolarization or depolarization respectively. The parameter n represents a "potassium activation" process that gives a delayed increase of the potassium conductance on depolarization, the so-called delayed rectification.

The time dependence of these parameters can be written as first order equations. For example:

$$\frac{dm}{dt} = \alpha_m (1-m) - \beta_m m \tag{2.10}$$

where $\alpha_m$ may be considered the forward rate constant of a process that produces "m" from something represented by "1-m" as suggested in the following reaction scheme:

$$1\text{-}m \underset{\beta_m}{\overset{\alpha_m}{\rightleftharpoons}} m \tag{2.11}$$

The rate constants are a function of voltage and temperature. If the voltage is held constant, as in the voltage clamp, equation 2.10 becomes a linear equation with constant coefficients with the following solution:

$$m = m_\infty - (m_\infty - m_o) \exp(-t/\tau_m) \tag{2.12}$$

where $m_\infty$ is the steady state value of m given by

$$m_\infty = \alpha_m / (\alpha_m + \beta_m) \tag{2.13}$$

and $\tau_m$ is the time constant of the exponential change of m from the initial value $m_o$ to the final value $m_\infty$. It is given by

$$\tau_m = 1 / (\alpha_m + \beta_m) \tag{2.14}$$

The time dependence of the parameters h and n can be written in exactly the same form as equations 2.10, 2.11, and 2.12.

All the equations of the model together with a set of empirical values of the steady states and time constants for m, h, and n are summarized in Fig. 3 and Table I. Empirical formulae for the rate

constants are listed in Appendix III. If the model is correct, then all voltage clamp experiments on a normal node should be described by these equations. Experiments show, however, that each node differs slightly from the next in the values of the empirical parameters given in Table I, so that individual differences have to be taken into account. The particular values chosen here will be called the standard parameters. They are slightly modified from the description given by Dodge (1963) of what he called "Node 7" studied at 22°C. One particular modification needs comment. In Xenopus and Rana nerves the value of $\bar{g}_{Na}$ is not strictly constant, rather it is larger when the sodium current flows inward from the 120 mM Na exterior than when it flows outward from the lower sodium concentration of the interior. This variation is like the rectification expected theoretically and seen experimentally under certain conditions for ions permeating membranes. Dodge and Frankenhaeuser (1959) showed that the small rectification could be incorporated into the model by using a particular solution of the Nernst-Planck diffusion equations that assumes a homogeneous membrane with a constant field at every point inside. Because this "constant field equation" depends on conditions that could not be verified with present techniques, I have chosen to use the empirical equation 5 of Fig. 3 to represent the small variation of the maximum sodium conductance with voltage. Equation 5 applies only to the range of potentials that is normally studied (from -100 to +100 mv).

The operation of the model can be illustrated by some solutions of the equations. It is easiest to consider the individual components of the ionic current separately. The leakage component is the major contributor to the resting potential and resting conductance of the node. A 100 mv depolarization from the resting potential produces a 2.5 na outward leakage current:

$$I_L = g_L (E-E_L) = 0.025 \times 10^{-6} \times 0.100 = 2.5 \text{ na}$$

$$I_i = \bar{g}_L (E-E_L) + m^3 h \bar{g}_{Na} (E-E_{Na}) + n^4 \bar{g}_K (E-E_K) \quad (1)$$

$$m = m_\infty - (m_\infty - m_o) \exp(-t/\tau_m) \quad (2)$$

$$h = h_\infty - (h_\infty - h_o) \exp(-t/\tau_h) \quad (3)$$

$$n = n_\infty - (n_\infty - n_o) \exp(-t/\tau_n) \quad (4)$$

$$\bar{g}_{Na} = (1 - \frac{E}{183}) \bar{g}_{Na,0mv} \quad (5)$$

STANDARD PARAMETERS AT 22°C

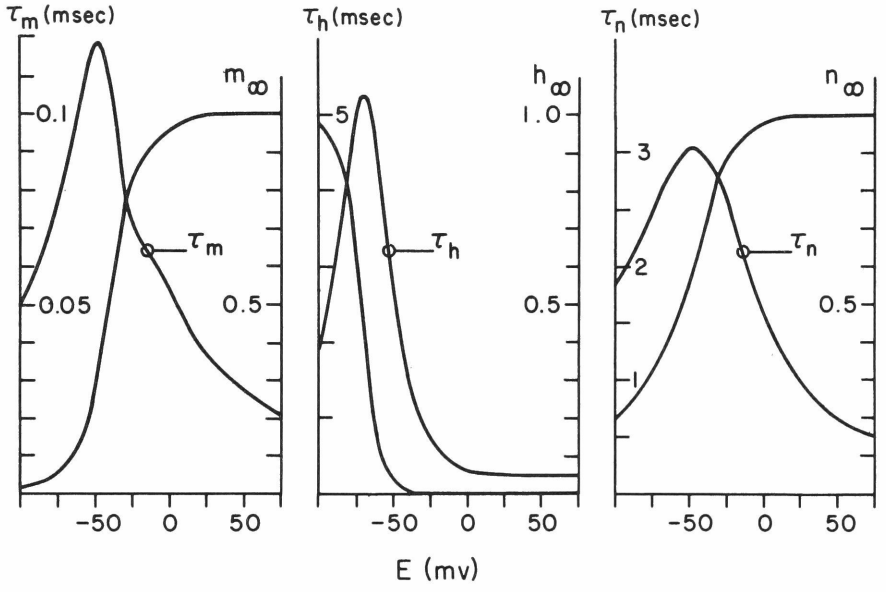


$\bar{g}_L$ = 0.025 μmho $E_L$ = -75 mv

$\bar{g}_K$ = 0.130 μmho $E_K$ = -75 mv

$\bar{g}_{Na,0mv}$ = 0.750 μmho $E_{Na}$ = 48 mv

Figure 3. Mathematical model of the frog node. A mathematical model slightly modified from "Node 7" of Dodge (1963) expressed in a form that is convenient for voltage clamp calculations. The resting potential is approximately -75 mv. The model is a close fit to data from a normal node at 22° C bathed in a solution identical with the Ringer's solution used in this thesis except that bicarbonate buffer was used instead of Tris. Tabular information on the model can be found in Table I and the empirical formulae for the rate constants are listed in Appendix III.

Table I

EMPIRICAL CONSTANTS FOR STANDARD RANA NODE OF RANVIER

IN STANDARD RINGER'S SOLUTION AT 22° C

| E | $\tau_m$ | $m_\infty$ | $\tau_h$ | $h_\infty$ | * | $\tau_n$ | $n_\infty$ | $n_\infty^4$ |
|---|---|---|---|---|---|---|---|---|
| -100. | .050 | .0166 | 1.84 | .9759 | .000006 | 1.82 | .1988 | .0015 |
| -95. | .054 | .0203 | 2.23 | .9589 | .000012 | 1.93 | .2158 | .0021 |
| -90. | .059 | .0253 | 2.75 | .9286 | .000022 | 2.06 | .2358 | .0030 |
| -85. | .064 | .0320 | 3.42 | .8753 | .000042 | 2.19 | .2597 | .0045 |
| -80. | .070 | .0410 | 4.19 | .7850 | .000077 | 2.32 | .2882 | .0069 |
| -75. | .077 | .0533 | 4.90 | .6469 | .000138 | 2.47 | .3221 | .0107 |
| -70. | .085 | .0707 | 5.25 | .4700 | .000230 | 2.62 | .3621 | .0172 |
| -65. | .093 | .0955 | 5.01 | .2935 | .000347 | 2.76 | .4089 | .0279 |
| -60. | .102 | .1317 | 4.28 | .1591 | .000483 | 2.88 | .4626 | .0458 |
| -55. | .111 | .1852 | 3.39 | .0777 | .000643 | 2.98 | .5225 | .0745 |
| -50. | .117 | .2644 | 2.58 | .0356 | .000838 | 3.03 | .5870 | .1187 |
| -45. | .117 | .3756 | 1.94 | .0157 | .001040 | 3.04 | .6534 | .1823 |
| -40. | .109 | .5124 | 1.46 | .0068 | .001125 | 2.99 | .7185 | .2666 |
| -35. | .095 | .6478 | 1.11 | .0029 | .000966 | 2.88 | .7789 | .3681 |
| -30. | .081 | .7543 | .86 | .0013 | .000652 | 2.73 | .8318 | .4789 |
| -25. | .071 | .8251 | .68 | .0005 | .000369 | 2.54 | .8759 | .5886 |
| -20. | .066 | .8701 | .55 | .0002 | .000191 | 2.33 | .9107 | .6881 |
| -15. | .064 | .9017 | .46 | .0001 | .000095 | 2.13 | .9372 | .7717 |
| -10. | .061 | .9265 | .40 | .0000 | .000047 | 1.92 | .9566 | .8376 |
| -5. | .057 | .9462 | .35 | .0000 | .000024 | 1.73 | .9705 | .8871 |
| . | .053 | .9615 | .32 | .0000 | .000012 | 1.56 | .9801 | .9228 |
| 5. | .049 | .9728 | .30 | .0000 | .000006 | 1.41 | .9867 | .9479 |
| 10. | .046 | .9810 | .28 | .0000 | .000003 | 1.27 | .9911 | .9652 |
| 15. | .042 | .9868 | .27 | .0000 | .000001 | 1.16 | .9941 | .9769 |
| 20. | .039 | .9909 | .26 | .0000 | .000000 | 1.05 | .9961 | .9847 |
| 25. | .036 | .9937 | .26 | .0000 | .000000 | .96 | .9974 | .9899 |
| 30. | .034 | .9956 | .25 | .0000 | .000000 | .88 | .9983 | .9933 |
| 35. | .032 | .9970 | .25 | .0000 | .000000 | .82 | .9989 | .9956 |
| 40. | .030 | .9979 | .25 | .0000 | .000000 | .76 | .9992 | .9971 |
| 45. | .028 | .9986 | .25 | .0000 | .000000 | .70 | .9995 | .9981 |
| 50. | .026 | .9990 | .25 | .0000 | .000000 | .66 | .9996 | .9987 |
| 55. | .025 | .9993 | .25 | .0000 | .000000 | .61 | .9997 | .9991 |
| 60. | .024 | .9995 | .25 | .0000 | .000000 | .58 | .9998 | .9994 |
| 65. | .023 | .9996 | .25 | .0000 | .000000 | .54 | .9999 | .9996 |
| 70. | .021 | .9997 | .25 | .0000 | .000000 | .51 | .9999 | .9997 |
| 75. | .021 | .9998 | .25 | .0000 | .000000 | .49 | .9999 | .9998 |
| 80. | .020 | .9999 | .25 | .0000 | .000000 | .46 | .9999 | .9998 |
| 85. | .019 | .9999 | .25 | .0000 | .000000 | .44 | .9999 | .9999 |
| 90. | .018 | .9999 | .25 | .0000 | .000000 | .42 | .9999 | .9999 |
| 95. | .017 | .9999 | .25 | .0000 | .000000 | .40 | .9999 | .9999 |
| 100. | .017 | .9999 | .25 | .0000 | .000000 | .39 | .9999 | .9999 |

explanation

E : Potential in millivolts where -75 is the approximate resting potential

$\tau$ : Time constants in milliseconds

* : Relative steady-state sodium conductance

$$* \equiv m_\infty^3 h_\infty \left\{1 - \frac{E}{183}\right\}$$

The inward sodium current through the nodal membrane during a normal action potential is just of this order of magnitude. Thus the leakage is of the utmost importance for normal function. Nevertheless in the experiments to be reported very little reference will be made to the leak because it seems to be constant under almost all the conditions used. To facilitate the inspection of the sodium and potassium currents the leakage current has been subtracted from most of the experimental records of ionic current to be discussed.

The membrane undergoes dramatic changes when the node is depolarized. In the model this can be seen as large changes in the steady-state values of m, h, and n. Notice in Fig. 3 that $m_\infty$, $h_\infty$, and $n_\infty$ undergo fairly sharp transitions when the membrane potential is displaced from -75 mv to 0 mv. In general the value of m changes more rapidly than the values of n or h, i.e., $\tau_m$ is small.

The steady-state potassium conductance is minute at all potentials more negative than -55 mv ($n_\infty$ is small). Thus hyperpolarization and small depolarizations lead to minute potassium currents. Stronger depolarizations elicit the slow potassium conductance increase (n increases). The time courses of a typical family of potassium currents obtained from the model are shown in Fig. 4. These are solutions of the equations at voltages from -60 mv to +75 mv, spaced at 15 mv intervals. The calculations were initiated with n starting at its steady-state value ($n_\infty$) for -116 mv. These curves are meant to mimic the potassium currents from a voltage clamp experiment in which the node is held at -116 mv for a long time and then suddenly depolarized to another voltage.

Similarly a sodium conductance increase can be elicited only by depolarizations. Fig. 4 shows the sodium currents calculated from the model under the same conditions as in the previous calculation. These curves seem more complex both because the sodium conductance is first activated (m increases) and then inactivated (h decreases) and because at a certain voltage, the sodium equilibrium potential, the direction of the currents reverses. The reversal is of course due to

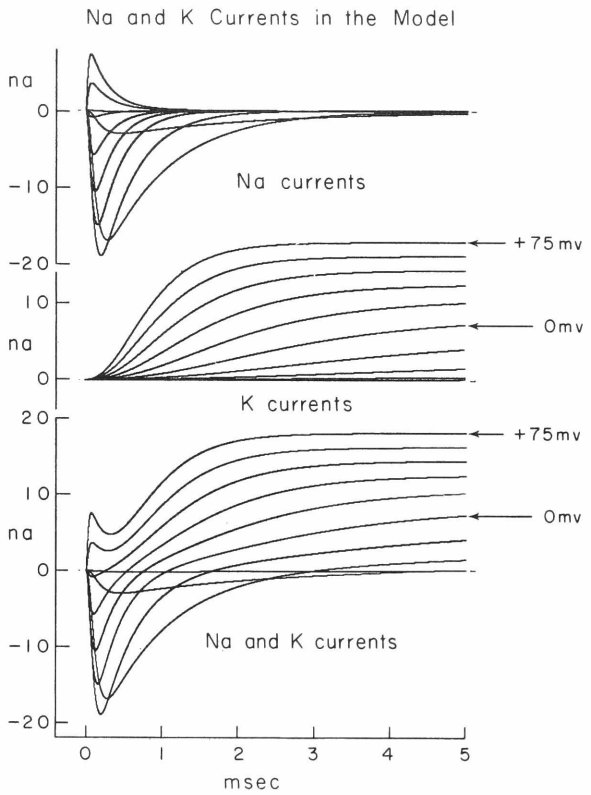


Figure 4. Voltage clamp currents in the model. The time courses of the voltage clamp currents of a frog node of Ranvier calculated from the mathematical model in Fig. 3. The calculations were started with m, n, and h set at their steady-state values for -116 mv, and the voltages of the test pulses spanned the range from -60 mv to +75 mv at 15 mv intervals. The top two families of curves are the sodium and the potassium currents and the bottom family is the algebraic sum of the two. The leakage current has not been included. T = 22° C.

a reversal of the electrochemical driving force at $E_{Na}$. Fig. 4 shows the sum of the sodium and potassium currents as they might be seen in a voltage clamp experiment.

Despite the exact quantitative nature of our knowledge, the molecular nature of the changes described by the model remains entirely unknown. My experiments are an attempt to modify the responses of the nerve membrane by applied chemical reagents in the hope that some clues will emerge concerning the physico-chemical structure of the excitability mechanism.

The results in Chapter IV are presented in three main formats: currents as a function of time, time constants as a function of voltage, and current-voltage relations. An understanding of why the sodium and potassium currents have the time courses they have will not be important for understanding the experiments, but it will be necessary to bear in mind the general shape of the whole family of these currents and of their sum as illustrated in Fig. 4. Likewise the overall appearance of the time constants as a function of voltage (Fig. 3) should be remembered. Finally an understanding of current-voltage relations will be useful. They will be described now.

The relationship between current and voltage across a nerve membrane is the electrical analog of the relationship between ionic fluxes and their driving forces. In this paragraph the electrical responses of equivalent circuits will be stressed. Current-voltage relations of a number of simple circuits are drawn in Figs. 5, 6, and 7. The plot for a constant ohmic resistance is always a straight line whose slope is equal to the conductance (Fig. 5) and whose voltage-intercept is equal to the electromotive force in the circuit (Fig. 6). The behavior of voltage-dependent resistances is more complicated. A familiar example is the diode that has a high conductance in one direction of current flow and a low conductance in the other. Figure 7 shows the current voltage relations of four circuits combining voltage-dependent resistances with series electromotive forces. Curve 1a is drawn for the case where there is an electromotive force -E in

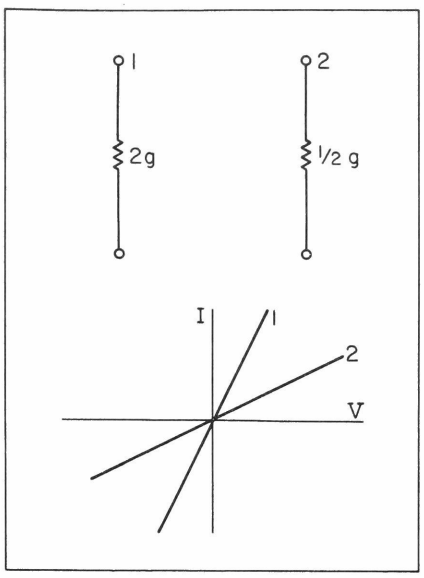


5

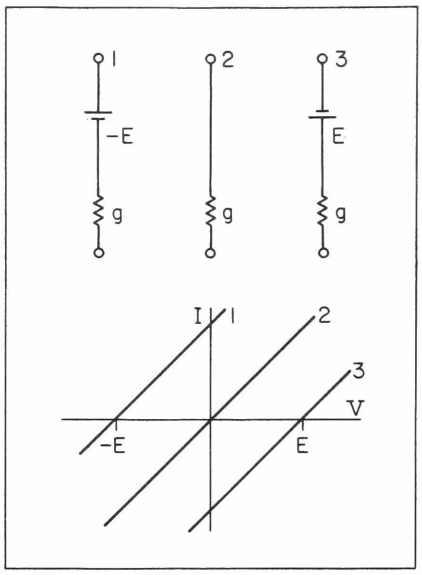


6

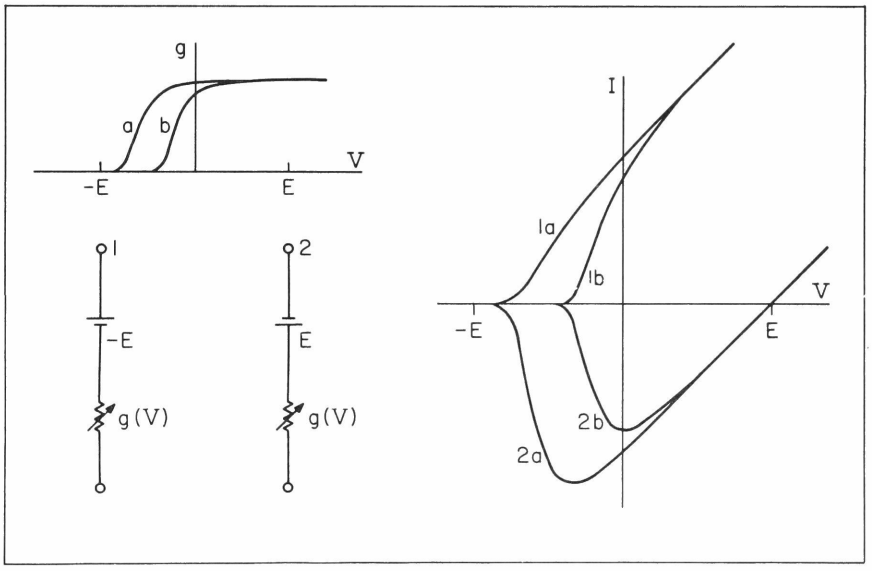


7

Figures 5, 6 and 7. Current-voltage relations of simple circuits. The current-voltage relations of constant conductances (5), of constant conductances with E.M.F.s in series (6), and of voltage-dependent conductances with E.M.F.s in series (7). The conductances in 7 are indicated as chord conductances which remain positive although a negative slope may appear in the current-voltage diagram. The sign convention used in these figures is the same as that in Fig. 3 in which upward current flow in the equivalent circuit is defined as positive.

series with a conductance that is zero when the potential is very negative and finite when the potential is more positive. The plot for these conditions has three limbs: a zero current limb at very negative potentials, a linear, high conductance limb at positive potentials, and a non-linear limb at intermediate potentials where the conductance is changing. The non-linear limb can be referred to as the region of rectification. If the region of rectification is moved further from the potential -E as in case 1b, the non-linearity becomes more pronounced. When the electromotive force is changed from -E to +E, the lines labelled 2a and 2b, the appearance of the current-voltage relation is markedly changed. The three limbs of the curves are still identifiable although the region of rectification shows a negative slope conductance as defined by relation 2.4. The reader can verify for himself that the relative position (on the voltage axis) of the zero conductance region of the variable conductance and of the electromotive force of the battery in the circuit determines whether the negative slope conductance will appear, as suggested by the example in Fig. 7.

The discussion of the previous paragraph is concerned with the phenomenological properties of some simple electrical circuits. Their behavior is like that of the nerve membrane. Specifically circuit 1 in Fig. 6 is like the leakage branch of the equivalent circuit of Fig. 1, and circuits 1a and 2a of Fig. 7 are like the potassium and sodium branches, respectively, with <u>one stringent reservation</u>: the conductances of the sodium and potassium branches are time-dependent as well as voltage-dependent. Consideration of Fig. 3 shows that the functions $m_\infty^3$ and $n_\infty^4$ resemble the function g(V) used in Fig. 7. The following relationship holds approximately for the peak of the sodium current (because at the peak, h has from 1.0 to approximately 0.6 and $m^3$ has risen to approximately 0.8 $m_\infty^3$ )

$$g_{Na,peak} \approx 0.6 \times 0.8\ m_\infty^3\ \bar{g}_{Na} \approx 0.5\ m_\infty^3\ \bar{g}_{Na} \qquad (2.15)$$

and the following is true for the steady-state potassium currents

$$g_{K,steady\ state} = n_\infty^4\ \bar{g}_K \qquad (2.16)$$

Thus the functions $g_{Na,peak}$ and $g_{K,steady\ state}$ closely resemble the function g(V) of Fig. 7, and comparison of the peak sodium current-voltage relation with curves 2a and b of Fig. 7 and of the steady-state potassium current-voltage relation with the curves 1a and b of Fig. 7 is therefore possible. Current-voltage plots are a convenient method of displaying any changes in the maximum conductances $\bar{g}_{Na}$ and $\bar{g}_{K}$. They also make it easy to observe alterations in the region of rectification. It might be helpful to refer ahead to some of the current-voltage diagrams that are derived from my experiments to see how they look in practice (Figs. 16, 20, 22, 23, and 28).

Readers with a background in electronics will note that a negative slope conductance is a sign of instability in any circuit. In the case of the nerve membrane it is an expression of the instability or electrical excitability of the membrane. Conditions that remove the negative slope resistance will abolish the nerve impulse. Some readers will be interested to read a discussion of the consequences of the simultaneous voltage and <u>time</u> dependence of the resistances of the equivalent circuit of the membrane by Mauro (1961). That article shows how various anomalous impedances can arise in simple circuits that contain resistors with a time-lag.

# Chapter III

## THE EXPERIMENTAL METHODS

The experiments in this thesis are basically of one type that is designed to examine the effects of drugs on the electrical behavior of nodes of Ranvier. The measurements are mainly of voltage clamp currents analysed in terms of the mathematical model described in the previous chapter. Thus the conclusions are statements of which parameters in the model are sensitive to a particular drug.

The execution of an experiment falls naturally into three phases, the dissection and mounting of the nerve preceding the measurements, the electronic measurement and recording, and the subsequent analysis of the data in terms of the mathematical model. The methods used in these phases will be described in this section. Except for the use of the digital computer the methods and instruments are identical with those used by Dodge (1963).

### The Biological Preparation

The sciatic nerve of Rana pipiens is removed from the knee to above the hip, desheathed, and split into the two bundles giving rise to the peroneal and tibial nerves. The middle of a 3 cm section of one of these bundles is teased apart with sharpened metal needles according to the technique of Tasaki (1954) until 3 or 4 mm of a single large myelinated fiber is freed of all other fibers. The remaining fibers are trimmed back to leave the large stumps of the nerve bundle on either side, connected by the single fiber. The fiber is transferred, always under Ringer's solution and handled by the stumps, into a four compartment lucite chamber shown in Fig. 8. The node to be studied is centered in the pool labelled A, and a narrow band of vaseline represented by crosshatching is laid across the fiber at the partitions separating the pools. Lowering the Ringer's level breaks the fluid continuity between the chambers and leaves four pools, each electrically isolated from the next by a

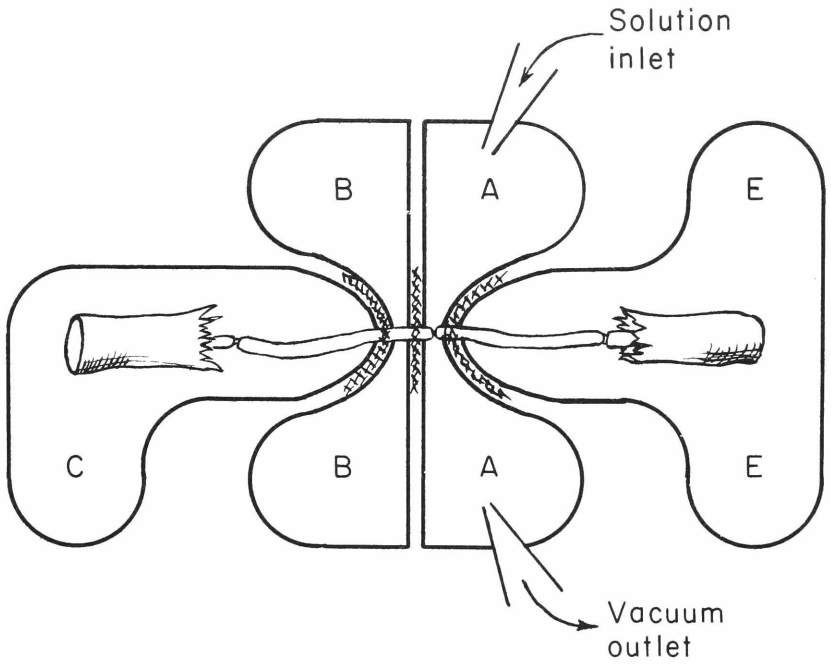


Figure 8. The Nerve chamber. A schematic drawing of the single fiber and the stumps of the nerve trunk lying in the four fluid-filled compartments C, B, A, and E of the lucite nerve chamber. The cross hatching on the partitions separating the pools represents the positions of the ribbons of vaseline that are laid across the nerve after it is in place to increase the electrical resistance between the pools. The three constrictions on the nerve fiber are the nodes of Ranvier. The node to be studied is placed in pool A.

vaseline seal of about 2 megohms resistance.

The lucite chamber is placed in a brass housing cooled to a constant temperature by water circulating from a thermostatically controlled water bath. To depolarize and lower the resistance of all nodes outside of pool A, the Ringer's solution in pools E and C is replaced by 120 mM KCl containing no calcium. This solution is allowed to penetrate the ends of the cut nerve stump for at least half an hour before measurements are made. Sometimes as much as two hours elapses before measurements are begun. Two small tubes touch the surface of the solution in pool A and serve as an inlet and a vacuum outlet for rapid solution changes.

The Ringer's solution has the following composition (mM): NaCl 110, KCl 2.5, $CaCl_2$ 2.0, tris-(hydroxymethyl) aminomethane buffer (pH 7.3) 5 mM. Solutions with extra calcium are the standard Ringer's made hypertonic by dissolving more $CaCl_2$. All other solutions are made by replacing some of the NaCl by an equimolar amount of the reagent to be studied. Table II is a list of the reagents used, showing the manufacturer and the names of individuals or manufacturers who were kind enough to donate them. The solutions to be used during an experiment are kept in an insulated box cooled by the same water bath that cools the preparation. One or two milliliters of the solution are taken into a cooled syringe and injected through the inlet tube to change the solution in pool A. The volume of this pool is about 0.15 ml, and so between 7 and 15 volumes are flushed through in any particular solution change.

The thermostatically controlled water bath and the circulation pump are placed in operation at least an hour before measurements are made, and the solutions are placed in their cooled box at least half an hour before use. With these precautions the temperature of the system measured in the box with the solutions does not vary more than 0.2° C in any half hour period during the experiment. This amount of regulation is extremely important because a 1° C change of temperature changes the rate constants $\tau_n$ and $\tau_h$ by 12%. The rate

Table II

SOME OF THE DRUGS USED

Tetrodotoxin (SC)
Xylocaine hydrochloride (Lidocaine) (AP)
QX314 chloride (AP)
QX-222 chloride (AP)
QX-572 chloride (AP)
Procaine hydrochloride (Novocaine) (AD)
Dibucaine hydrochloride (Nupercaine) (C)
Prochlorperazine ethanedisulfonate (Compazine) (SKF)
Chloretone (PD)
Veratrine hydrochloride (M)
Tetramethylammonium bromide (E)
Ethyltrimethylammonium iodide (E)
Diethyldimethylammonium iodide (S)
Triethylmethylammonium iodide (E)
Tetraethylammonium iodide (E)
Triethyl-n-propylammonium iodide (E)
Tetra-n-propylammonium iodide (E)
Tetra-n-butylammonium iodide (E)
Choline chloride (E)
(2-hydroxyethyl) ethyldimethylammonium iodide (S)
(2-hydroethyl) triethylammonium iodide (AC)

Abbreviations:

AC Aldrich Chemical Company, Inc., Milwaukee
AD Amend Drug and Chemical Co., Inc., New York
AP Gift of Astra Pharmaceutical Products, Inc., Worcester, Mass.
C CIBA, Summit, New Jersey
E Eastman Organic Chemicals, Rochester
M E. Merck, Darmstadt
PD Parke Davis and Company, Detroit
S Gift of Dr. F.G. Standaert, Cornell University Medical School, New York
SC Gift of Dr. T. Narahashi, Duke University Medical School, Durham; and Sankyo Company, Tokyo
SKF Gift of Smith, Kline, and French, Labs., Philadelphia

constant $\tau_h$ is somewhat less sensitive.

## The Electronic Measurements and Recording

The electronic apparatus has two main components. There are first the amplifiers and stimulus generators that achieve the voltage clamp and second the digital computer that records the data automatically.

### The voltage clamp

The explanation of the operation of the voltage clamping method should be prefaced by a remark about voltage clamping in general. In all voltage clamps one needs an accurate measure of the transmembrane potential of the cell. This signal is then compared with some reference signal (generated by the experimenter). If the signals differ, a current is passed through the membrane by a second device until the signals are equal. The comparison of signals and adjustment of current is accomplished by electronic feedback. A last requirement is that the dependent variable of the experiment, the current, needs to be measured. Therefore the method to be described has to provide a measure of the transmembrane potential and a procedure for passing a measurable transmembrane current that does not interfere with the potential measurement. As will be seen, the part of the axon projecting into pool C serves as a kind of insulated intracellular lead that is used to observe the potential of the node in pool A, while the part projecting into pool E is used as a lead through which the current can be supplied.

In the following paragraphs the electronic method is outlined in a simple manner. The details of the circuits and theory are given by Frankenhaeuser (1957), Frankenhaeuser and Dodge (1958), and Dodge (1963). Also, Appendix II of this thesis is a discussion of two significant sources of error in the method.

Salt bridges from the fluid pools of the nerve chamber to calomel half-cells establish the electrical contact with the nerve.

The bridges are filled with 1% agar in 3M KCl and a fine shiny platinum wire. The calomel cells contain a 3M KCl solution and are embedded in the temperature-controlled brass housing. In all, seven electrical connections are made to the seven fluid filled wells labelled in Fig. 8. Three of these, from pools C, A, and E go to cathode followers as part of the high impedance measuring circuit, and the remaining four are attached to low impedance sources used for sending current into the preparation.

Fig. 9 is an equivalent circuit of the preparation and amplifiers. The large triangles labelled 1 and 2 are high gain, wide bandwidth differential amplifiers, and the resistors represent the electrical resistance of some of the fluid paths in the preparation, including the longitudinal resistances, labelled "internode," of the axoplasm of the fiber. The points labelled A, B, C, and E correspond to the pools with the same labels in Fig. 8. D is in the axoplasm of the node under investigation.

The membrane potential measuring system is a potentiometric device employing electronic feedback developed by Frankenhaeuser (1957) as an extension of the static potentiometric method of Huxley and Stämpfli (1951a). Similar methods are rarely seen in neurophysiology. Amplifier 1 serves as an operational amplifier applying negative feedback to its input (C) through the circuit A-D-C. Point C can be called the summing point of the amplifier and is a virtual ground due to the negative feedback. While the feedback is in operation, no longitudinal current can flow to pool C from point D and therefore point D is also maintained at ground potential. If the internal potential (at D) of the node under investigation is zero, the external potential (at A) must be $-E_M$, where $E_M$ is the membrane potential defined in the usual sense of inside potential minus outside potential.

The membrane potential can therefore be measured by displaying the potential of pool A on an oscilloscope with inverted sign. This signal appears at the low impedence output of amplifier 1, so that no

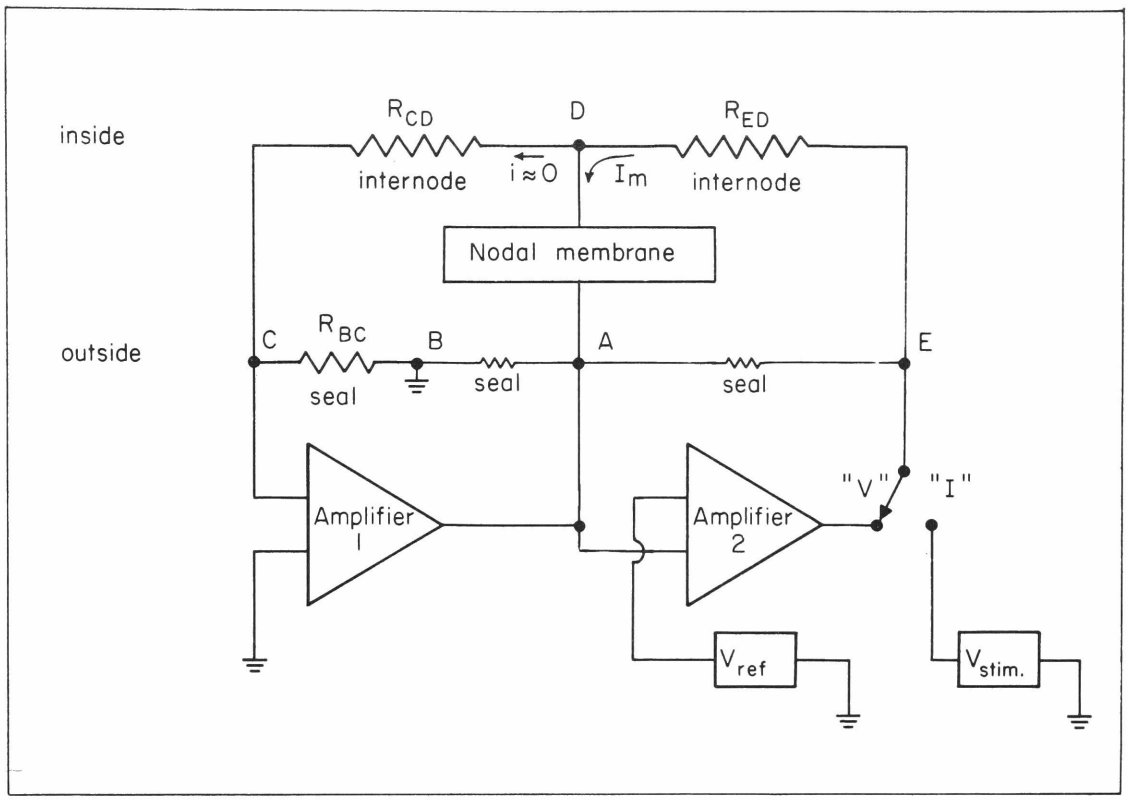


Figure 9. Equivalent circuit of the voltage clamp. A schematic diagram of the potential measuring and voltage clamp circuits including an abbreviated equivalent circuit of the preparation. The top line is meant to be inside the axon and the second line is in the chamber showing the four fluid filled wells C, B, A, and E. The bottom line shows the connection of the amplifiers. A more complete equivalent circuit can be found in Appendix II. (Figure taken from Dodge, 1963).

special apparatus is needed for this measurement. Nevertheless, although the voltage at the output of amplifier 1 is easily measured, it is not always a true indication of the D.C. level of the resting potential. The origin of this significant error is discussed in Appendix II.

Throughout this thesis membrane potentials will be given on the absolute scale of inside minus outside (the "E" scale) rather than on the relative scale of displacement from the resting potential (the "V" scale) used by Hodgkin, Huxley, and Katz (1952). The word depolarization will be taken to mean any displacement of the membrane potential in the positive direction and hyperpolarization, a displacement in the negative direction. Outward currents are called positive currents.

Since no current flows from D to C, any current that flows from E to D will of necessity pass through the nodal membrane. Thus a variable voltage source applied to pool E will permit polarization of the membrane by variable currents. When the switch in the lower right hand side of Fig. 9 is in the "I" position, a pulse generator ($V_{stim}$) is connected to pool E, and the node may be stimulated and polarized. This condition is called current clamp. When the switch is in the "V" position, the output of amplifier 2 is applied to pool E closing a negative feedback loop E-D-A. The feedback amplifier applies transmembrance current appropriate to equalizing the membrane potential and reference voltage ($V_{ref}$). This is the voltage clamp condition. Remembering that all the membrane current passes from E to D and that D is at zero potential, it is easy to see that the current will be proportional to the voltage applied in pool E provided the resistance in this path ($R_{ED}$) remains constant. One generally assumes that $R_{ED}$ is constant, so the voltage at E is displayed on the oscilloscope as a measure of the membrane current. It is shown in Appendix II that $R_{ED}$ may change especially when the applied current is large and that this leads to a significant error in the measurement of current under certain conditions. Other errors in the voltage

clamp have been discussed by Dodge and Frankenhaeuser (1958 and 1959) and by Dodge (1963).

In my measurements the membrane potential of the node was held clamped near the normal resting potential (approximately -75 mv) throughout the experiment except when depolarizing or hyperpolarizing test pulses were applied. This procedure keeps the node in good condition for a long time. The clamp was not turned off during the solution changes making it possible to take measurements soon after the solution change. If the node is allowed to depolarize for more than a few seconds, it must be repolarized for more than a minute before certain deleterious effects of depolarization are reversed and the electrical properties of the node return to normal. This and related hysteresis effects are discussed in Chapter V. The method for setting the membrane potential near -75 mv at the beginning of the experiment is discussed in Appendix II.

Analog-to-digital recording

The observables of a voltage clamp experiment are the current and voltage as a function of time. From this information the time and amplitude parameters of the quantitative model are extracted. The complete analysis of voltage clamp experiments requires lengthy mathematical calculations that can be performed by a digital computer if the observations are recorded in an appropriate form. The traditional photograph cannot be conveniently read by computers. Conventional AM or FM analog tape recording lacks the high frequency response needed in the voltage clamp. The only practical technique is on-line analog-to-digital (A-to-D) conversion using fast digital logic and memory. Fortunately, I was able to use Dr. H. K. Hartline's Control Data Corporation 160 A digital computer and its A-to-D conversion devices both for recording and for analysing my experiments. In this section the recording process is outlined in general terms that will be sufficient for an understanding of the main advantages and limitations of the method. Some of the practical considerations

such as the computer program and the interconnections between electronic components are discussed in greater detail in Appendix III. It should be understood that the computer serves only as a recording apparatus during the experiment. It does not control the voltage clamp, the reference voltages, or the frequency of repetition in any manner. Rather the experimenter by turning switches on the voltage clamp apparatus informs the computer when to record and when not to.

Of the two signals to be recorded, the voltage signal is by far the simpler, being (except for a brief transient at the transitions) rectangular steps of long duration. The current signals are complex waveforms like those calculated from the model (Fig. 4), with high frequency components associated with the rise of the sodium currents that can be resolved only if the time intervals between successive digital measurements are very short. In my experiments current measurements are made every 50 μsec and voltage measurements are made about 14 μsec after the current measurements. For convenience each measurement will be called a "point". This rate of sampling is not adequate for the curves of Fig. 4 calculated for 22° C; however, the cooled nerve used in my experiments has more slowly varying currents and the resolution is adequate. As is discussed in Appendix III it is practical to use one memory bank of the computer (4096 memory locations) for the initial storage of the current and voltage points thus limiting the total duration of an experimental record to 100 msec. In practice less than 50 msec of record contains enough information for the extraction of all the time constants and amplitudes of the model at one particular test voltage, so that two records may be taken before the memory is full.

Fig. 10 shows schematically a pair of simultaneous current and voltage signals associated with a 40 msec hyperpolarizing prepulse and a 25 msec depolarizing test pulse. During the 50 msec period from A through D the memory receives 1000 current points and 1000 voltage points. About 350 msec later, exactly the same prepulse and test pulse are repeated and a second list of similar points is

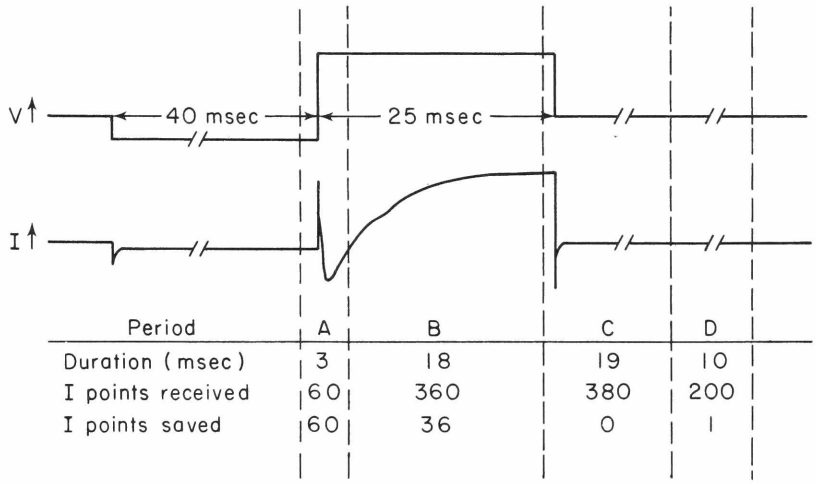


| Period | A | B | C | D |
|---|---|---|---|---|
| Duration (msec) | 3 | 18 | 19 | 10 |
| I points received | 60 | 360 | 380 | 200 |
| I points saved | 60 | 36 | 0 | 1 |

Figure 10. Digital sampling of voltage and current. The time courses of the voltage and current signals (above) and the four periods A, B, C, and D that constitute the 50 msec of digital sampling (below). The bottom two lines give the count of the current points as originally received and after the computer has condensed the data. The curves are drawn schematically and are not to scale.

received. The memory bank is now full, and the lists of points must be condensed as much as possible and transferred to digital magnetic tape before more points can be taken. First the two lists are added together to make a single list with an improved signal-to-noise-ratio. Then the average voltage of the prepulse, of the test pulse, and of the following baseline are calculated by averaging the appropriate voltage numbers. Several points on either side of the voltage step are left out so as not to include the transient in the average. In this way the 1000 voltage points are reduced to the three numbers of interest. Similarly the current points in period D are averaged for the current baseline. Aside from these four averages, only the current points from periods A and B need to be saved. After the early rise of the sodium current in period A, the currents vary so slowly that they are satisfactorily represented by one point every 500 μsec instead of every 50 μsec. This is accomplished by averaging each ten consecutive current points during period B. Averaging these points markedly improves the signal to noise ratio as can be seen in almost any of the experimental records illustrated later. The computer takes less than 0.5 sec on-line to compute all the averages and to reduce the data from the 4000 points received to the 100 to be saved. In another small fraction of a second the 100 points are recorded on magnetic tape for later analysis, and the whole system is ready to receive a new pair of lists from a new test pulse. The durations of the periods A, B, C, and D chosen for Fig. 10 are representative, but various values were used in actual experiments.

The measurements on a node are considered complete when the responses to one hyperpolarizing voltage (-120 mv or -135 mv) and to 19 different depolarizing voltages (spaced at 7.5 mv intervals) have been recorded. The measurements are taken in less than a minute. Then the solution around the node is changed by an injection of 1 or 2 ml of the new solution through the inlet of the chamber. Between ten and twenty solution changes and measurements constitute a good experiment. A typical experimental protocol consists of five changes

spaced 5 min apart, a 15 min rest, five more changes, another 15 min rest, and a final five changes. The measurements in consecutive solutions are given consecutive identifying numbers. These numbers are included in all the figures in Chapter IV so that the chronological relationships of the measurements can be determined. One caution should be noted in the interpretation of these numbers. They are in the octal notation used by the computer, rather than in the more familiar decimal notation. In octal the digits from "0" to "7" are used, for example, $7_8$ plus $1_8$ is $10_8$ and $377_8$ plus $1_8$ is $400_8$.

## Analysis of Voltage Clamp Records

Conceptually the complete analysis of voltage clamp experiments is first the resolution of the total current into the capacity, sodium, potassium, and leakage components and then the extraction of the time and amplitude parameters from these separated components. In practice these phases overlap as will be explained. However, the principles of the separation of the current components are so important for this thesis that I shall discuss them in general terms before describing the analysis of the records by the computer.

### The separation of the components of the current: methods

Whenever an excitable membrane is studied by the voltage clamp technique, an attempt should be made to resolve the observed currents into independent components. A simple method of limited usefulness is to clamp the membrane potential at the equilibrium potential of one of the ions. The contribution of this ion will disappear from the record and the time course of the remaining currents can be studied. A more general method of separating the currents is the ionic substitution method of Hodgkin and Huxley (1952). When one of the permeant ions in the bathing solution such as sodium is replaced by an impermeant ion such as tetramethylammonium, the currents formerly carried by an influx of sodium disappear or are replaced by a small efflux of sodium. The substitution of the

tetramethylammonium ion for the sodium ion has no effect on the potassium or leakage currents of the node, so the difference between the experimental records before and after the substitution yields the time course of the sodium currents. Once the size and shape of the sodium currents are determined, they may be subtracted from the experimental records to permit further study of the remaining currents. The details of these methods are discussed by Hodgkin and Huxley (1952) and by Dodge (1963). In principle the potassium currents can also be derived by substituting an impermeant cation for the potassium in the axoplasm and subtracting the records as in the sodium substitution method.

One important assumption of the substitution method is that only the amplitude of the sodium current changes when the ionic substitution is made. If the time course of the sodium current were changed also, the method would fail. As it happened the sodium substitute used by Hodgkin and Huxley and by Dodge was choline. In choline the potassium currents are not as large as they are in Ringer's solution, an undersirable perturbation that had to be corrected mathematically before the subtraction of currents could yield a true time course of the sodium currents. The reduction of the potassium currents by choline is part of a general class of phenomena to be described in Chapter IV.

The ionic substitution method is the only direct method that can show which ions are carrying the ionic currents and how the componets of current depend on time and voltage, but it suffers from the lengthy calculations and from the need of taking sets of measurements in two different bathing solutions. Dodge (1963) showed that it is possible to obtain an equivalent separation of the ionic currents from measurements taken in only one solution, once the form of the kinetic equations for the conductance changes has been determined by the substitution method. The procedure he developed is simply mathematical curve fitting. It has been used exclusively in the analysis of my experiments. In the following discussion it is

assumed that the capacity current has already been removed from the record. This problem is treated later and in Appendix I.

Given the problem of curve fitting, one can devise many procedures to match solutions of the equations of Fig. 3 to experimental records. Dodge's method fits the parameters a few at a time. First the leakage conductance is calculated from the current flowing in response to a single hyperpolarizing voltage clamp. The leakage current can then be calculated and subtracted from all other voltage clamp records. The resulting curves consist mainly of sodium current at early times and only of potassium current at late times. In general they look like the curves in Fig. 4. Hyperpolarization of a node preceding the voltage clamp test pulse brings about a delay of the turn-on of the potassium conductance explained in the model by the small value of $n_\infty$ at very negative potentials. Fortunately hyperpolarizations beyond -100 mv delay the potassium current enough so that its later time course is not obscured by the presence of sodium currents. Under these conditions it is possible to fit the equation for the potassium current to the late part of the experimental record. The currents predicted by the equation can then be subtracted from all parts of the record leaving the sodium currents and completing the separation of currents.

Dodge found a simple way to fit the potassium current function. He observed that the form of the potassium currents following a strong hyperpolarization (where $n_\infty$ approaches zero) is

$$I_K = A\,[1 - \exp(-t/\tau_n)]^4 \qquad (3.1)$$

where A is the steady-state amplitude of the potassium current. All curves of this form with different values of A and $\tau_n$ are the same but for dilatations in the amplitude and time axes. Thus when the logarithm of the amplitude is plotted against the logarithm of the time all the curves look identical but for a vertical and horizontal displacement. In practice it is convenient to make a template of the logarithm of function 3.1 versus the logarithm of time that can be moved over the "log-log plot" of the experimental records to

obtain the best fit to the middle or late portion of the curves. The position of the template on the graph permits a quick calculation of A and $\tau_n$ for the curve being fit. The sodium currents are then obtained by subtracting the function 3.1 from the currents.

A valuable feature of this mathematical procedure is that it and the classical ion substitution method give the same separation of the current components, i.e., they are equivalent. The experiments in this thesis and many recent papers indicate that a third method of current separation can be used. It yields the same result as the previous two. This is the pharmacological inhibition of the ionic conductances by drugs. In particular the poison tetrodotoxin is a specific inhibitor of the sodium conductance and the cation tetraethylammonium is a specific inhibitor of the potassium conductance.

The separation of the currents in practice

The record for a node in a test solution usually consists of the responses to one hyperpolarizing voltage and to 19 depolarizing voltages. The computer program is designed to extract from these numbers the time constants and amplitude parameters of the model by carrying out almost exactly the procedures outlined by Dodge (1963). It is convenient to summarize how this is done by a block diagram that in itself resembles a computer program (Table III). Before the calculation the computer is told which record is to be analysed and which of the four kinds of graphical display is to be drawn. Indeed, additional displays are also used but are not important for the analysis. The appropriate part of the magnetic tape is found and parts I and II of the analysis are executed (Table III). Part I is done once. It determines the leakage conductance from the response to a hyperpolarizing voltage. Part II is done 19 times and results in a family of 19 curves that must be analysed in some way by the operator. The meaning of each of the statements in Table II will now be defined more precisely.

Table III

OUTLINE OF THE GRAPHICAL ANALYSIS OF EXPERIMENTS

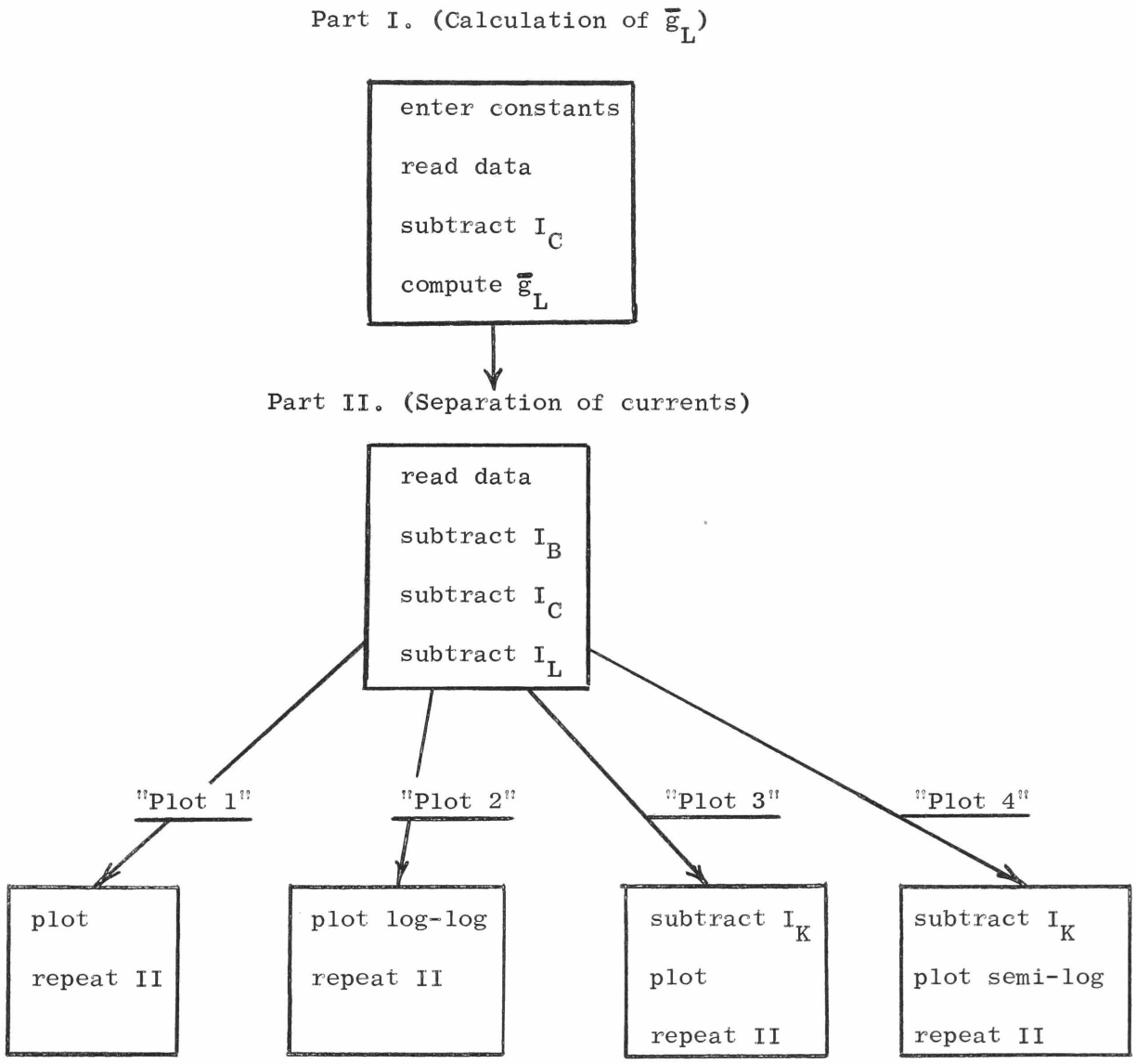

Enter constants: Various numbers are entered into the computer by the typewriter and by the paper tape reader. These initiate the proper program and include whatever adjustable parameters are needed for the execution.

Read data: The list of 100 numbers corresponding to current points, several averages of voltage and of current, and information on the timing of the test pulse are read into memory.

Subtract $I_C$: An exponentially decreasing "extra capacity" current is subtracted from the data. This component described in Appendix I has not been mentioned before. The two adjustable parameters for this current are entered at the beginning of part I. Frequently this subtraction can be skipped because the capacity currents are negligible in many cases.

Compute $\bar{g}_L$: The difference between the current during the hyperpolarizing pulse and the current baseline is divided by the difference between the voltage of the hyperpolarizing pulse and the voltage baseline. This is the value of $\bar{g}_L$ used in part II.

Subtract $I_B$: The average value of the current baseline (determined during the original data recording) is subtracted from every point in memory.

Subtract $I_L$: $I_L$ is defined as the product of $\bar{g}_L$ and the voltage displacement from the baseline. This number is subtracted from the data in memory.

Subtract $I_K$: The function 3.1 is calculated for each point in memory and subtracted from it. The two adjustable parameters for each of the 19 voltages are entered at the beginning of part I.

Plot: The data points in memory (modified by the preceding subtractions) are plotted as a function of time starting at the beginning of the step of voltage and joining the points by straight line segments. The scale factors to be used in this and the following plots can be varied widely. They are entered at the beginning of part I.

Plot log-log: The logarithms of the modified data are plotted against the logarithm of time.

Plot semi-log: The logarithms of the modified data are plotted against time.

The outcome of some of these operations is illustrated in Fig. 11. The upper part of the figure labelled "stored data" shows actual data points as they are stored on magnetic tape. Three traces from the same node are drawn including the end of the 40 msec prepulse. They correspond to a hyperpolarization to -135 mv and to depolarizations to 0 mv and to +75 mv. The dotted line is the current baseline. The vertical arrow indicates the point after which the data were condensed ten-to-one by averaging during the original data recording. The middle and lower parts of Fig. 11 will be discussed in the following paragraphs.

Plot 1 (of Table III) is the family of voltage clamp currents with the leakage current (and the capacity current if necessary) subtracted. The middle part of Fig. 11 and many of the figures in Chapter IV are of this type. Notice that the arrow indicating the beginning of condensed data has moved to the left because the horizontal scale has been adjusted to reproduce the true time course. Either this plot or plot 3 can be used to determine the peak sodium current-voltage relation, the results being nearly identical.

Plot 2 (not illustrated) is the "log-log" plot, referred to earlier, that can be used to determine the amplitude and time constant of the potassium current. The operator must do this manually by matching a template to the middle or late part of the curve (see comments at the end of Appendix II). Note that the steady-state amplitude can be determined this way even if it has not quite been reached on the record. The amplitudes are used in drawing the steady-state current-voltage relation. They are also punched with the time constants $\tau_n$ on paper tape for use in plots 3 and 4.

Plot 3 is the family of sodium currents. The bottom of Fig. 11 and several figures in Chapter IV are of this type. Plot 3 is used

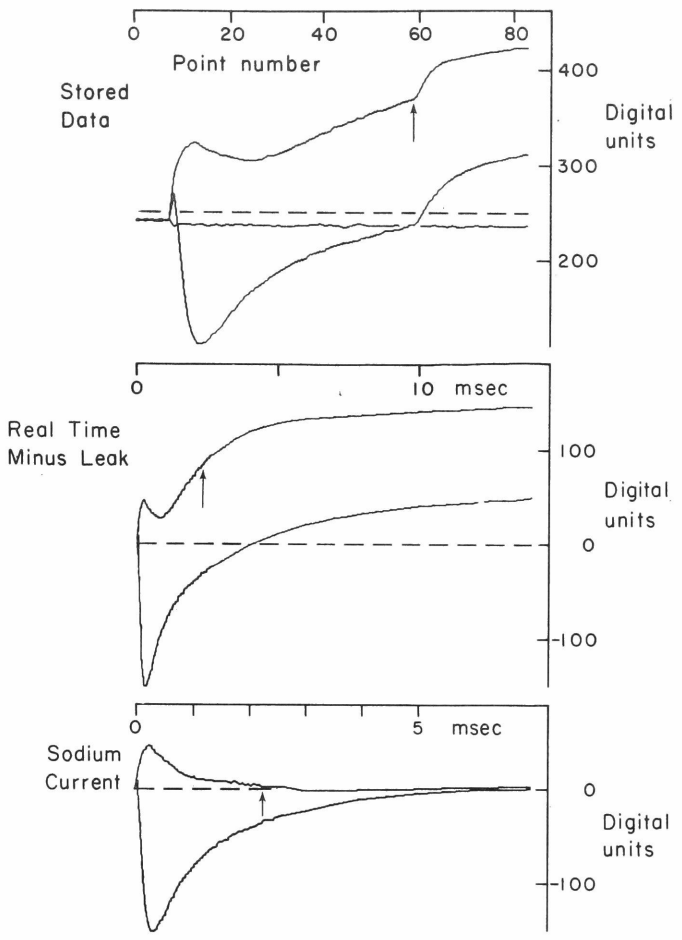


Figure 11. Separation of the currents with the computer. Three stages in the analysis of voltage clamp data. In each frame the currents at 0 mv and at +75 mv (solid lines) and the zero-current baseline (dashed line) have been drawn. The top frame also includes the currents at -135 mv as well as a few points in the beginning from the last 300 μsec of the 40 msec prepulse at -120 mv. The top frame shows the points as stored on the magnetic tape using the digital current scale from 0 to 512 and with a compressed time axis after the arrow. The middle frame shows the currents with the baseline and leakage currents removed and with the time scale linearized. In the bottom frame the potassium currents have been subtracted and the time scale has been expanded to improve the visibility of the sodium currents. The curves used in this figure are from the same experiments as the curves in Fig. 13. T = 13° C.

to verify that the parameters for $I_K$ have been chosen and recorded correctly.

Plot 4 is a semilogarithmic plot of the family of sodium currents. The late part of each sodium current curve falls with a single exponential time constant, $\tau_h$, that is readily determined from the final slope of the curve in plot 4. $\tau_m$ is also determined from this graph. A line is drawn parallel to the linear falling phase of the sodium current but at distance of log (0.5) below it. This line intersects the rising part of the sodium current at the point where the fraction $m^3/m_\infty^3$ equals one half. According to the model $t/\tau_m$ equals 1.58 at this point.

When these four plots have been completed and analysed, the data analysis is finished. In practice this method does not permit a determination of all the constants at each voltage. The sodium currents near $E_{Na}$, for example, are too small to be analysed reliably. Thus the experiments here do not result in a description of the nodal membrane that is as complete as the model discussed earlier; however, it will be seen that the measurements are adequate to reach clear conclusions about the actions of some of the chemical agents that I have studied.

In some experiments, especailly in those executed without chopper stabilization (see Appendix II), it is clear that the membrane potential measuring amplifier was drifting out of balance. Some procedure has to be used to correct for this drift in comparing records taken at different times during an experiment. The sodium equilibrium potential is a stable reference point in myelinated axons because the large internodal volume of axoplasm serves as an ionic reservior that buffers the small ionic changes taking place at the node during an experiment. In unmyelinated fibers the buffering capacity of the axoplasm is not so great and there is a measurable lowering of $E_{Na}$ in an hour's time. With squid axons $E_{Na}$ may decrease by 10 mv in 60 min (Moore and Adelman, 1961). I use $E_{Na}$ as a reference point for comparing records. Frequently this requires shifting the records

about 5 mv to compensate for drift. If there is a question of drift and the measurement of $E_{Na}$ is ambiguous, the records are not used. The values of $E_{Na}$ of most of the nodes described in this thesis are in the range from 38 to 48 mv.

The magnitude of the errors

This section is a brief list of the estimated magnitudes of the errors or more correctly a statement of the reproducibility of the methods for obtaining the empirical constants for a node of Ranvier. It is the reproducibility that is important here because the experiments are always based on the comparison of the properties of the same node in several different solutions.

The basic instrumental limitations are that the analog-to-digital conversion uses 8 bits (a scale from 1 to 256) and that the time points are spaced by 50 μsec. Because of the various averaging techniques I used, the 0.4% uncertainty in the current and voltage points is never a significant limitation. On the other hand, the 50 μsec uncertainty in timing is significant, because with my "analog timing" system the step change of voltage at the beginning of the prepulse could have fallen anywhere in the 50 μsec clock interval (see Appendix III). Had digital timing been available, the step change would have been synchronized to the 50 μsec clock, and part of the difficulty could have been avoided. Because the recorded signal also included noise from the feedback amplifiers, rapidly changing currents such as the rising part of the sodium currents of a node at room temperature could not be resolved successfully.

The calculation of $\bar{g}_L$ is performed automatically by the computer. Different measurements on the same node indicate a reproducibility of better than 2%. The determinations of $\tau_n$ and A (see formula 3.1) are performed manually by moving a template on the log-log plot described earlier. The numbers are noted to an accuracy of 2% and repeated determinations from the same graph are always reproducible to within 5% for potassium currents that are larger than 2 na. The

errors in the parameters of the sodium currents can be larger than those for the potassium and leakage currents. The 50 μsec uncertainty is usually the most significant factor for $\tau_m$. For the smallest observed values of $\tau_m$ (100 μsec) this leads to an uncertainty of 50% and for larger values (400 μsec) and uncertainty of 13%. The value of $\tau_h$ usually cannot be determined to better than 8% because it depends on the value chosen for $\tau_n$ in the current separation. Also it should be noted the potassium current formula (3.1) is not a perfect fit to the actual potassium currents, and therefore after the current separation the "sodium currents" do not fall exactly exponentially. I did not investigate this problem in a systematic way. The measurement of the peak sodium current was reproducible in successive runs to better than 0.5 na.

# Chapter IV

## EXPERIMENTAL RESULTS

My experiments are designed to show how the parameters of the quantitative model of voltage-clamp currents are changed in nodes of Ranvier by treatment with drugs. The puffer fish poison, tetrodotoxin, and the quaternary ammonium ion, tetraethylammonium, are the two most interesting agents used, as their actions are the most specific. Local anesthetics and the calcium ion also produce fairly specific effects.

The selection of the drugs has been guided by published experiments of other investigators. Many of their experiments were on other nerve fibers or bundles of fibers and many were not voltage clamp studies. Thus, while the effects I observe have been expected in large part, they remained to be demonstrated in quantitative experiments. I have attempted to concentrate on agents that show the greatest specificity in their actions, because these can lead to results of some theoretical usefulness. During my work many similar studies have been published, mostly of invertebrate fibers. The conclusions were gratifyingly like mine. In this chapter I present the results of my experiments. Some of my observations have been published (Hille, 1966a and b, 1967a and b). The comparison with the published results of other workers is saved for Chapter V.

In the course of this work I have been impressed by the difference in action between lipid-soluble compounds (neutral and aromatic molecules) and lipid-insoluble compounds (permanently charged molecules). In general the permanently charged molecules produce their effects as soon as they are applied, without causing additional changes on long exposures. They usually may be washed away and the normal responses of the node return. On the other hand the lipid-soluble compounds have irreversible, deletrious effects when they are applied at high concentrations. The irreversible effects increase

with the time of exposure and in extreme cases lead to lysis. Whatever the normal mode of action of these compounds that produces the interesting change in electrical properties, the molecules must also be dissolving in the axolemma and myelin, gradually disrupting the normal structure. Another effect of sublytic concentrations of lipid-soluble compounds is to increase the mechanical fragility of the preparation to the point that the changes of solution frequently ruin the node. Because of the experimental difficulties in dealing with partly irreversible effects and in distinguishing primary from secondary changes, the lipid-soluble molecules are not as useful as I had originally hoped. The first three sections of this chapter deal with the three permanently charged compounds: tetrodotoxin, tetraethylammonium ion and related ions, and calcium ion. The effect of these molecules is easy to determine experimentally. The last two sections deal with lipid-soluble anesthetics and veratrine. The information gained from these latter experiments is not so reliable nor is it so useful from the theoretical point of view.

## Tetrodotoxin

Tetrodotoxin (TTX) is the water soluble toxin found in most tissues of the Japanese puffer fish (Spheroides rubrides and many other members of the same suborder) and in tissues of American west coast salamanders (Taricha torosa and many other members of the same family). The structure of TTX is shown in Fig. 12. It is a remarkable example of evolutionary convergence that such a complicated molecule could have been produced twice by the opportunistic mechanisms of natural selection, and this speaks for the special potency that resides in this structure. Indeed TTX ranks with a different molecule, saxitoxin (also called paralytic shellfish poison and mussel poison), as the most poisonous small molecules known. As the Japanese people consider the puffer fish a great delicacy, special legislation has been adopted to license cooks to prepare it in safe form. Saxitoxin is the cause of deaths when shellfish are eaten during periods of "red tides". The poison is

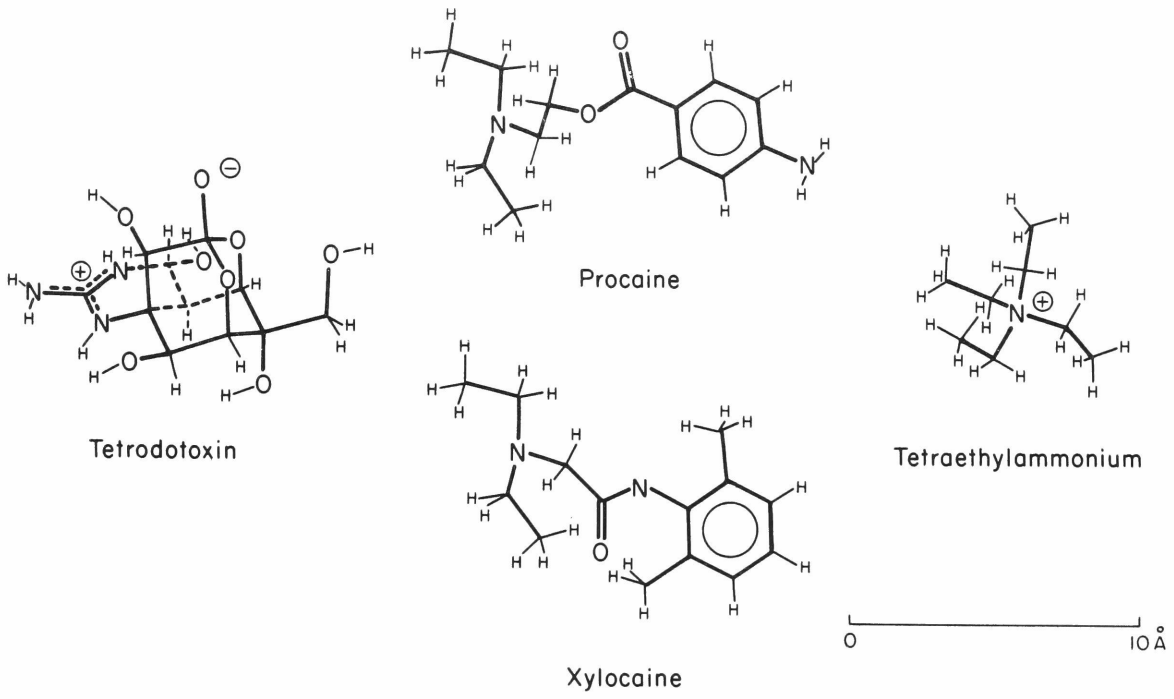


Figure 12. Structure of Drugs. The chemical structures have been drawn in perspective and approximately to scale by tracing photographs of molecular models.

actually produced by certain dinoflagellates, including Gonyaulax catanella, that are filtered out of the water by the shellfish. See Kao, 1966, for a beautiful discussion of the history, natural history, and pharmacology of both of these poisons.

Before I started my experiments it was known that TTX is a neurotoxin, that it is a specific poison of the action potential mechanism, and that it depresses the sodium currents of the excitatory process. The literature has been reviewed by Kao (1966).

The curves in the upper half of Fig. 13 are the voltage clamp currents of a node in Ringer's solution. There are 18 traces, superimposed to the same baseline, corresponding to 18 voltages spaced at 7.5 mv intervals from -52.5 mv to +75.0 mv. As in all the other figures of this chapter, the leakage current has been subtracted. Two of the curves in the family, the ones for 0 mv and the ones for +75 mv, were used in Fig. 11 to illustrate the mathematical separation of currents. It is helpful to compare visually the currents calculated from the model (Fig. 4) with the measured currents of Fig. 13 and with the separated currents illustrated in Fig. 11 to facilitate the identification of the sodium and the potassium components of current. It should be observed that the calculated currents in Fig. 4 correspond to 22° C and therefore change more rapidly than the currents observed at 13° C.

The voltage clamp currents are markedly changed by 300 nM TTX. Comparison of the lower family of curves in Fig. 13 with the calculations in Fig. 4 shows that this concentration of TTX entirely abolishes the sodium currents. In fact, in no case has evidence of sodium currents been found when the concentration of TTX was higher than 10 nM. The blockade prevents the outward flow of sodium ions as well as the normal inward flow. This can be seen more clearly in a preparation with artificially enhanced outward sodium currents. Figure 23 (in the next section) shows the outward sodium currents of a node in which the normal distribution of sodium ions has been reversed. The axoplasm contains nearly isotonic sodium and the

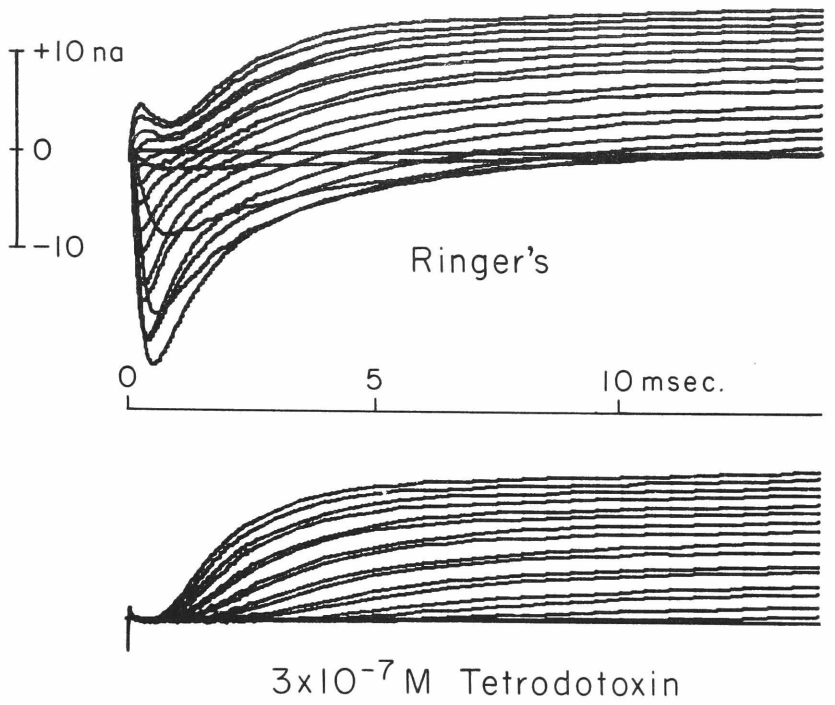


Figure 13. Sodium and potassium currents in TTX. The time courses of the voltage clamp currents minus leakage currents before and during treatment with TTX. The maximum depolarization is to +75 mv. Some of these curves are shown in Fig. 11 also. T = 13° C.

bathing fluid contains none. How this unusual condition was achieved will be discussed later (see "Tetraethylammonium ion and related ions"). The point to be made here is that the expected transient outward sodium currents seen in record 472 are entirely blocked by 10 nM TTX in record 473.

Cations that usually restore conduction to a sodium deprived sciatic nerve, such as lithium, ammonium, or guanidinium ions (see Chapter V) do not restore conduction in the presence of 10 nM TTX. This is because the permeability to these ions is also blocked. Figure 14 is an example of lithium currents in the voltage clamp. The inward lithium currents of record 452 are very similar to the inward sodium currents of record 451 in time course and magnitude. The reversal potential of the early currents is possibly 5 mv less positive in Li-Ringer's than in Na-Ringer's. Like the sodium currents of Fig. 13, the lithium currents are eliminated by 10 nM TTX. Thus TTX simply blocks the voltage-dependent transient permeability of the nerve that is normally associated with sodium currents irrespective of the direction of the expected current flow or of the kind of cation carrying the current.

Partial reduction of sodium currents is found in concentrations of TTX between 0.1 and 10 nM. An example is illustrated in Fig. 15. In this figure the potassium and leakage currents have been a subtracted by the computer, leaving only the sodium currents. They are plotted on two different time bases to facilitate inspection of the fast turn-on and the slower inactivation.

The sodium currents of Fig. 15 can be analyzed to give the time constants $\tau_h$ and $\tau_m$ (Fig. 16, left) and the peak current-voltage relation (Fig. 16, right). The sodium currents turn on in a few hundred microseconds, and the measurements are made only every 50 μsec. The separation between the two lines drawn on the graph of $\tau_m$ (Fig. 16) represents the 50 μsec band of uncertainty attributable to the timing problem. Within the limitations of the method, the time constants $\tau_h$ and $\tau_m$ are <u>not</u> <u>changed</u> by 0.8 nM TTX;

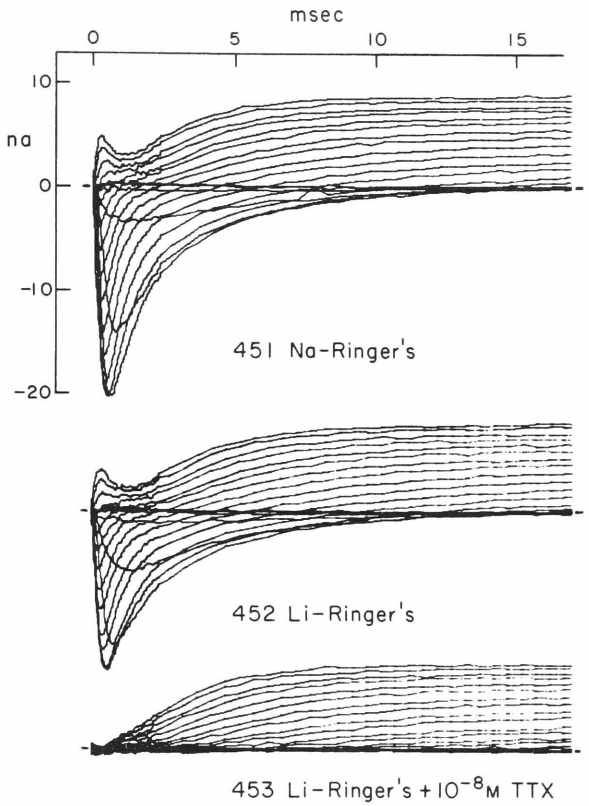


Figure 14. Lithium currents and TTX. The time courses of voltage clamp currents minus leakage currents in lithium and TTX solutions. The maximum depolarization is to +67.5 mv. This node was also used in the experiments illustrated in Figs. 21, 22, 27, and 28. T = 11° C.

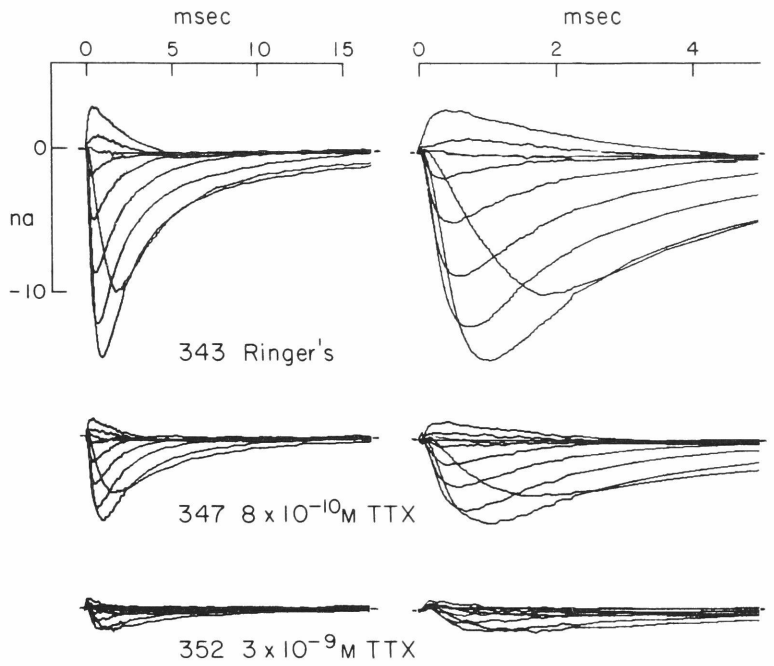


Figure 15. Sodium currents in TTX. The time courses of voltage clamp currents with both the potassium and the leakage currents subtracted mathematically. The sodium currents are drawn at two different time scales on the left and right but with the same vertical scale. The maximum depolarization is to +67.5 mv. T = 2.5° C.

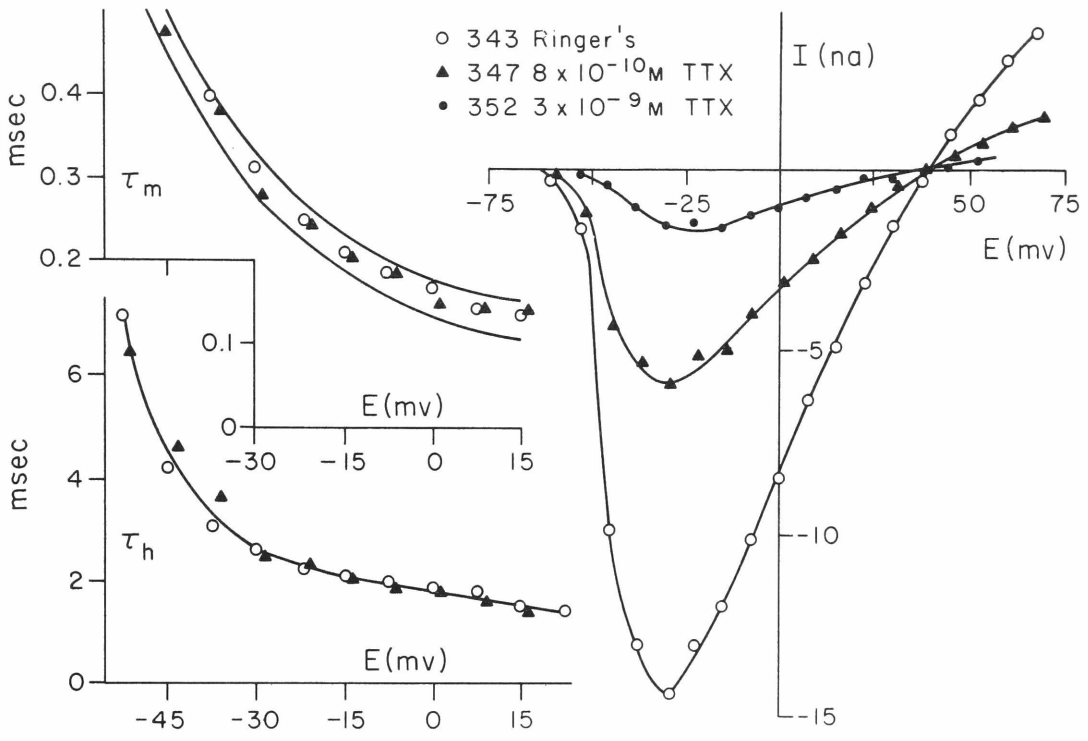


Figure 16. Analysis of sodium currents in TTX. The time constants $\tau_m$ and $\tau_h$ (left) and the peak current-voltage diagram (right) of the sodium currents of Fig. 15. The two lines drawn on the graph of $\tau_m$ indicate the band of uncertainty in the measurement. T = 2.5° C.

however, 0.8 nM and 3 nM TTX reduce the amplitudes of the sodium currents to 40% and to 10% of the normal, respectively. As the same percentage change occurs at all voltages, the effect of TTX can readily be summarized as a reduction of the maximum sodium permeability $\bar{g}_{Na}$. About 0.5 nM TTX reduces $\bar{g}_{Na}$ to one half of its normal value.

TTX also blocks the prolonged sodium currents that appear in veratrine. This phenomenon is described later in this chapter.

The potassium currents are not affected by TTX. Since the sodium currents disappear in these experiments, it is not possible to correct drifting of the membrane potential amplifier by using the sodium equilibrium potential as a reference. However, with chopper stabilization (see Appendix II) and with equilibration of the temperature of all solutions, the potassium currents can be made identical in Ringer's and TTX. Figure 17 is an example of superimposed records of a node in Ringer's (dashed lines) and in 10 nM TTX (solid lines). Observe that the late portions of the current curves for the control and for the TTX-treated node merge and become indistinguishable. It may be helpful to refer to Fig. 19 in which the currents of record 375 have been drawn alone, if the superposition of Fig. 17 causes difficulty in reading the curves.

The first experiment ever to demonstrate that TTX acts specifically to reduce the sodium conductance was done by Narahashi, Deguchi, Urakawa, and Ohkubo (1960). They passed constant currents through a microelectrode into frog muscle fibers, observing that while the spike (action potential) mechanism is inhibited by TTX, delayed rectification still takes place. It was instructive, and of historical interest, to repeat this observation on the node of Ranvier using the current clamp mode (see Chapter III). The results of this experiment are shown in the upper half of Fig. 18. The superimposed traces are the time courses of the membrane potential for different steps of intensity of a depolarizing current with the potential starting from a hyperpolarized value. The dotted line is

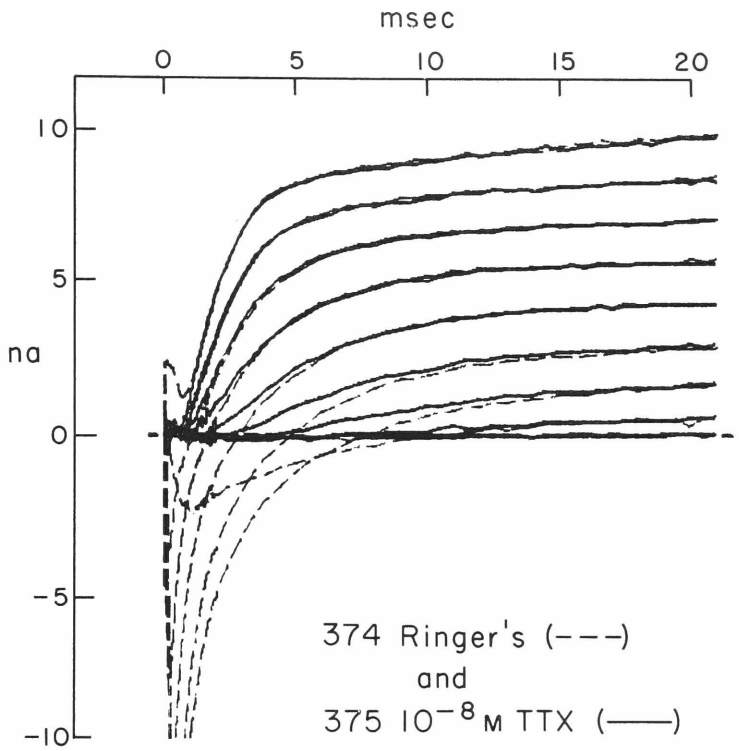


Figure 17. Potassium currents in TTX. The superimposed voltage clamp currents minus leakage currents of a node before and during treatment with $10^{-8}$ M TTX. The maximum inward sodium current in the Ringer's solution is about -17 na, but the records are truncated at 10 na in this figure. The maximum depolarization is to +67.5 mv. Further experiments with this node are shown in Fig. 19. T = 17° C.

the baseline at -75 mv. Small currents produce a simple exponential rise to a steady-state, reflecting the "passive" response of the leakage conductance and the membrane capacitance. The exponential time constant is about 0.2 msec which corresponds to a capacitance of 5 pF in pool A, assuming that the resting resistance is 40 megohm. Stronger currents depolarize enough to activate the delayed rectification. As the potassium conductance increases with time, the membrane resistance decreases and the voltage response to the constant current falls again. These records reproduce in every respect the observations of Narahashi et al. Before TTX was applied this node gave a 1.5 msec action potential with a threshold at -50 mv. The lower half of Fig. 18 is the expectation calculated from the membrane model using the standard parameters except that $\bar{g}_{Na}$ is set equal to zero to imitate the effect of TTX, the membrane capacity is 4 pF, and the rate constants have been scaled to 12° C assuming a temperature coefficient ($Q_{10}$) of 3.0 (Frankenhaeuser and Moore, 1963). The experiment and the model give similar results except that the measured curves cross briefly. Undoubtedly a closer correspondence between theory and experiment would be obtained by basing the calculations on measured voltage clamp parameters of the node studied rather than on the node of the model.

The leakage current of nodes treated with TTX is also untouched. If the normal leakage conductances is called 100, the mean conductance in 15 measurements on 9 different nodes in TTX is 99.5 ± 5.5 (mean ± S.D.).

TTX is thus a highly specific poison of the voltage-dependent sodium carrying system of the frog node. It blocks all the ionic movements whether inward or outward that are mediated by this system. The effect of TTX appears as rapidly as the solution can be changed (about one second) and does not intensify with time thereafter. It is at times completely reversible in a few seconds and on other occasions at least 50% reversible in seconds with slow further recovery over several minutes. TTX probably acts by binding

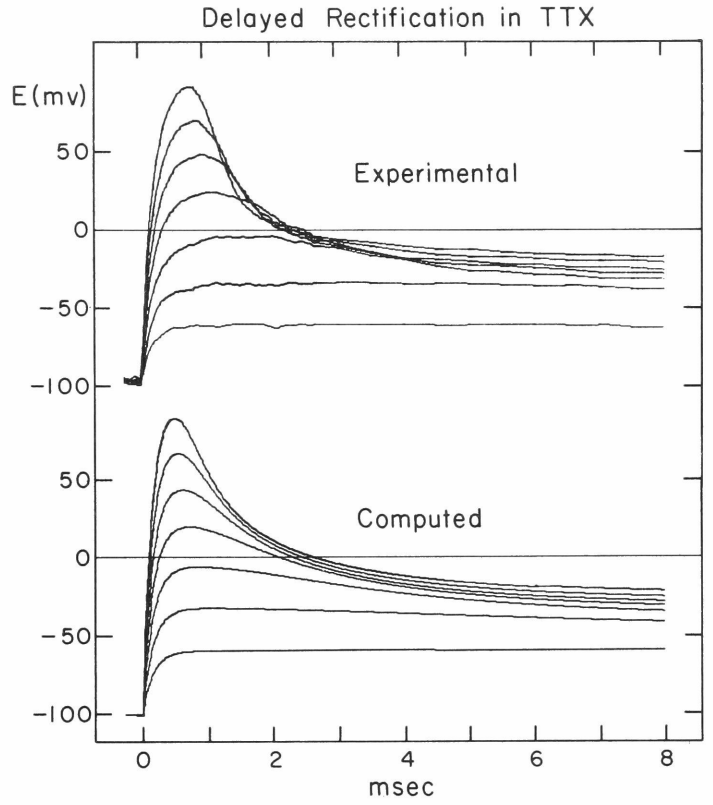


Figure 18. Delayed rectification in TTX. The time courses of the membrane potential in a current clamp experiment on a node in 100 nM TTX at 12° C (upper) and in a computer simulation (lower) using the standard mathematical model (Fig. 3) modified in three ways: $\bar{g}_{Na} = 0$, $C_M = 4pF$, and $\alpha_n$ and $\beta_n$ divided by three. The last change imitates the effect of cooling ten degrees from the standard 22° C to 12° C. For the computation, the model was first hyperpolarized for a long time by a -0.7 na current and then depolarized by currents ranging from +0.35 na to +4.55 na in 0.7 na steps. See Appendix III for method of calculation.

reversibly to some substance on the axon membrane that is easily accessible from the bathing medium. It is convenient to use the term TTX receptor to refer to this membrane component.

The structure of TTX drawn in Fig. 12 indicates a negative charge on the hemilactal oxygen and a positive charge on the quanidinium group. In fact the pKa's of these two groups are about 8.7 and 12.5 (Goto et al., 1965; Woodward, 1964), so that at pH 7.3 less than 2% of the TTX molecules have the indicated structure and the remainder lack the negative charge. The pH dependence of the blocking action of TTX could be studied to determine whether the cation, the zwitterion, or both are the active forms. This information should be useful in determining whether TTX and other anesthetic drugs share the same receptor.

## Tetraethylammonium Ion and Related Ions

The tetraethylammonium (TEA) ion is a non-biological, water soluble substance of unusual interest to neurophysiologists. Its many actions seem to center in two fundamentally different biological processes. On the one hand, as a quaternary ammonium ion, TEA can mimic natural chemical transmitter agents or their precursors. In these cases the TEA ion will excite or block synaptic activity or interfere with enzymes which transport, synthesize, and destroy transmitters or their precursors. The principle medical use of TEA has, indeed, been as a sympathetic ganglion blocking agent. Many references to these phenomena can be found in Raventós (1937), Schmidt (1965), and Grundfest (1961). The other action of TEA is a direct modification of the normal voltage-dependent permeability changes of nerve and muscle membranes manifested as prolonged action potentials (Loeb and Ewald, 1916; Cowan and Walter, 1937; Schmidt, 1965). In some cases the prolongation is known to be caused by a depression of the potassium conductance. This is the phenomenon I studied.

The voltage-dependent potassium carrying system is most conveniently studied in the absence of the transient sodium currents seen in normal nerves. Tetrodotoxin (TTX) achieves this condition. Figure 19 shows the time courses of the voltage clamp currents minus leakage currents of a node in $10^{-8}$ M TTX. As the leakage current is removed mathematically and the sodium current pharmacologically, the tracings represent potassium current alone. The five families of curves at increasing concentrations of TEA show a progressive abolition of the outward potassium current. Fig. 20 illustrates the analysis of these curves into the time constant $\tau_n$ (left) and the steady-state current-voltage relation (right) and demonstrates that the primary effect of TEA is to reduce the amplitude of the potassium currents without affecting the time constants of the changes of the potassium conductance. Because the amplitude is reduced by the same proportion at all voltages, the effect can be described as a reduction of the maximum potassium conductance, $\bar{g}_K$.

Similar results are obtained in the absence of TTX. Figure 21 shows the time course of the voltage clamp current minus leakage current of a node in Ringer's. Both early sodium currents and late potassium currents are present. As TEA is added to the Ringer's solution (records 443 and 444 of Fig. 21) the potassium currents are reduced. As in the previous experiment the steady-state current-voltage relations, given by the dotted lines of the right hand side of Fig. 22, show a uniform proportional reduction of the potassium currents at all voltages while the time constants $\tau_n$ (not illustrated) are unchanged. Again the effect is a reduction of $\bar{g}_K$.

If TEA reduces $\bar{g}_K$ in a simple manner, inward as well as outward potassium currents should decrease. This can be tested in two ways. When a normal node is hyperpolarized after a long depolarization there is a brief "tail" of inward potassium current during the return of the potassium carrying system from a high conductance state to a low conductance state. This tail is eliminated by TEA. Much larger inward potassium currents can be produced in isotonic KCl solutions.

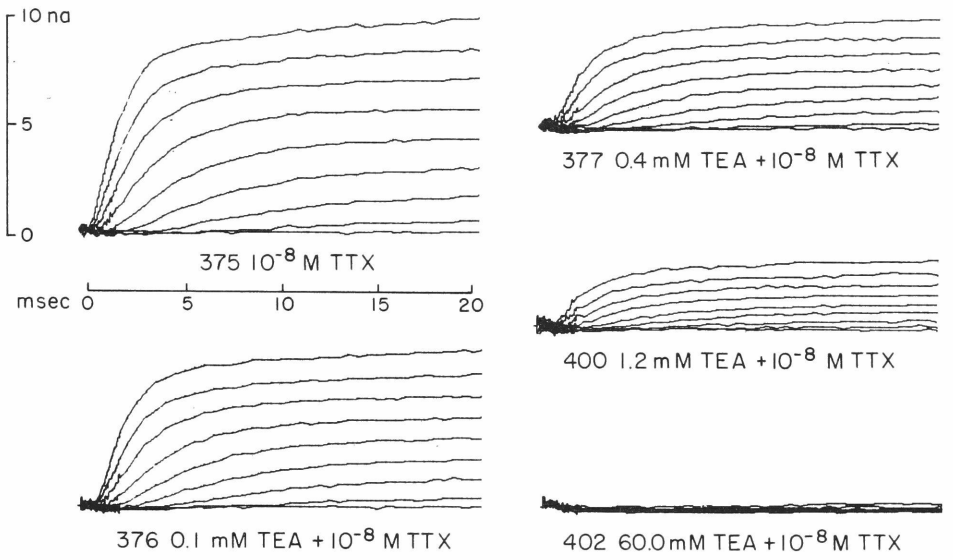


Figure 19. Potassium currents in TEA. The voltage clamp currents minus leakage currents of a node in TTX-containing solutions with increasing concentrations of TEA. The maximum depolarization is to +60 mv. Other experiments with this node are illustrated in Fig. 17. T = 17° C.

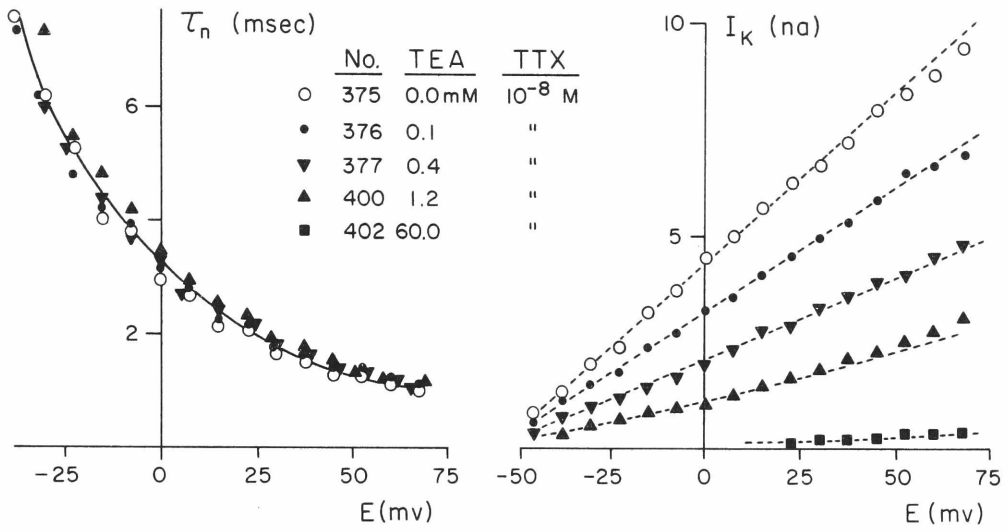


Figure 20. Analysis of potassium currents in TEA. The time constants $\tau_n$ (left) and steady-state current-voltage relation (right) of the potassium currents illustrated in Fig. 19 T = 17° C.

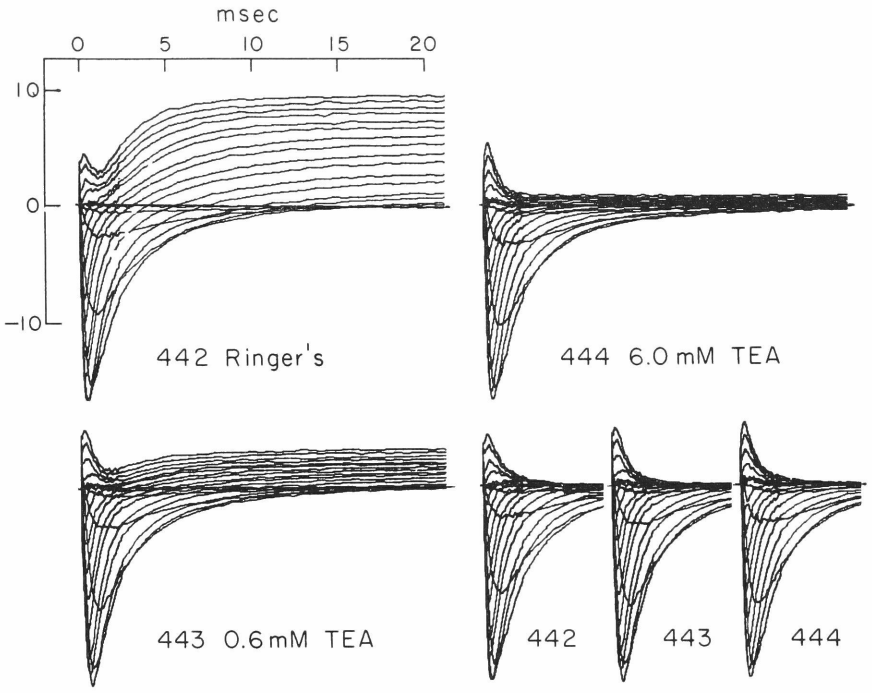


Figure 21. Sodium and potassium currents in TEA. The voltage clamp currents minus leakage currents in TEA. The maximum depolarization is to +67.5 mv. This node was also used for experiments illustrated in Figs. 14, 22, 27, and 28. T = 11° C.

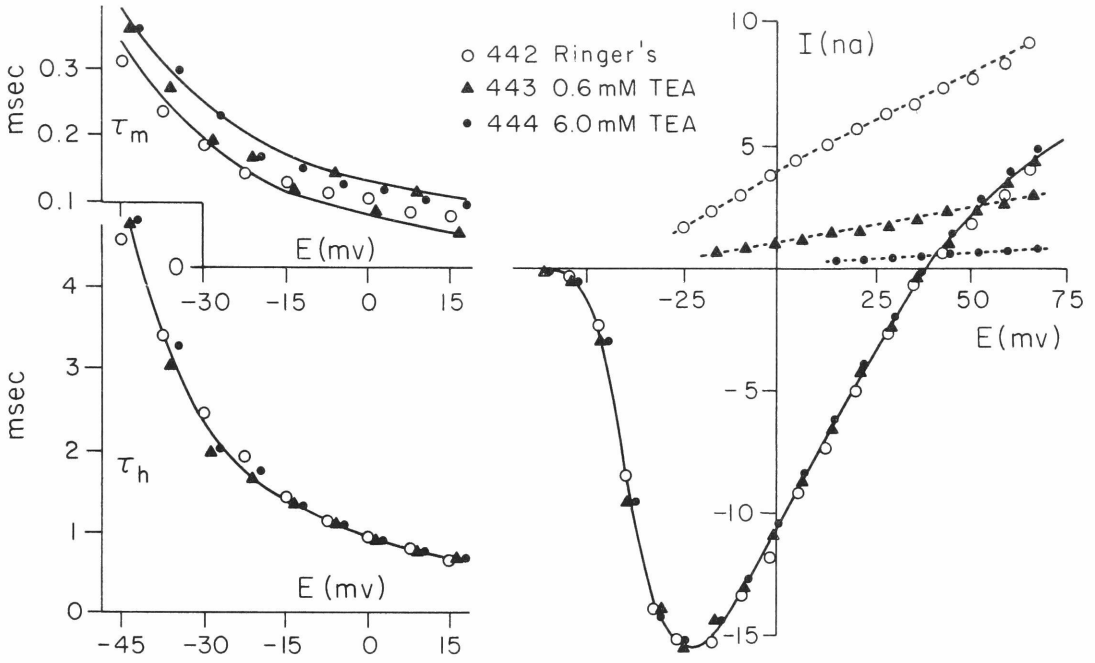


Figure 22. Analysis of the sodium currents in TEA. The time constants $\tau_m$ and $\tau_h$ (left) and current-voltage relations (right) from the experiment illustrated in Fig. 21. The two solid lines in the graph of $\tau_m$ define the band of uncertainty attributable to the non-synchronous timing used in the experiment. In the current-voltage diagram the solid line connects the points of the peak sodium current-voltage relation and the dashed lines the steady-state potassium current-voltage relation. T = 11° C.

Frankenhaeuser (1962) showed that with Xenopus nodes held at about -75 mv in high KCl, small depolarizations give rise to delayed inward potassium currents and depolarization beyond 0 mv give delayed outward potassium currents. On repolarization to -75 mv from any depolarization, there is a large "tail" of inward potassium current. Rana nodes exhibit all of these potassium currents in 115 mM KCl and all of them are abolished by 12 mM TEA. Thus the action of TEA is adequately represented as a simple reduction of $\bar{g}_K$ for both inward and outward currents.

The experiment of Figs. 21 and 22 also illustrates the insensitivity of the sodium permeability system to TEA. The three short records in the lower right hand side of Fig. 21 are from the same data as the three longer records in the figure but the potassium current has been subtracted mathematically. Thus these are sodium currents. They seem indistinguishable. The sodium currents are analyzed in Fig. 22. On the right hand side the solid line indicates the points of the peak current-voltage relation. On the left hand side are the time constants $\tau_m$ and $\tau_h$ of those currents that are large enough to permit measurement. The band of uncertainty in $\tau_m$ is fairly significant at 11° C. This experiment shows that within the uncertainty of the measurements there is no change of $\tau_m$, of $\tau_h$, or of the peak current-voltage relation attributable to TEA. This conclusion has been verified at concentration of TEA up to 60 mM in normal nodes. At 60 mM TEA the voltage dependence of the steady-state sodium inactivation (or $1-h_\infty$) is unchanged.

It seemed desirable to look for effects of higher concentrations of TEA on the sodium current, but in an isotonic TEA solution there is no sodium, so the sodium currents would be outward and very small unless the axoplasm were loaded with sodium. The nodal axoplasm can be loaded with ions by temporarily breaking down the diffusion barrier by a strong electric shock (i.e., a hyperpolarization to -220 mv). The resistance recovers, often completely, over a period

of a few seconds after the shock. If the shock is given in Ringer's solution, the sodium equilibrium potential is greatly reduced, outward sodium currents become large, and the potassium currents virtually disappear. After such treatment the potassium permeability system is permanently damaged, being unable to produce delayed inward currents in isotonic KCl, but the sodium system seems normal except for the unusual equilibrium potential, attributable to the high internal sodium concentration.

Figure 23 shows the time course of the voltage clamp currents minus leakage current (left) and the peak current-voltage diagram (right) of a node after several strong hyperpolarizing shocks. The curves represent sodium current alone because the damaged node has no potassium current. In normal Ringer's there are both inward and outward sodium currents with an equilibrium potential near 0 mv suggesting that the axoplasm contains nearly 110 mM sodium after loading. In 110 mM TEA there are almost no inward currents, but there are outward currents above -25 mv. At large depolarizations the outward currents are nearly identical in amplitude and in time course in Ringer's and in 110 mM TEA. The arrows on records 471 and 472 indicate the value of $\tau_h$ at +67.5 mv in Ringer's and TEA. It is essentially unchanged. Therefore nearly isotonic TEA is unable to produce a measurable change in the sodium carrying system. The third set of curves in Fig. 23 (record 473) shows that TTX abolishes all of the outward sodium currents in isotonic TEA.

The leakage conductance is not changed by 60 mM TEA. In the experiment illustrated in Figs. 19 and 20 the leakage conductances in the four concentrations of TEA are 97, 98, 100, and 100 relative to a control value of 100. The small variation is within the reproducability of such a measurement. However in 110 mM TEA three different nodes gave relative conductances of 60, 63, and 65.

TEA is an extremely stable compound in solution. There are no enzymes that can change its structure readily. Furthermore it is permanently charged and therefore will not pass readily through cell

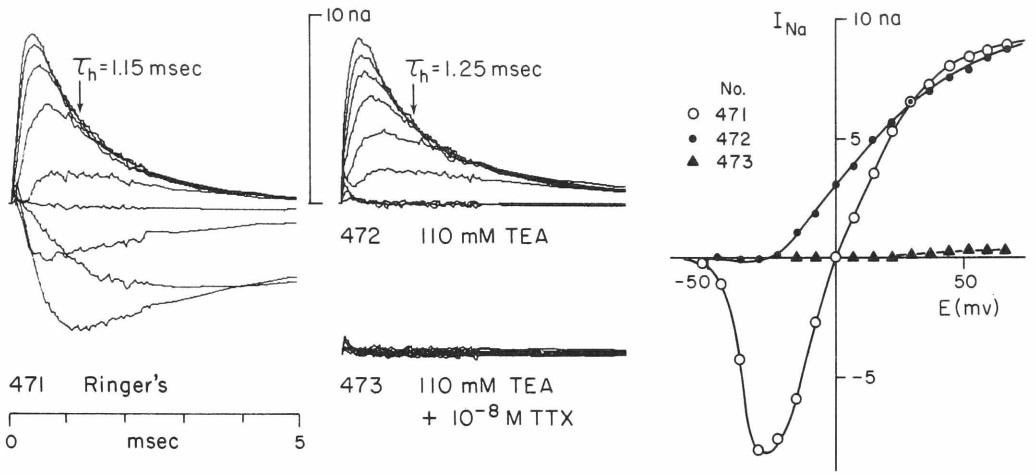


Figure 23. Sodium currents in isotonic TEA. The early part of the voltage clamp currents (left and center) and the peak current-voltage relations (right) of a node that has been loaded with sodium by the strong shock technique described in the text. The arrows labelled $\tau_h$ indicate the value of the time constant of the sodium inactivation process at the highest depolarization, +67.5 mv. T = 4° C.

membranes. For example, in experiments with human red blood cells and the tetramethylammonium ion (TMA) Askari (1966) found that the rate of entry was less than 0.2 mmoles (liter cells)$^{-1}$ hr$^{-1}$ from a 120 mM solution of TMA. Thus even with the large surface to volume ratio of a red blood cell, the half-time for equilibration would be many hundreds of hours. The block of $\bar{g}_K$ by TEA, on the other hand, appears as rapidly as the solution can be changed and is readily reversible in seconds, even after the node has been exposed to 10 mM TEA for one hour. Thus TEA interacts rapidly and reversibly with some component of the axon membrane that is easily accessible from the outside. This component can be called the TEA receptor.

One property of receptors is that they exhibit adsorption isotherms characterized by binding constants and saturation phenomena. These can be seen in dose-response studies. Figure 24 shows the relative potassium permeability as a function of the TEA concentration. The circles are individual experimental measurements from eleven different nodes. The line is the standard "rectangular hyperbola" that describes the simplest kind of receptor interaction commonly found. The assumption for drawing this line are:

1) There are many receptors on the membrane.

2) One TEA binds to one receptor reversibly.

3) The receptor-TEA complex has a dissociation constant of 0.4 mM.

4) $\bar{g}_K$ is proportional to the number of unoccupied receptors.

The filled circles are from the experiment discussed earlier and shown in Figs. 19 and 20 in which the sodium currents were abolished by 10 nM TTX. These filled circles fall near enough to the open circles to show that TTX does not affect the binding of TEA. More simply it can be said that the TEA receptor and the TTX receptor are <u>different</u> components of the membrane. Experiments will be discussed later that show that the TEA receptor is also different from the calcium receptor.

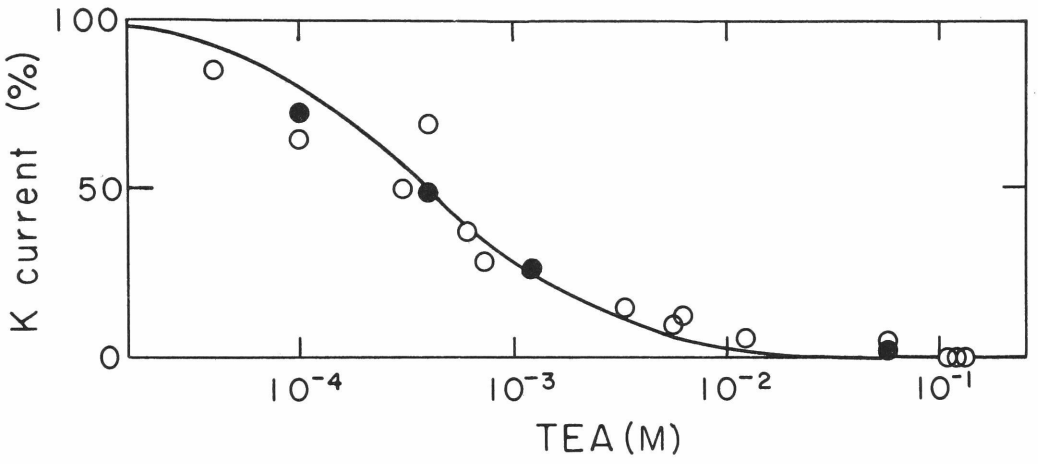


Figure 24. Dosage-response to TEA. The relative amplitudes of the potassium current (or of $\bar{g}_K$) as a function of the TEA concentration in the external solution. The filled circles are from the experiment in Figs. 19 and 20 in which the sodium currents had been eliminated by TTX. The open circles are from ten other nodes not treated with TTX. The solid line is the dose-response relationship of a hypothetical system in which one TEA ion binds reversibly to a receptor to produce a fraction of the inhibitory effect. The curve is identical with a simple adsorption isotherm of "rectangular hyperbola".

Another property of receptors is specificity. There are many quaternary ammonium ions very similar to TEA in size and shape. Some of these also depress $\bar{g}_K$, and it is possible to measure the apparent constant ($K_i$) by finding the concentration required for half maximal inhibition. Table IV is a list of quaternary ammonium ions and the estimated values of $K_i$. The dose-response behavior of these compounds has not been investigated in detail. $K_i$ is determined by finding one concentration giving more than 50% inhibition and one giving less and interpolating using the rectangular hyperbola. Values of $K_i$ above 120 mM (isotonic) are extrapolations from measurements at 115 mM. TEA has the greatest affinity for the receptor of all the quaternary ammonium ions tried. Addition or subtraction of single methyl groups decreases the binding considerably. The same kind of structure-activity relationship is seen in the series of ions related to choline (with the hydroxyethyl group). Isotonic choline depresses $\bar{g}_K$ to 75% of normal, but as the methyl groups are replaced by ethyl groups, the binding increases. It seems again that the more the structure resembles TEA the better the binding. The depression of potassium currents by choline has been seen by other investigators who used choline to achieve a separation of the ionic currents (see Chapter III). Dodge (1963) showed that $\bar{g}_K$ was reduced without any change in $\tau_n$.

Quaternary ammonium ions might themselves carry current through the membrane. It is already known that $NH_4$ ions carry current about one fourth as well as sodium ions in Rana nodes (Dodge, 1963). When care is taken to rinse away the external sodium from a normal node, there are no inward currents in 110 mM TEA or in 110 mM tetramethylammonium ion (TMA), and above -25 mv there are definite outward sodium currents of normal kinetics. These observations show that these quaternary ions are at least twenty times poorer current carriers than sodium ions. Indeed none of the ions of Table IV shows evidence of carrying current or of affecting the normal sodium current kinetics.

Table IV

QUATERNARY AMMONIUM IONS THAT BLOCK POTASSIUM CURRENTS

| Substituents on N | $K_i$ |
|---|---|
| 4Me | 500 mM |
| 3Me 1Et | 300 |
| 2Me 2Et | 60 |
| 1Me 3Et | 15 |
| 4Et | 0.4 |
| 3Et 1n-Pr | 2 |
| 4n-Pr | 60 |
| 4n-Bu | 60 |
| 3Me 1EtOH | 240 |
| 2Me 1Et 1EtOH | 30 |
| 3Et 1EtOH | 10 |

The ions are identified by the number of methyl, ethyl, hydroxyethyl, n-propyl, and n-butyl groups that are joined to the central nitrogen atom.

## Calcium

The calcium ion is an essential component of any physiological solution. The complete absence of calcium leads to electrical inexcitability in nerves and to the cessation of a spectrum of processes related to membrane irritability in non-nervous cells. On the other hand, low calcium leads to hyperexcitability and high calcium to depressed excitability in most nerves. This literature has been reviewed by Brink (1954). Voltage-clamp experiments by Frankenhaeuser and Hodgkin (1957) and by other authors more recently (see Chapter V) showed that the primary action of calcium is to shift the voltage-dependence of the parameters m, n, and h along the voltage axis. Thus in low calcium a small depolarization and in high calcium a large depolarization would be needed to elicit the same permeability changes. These shifts account for the increase of threshold found on increasing the calcium concentration. Although the effects of raising the calcium concentration can be loosely described as equivalent to the effects of hyperpolarization, it should be borne in mind that there is in fact only a slight change if any in the measured membrane potential.

A convenient index of shifts can be calculated from the peak (sodium) current-voltage relation. The sodium current is given by (see Fig. 3)

$$I_{Na} = m^3 h \bar{g}_{Na,O\ mv} \left(1 - \frac{E}{183}\right) (E - E_{Na}) \qquad (4.1)$$

and

$$m^3 h \bar{g}_{Na,O\ mv} = I_{Na} / \left[\left(1 - \frac{E}{183}\right) (E - E_{Na})\right] \qquad (4.2)$$

Expression 4.2 evaluated at the peak of the sodium current will be called the peak sodium conductance.

Figure 25 is a semi-logarithmic plot of the peak sodium conductance versus voltage of a node in solutions containing different concentrations of calcium. The lines are derived as follows. First

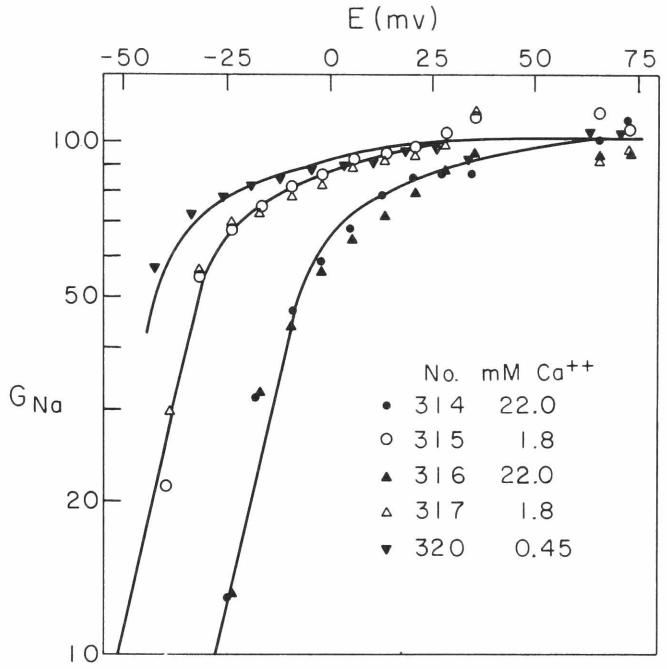


Figure 25. Peak sodium conductance and calcium. The peak sodium conductance as a function of voltage for a node in various concentrations of calcium. All points are plotted on the same conductance scale with 100 units corresponding approximately to 0.40 μmho. The value of $\bar{g}_{Na}$ for this node is then about twice as large or 0.80 μmho.

a smooth curve is drawn through the experimental points for records 315 and 317 (1.8 mM Ca). This same curve is then copied and fitted to records 314 and 316 (high calcium) and to record 320 (low calcium). The best fit is obtained by sliding the curve 24 mv to the right in the 22 mM Ca case and 11 mv to the left for 0.45 mM Ca. It is not necessary to slide the curve vertically and therefore in this experiment $\bar{g}_{Na}$ is not affected by the calcium concentration. However, the fit of the shifted curve to the points is imperfect suggesting that there is a more complex change than a simple shift. I did not investigate these complications. The reproducibility of the points shows that the effects of calcium are readily reversible. Note that the high calcium solutions are hypertonic and contain the normal amount of sodium. In this way the effects of sodium concentration changes on $\bar{g}_{Na}$ are avoided.

The convention for describing the effects of calcium - started perhaps by Frankenhaeuser and Hodgkin (1957) - has been to speak of a certain number of millivolts shift along the voltage axis per tenfold or per e-fold change in calcium concentration. This could be in analogy with the Nernst equation for a "calcium electrode" which specifies a 28 mv potential change per tenfold concentration change (at 10° C). The possible meaning of this relationship will be discussed in Chapter V. The shifts in the peak sodium conductance relation seen in four different nodes are summarized in Fig. 26. The points are the experimental results in solutions ranging from 0.45 mM to 22.0 mM calcium. The two lines have a slope of 20 mv per tenfold change or 8.7 mv per e-fold change and are separated by 3 mv, the estimated uncertainty of the measurement. The data seem to satisfy the logarithmic relationship except at the lowest calcium concentration. I do not know whether several more washes in the low calcium solution would give the larger shifts expected by the logarithmic relationship. In three experiments $\bar{g}_{Na}$ is not affected; however, in the fourth, $\bar{g}_{Na}$ is decreased by about 35% in 12 mM Ca.

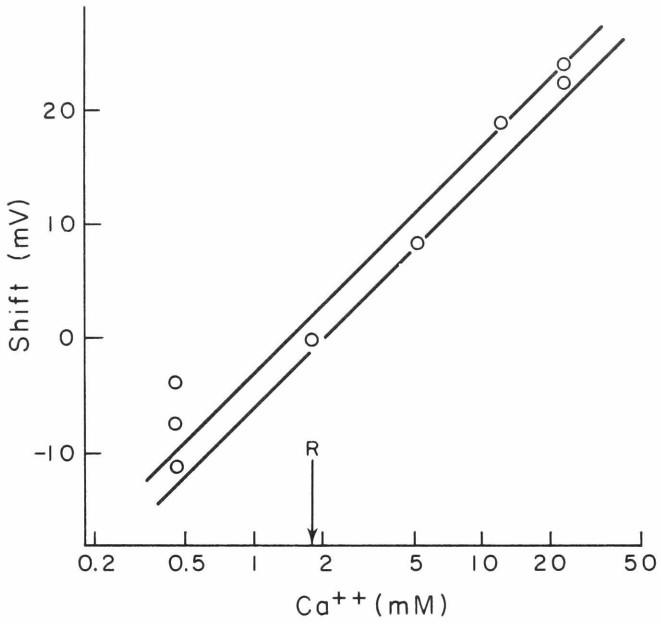


Figure 26. Voltage shifts and calcium concentration. The shifts of the peak sodium conductance relation along the voltage axis in solutions with various calcium concentrations. Please recall that raising the calcium causes the relation to shift in the direction of depolarization so that the node, whose resting potential is relatively unaffected, behaves as though it were hyperpolarized. The concentration of calcium in normal Ringer's solution (1.8 mM) has been indicated by the arrow labelled R. The value of the voltage shift at this point has arbitrarily been set at zero. The two straight lines have a slope of 8.7 mv per e-fold change of calcium concentration and a separation of 3 mv, the estimated uncertainty. The data are taken from four different nodes.

The voltage-shifts of the curves of the relations between $\tau_m$ and voltage and between $\tau_h$ and voltage are almost exactly equal to the shifts of the peak sodium conductance relation in all my experiments. The left side of Fig. 27 is an example of a 20 mv shift of the curve of $\tau_h$ in an 11-fold increase in calcium concentration. This corresponds to a shift of 8.4 mv per e-fold change. Notice that the displaced line fits the observations quite well. The line drawn for record 444 is in fact a theoretical line obtained directly from the model of the "standard" node with the one assumption that an 11° cooling from 22° C to 11° C lengthens $\tau_h$ by a factor of three, i.e. an assumed $Q_{10}$ of 2.9, exactly equal to the measured value of 2.9 (Frankenhaeuser and Moore, 1963a). The curve of $\tau_m$ was shifted by 22 mv in this experiment.

The results of a single experiment on steady-state sodium inactivation indicate a 14.5 mv shift of the curve of $h_\infty$ towards more negative potentials for a 12-fold increase in calcium concentration, i.e. there is less inactivation at the resting potential in elevated calcium concentrations. This corresponds to a 6 mv shift for an e-fold change, slightly less than the shifts for peak sodium conductance, $\tau_h$, or $\tau_m$.

In my experiments calcium concentration changes affect the potassium permeability system much less than the sodium system. Usually there is no effect whatsoever on $\tau_n$. The right side of Fig. 27 shows $\tau_n$ before, during, and after an 11-fold increase in calcium. Again the line on this side of the figure, like the line on the left side, is taken from the "standard" node assuming a $Q_{10}$ of 2.9, compared with the measured value of 3.0 (Frankenhaeuser and Moore, 1963a). Notice for the node in Fig. 27 that the process underlying $\tau_h$ can be affected by calcium changes without affecting the process underlying $\tau_n$. This point will be referred to in Chapter V. Because in published experiments on other nerves, increases in the calcium concentration are always accompanied by a positive shift of the curve of $\tau_n$, the lack of a shift in my

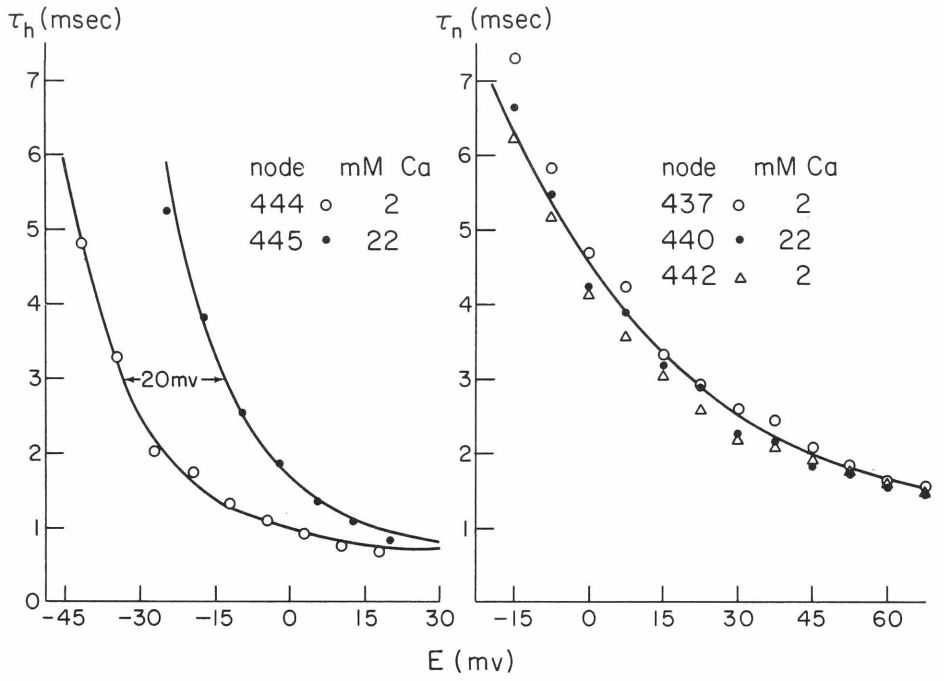


Figure 27. Calcium and the time constants. The time constants $\tau_h$ (left) and $\tau_n$ (right) of a node in normal and in high calcium solutions. The line drawn for $\tau_h$ of record 445 is the same as the line for record 444 but displaced 20 mv along the voltage axis. The lines for record 444 and for all the $\tau_n$ points are both taken directly from the theoretical "standard" node assuming a 3-fold increase in the time constants at 11° C compared to the standard 22° C. The solutions bathing the node in records 444 and 445 contain 6 mM TEA. Other experiments with this node are shown in Figs. 14, 21, 22, and 28. T = 11° C.

experiment is an unexpected finding. Of four nodes each bathed twice in 22 mM calcium and three times in Ringer's solution, three show no shift of the curve of $\tau_n$ and one shows a shift of 13 mv. One of the nodes with no shift also shows no shift on two exposures to 22 mM calcium containing 10 nM TTX as well. This last treatment checks against the possibility of improper separation of the sodium and potassium currents using the mathematical curve fitting method. In two nodes each exposed twice to 0.45 mM calcium there is also no shift of the curve of $\tau_n$. In none of the measurements with different calcium levels is $\bar{g}_K$ changed.

There is no interaction between the actions of TEA and of calcium. The current-voltage diagram of a node exposed to high calcium and to TEA, separately and in combination, is shown in Fig. 28. Data from this experiment have already been given in Figs. 21, 22, and 27. It may be helpful to refer to the idealized current-voltage relationship in Fig. 7 and to the peak sodium conductance relation in Fig. 25 to understand this figure. The solid lines connect the points of the peak current-voltage relationship and the dashed lines, the points of the steady-state relationship. All the open symbols are from measurements in normal Ringer's solution. Notice how reproducible these measurements are. When 6 mM TEA is applied (solid circles), the sodium currents are unchanged and the potassium currents are depressed. When 22 mM Ca is applied alone (inverted solid triangles), the potassium currents are of normal size, but the sodium currents show a 22.5 mv shift in the peak conductance relation. TEA added in the presence of elevated calcium (solid triangles) depresses the potassium currents as before and exerts no further change on the sodium currents. Thus the TEA receptor and the calcium receptor are different structures without interaction.

In summary the curves of the empirical constants for the sodium permeability mechanism ($m_\infty$, $h_\infty$, $\tau_m$, and $\tau_h$) are always shifted along the voltage axis by changes in the calcium concentration,

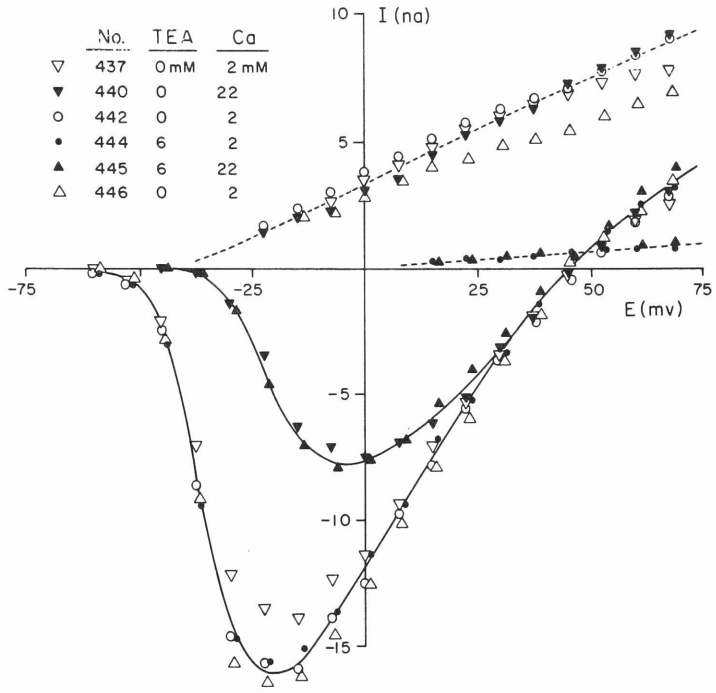


Figure 28. TEA and calcium. The peak (solid lines) and steady-state (dashed lines) current-voltage relations of a node in solutions containing TEA and calcium. It can be seen that TEA and calcium exert their effects independently. Other experiments with this node are shown in Figs. 14, 21, 22, and 27. T = 11° C.

The shift is proportional to the logarithm of the concentration change and amounts to about +8.5 mv per e-fold increase in calcium. In contrast, the potassium permeability changes are entirely unaffected by changes in calcium in most cases. The ability of TEA to inhibit the potassium conductance changes is also unaffected by the calcium level.

## Lipid-soluble anesthetic agents

Anesthetics depress electrical activity in the nervous system. Some depolarize nerves, e.g. ether, which in itself is sufficient reason for loss of excitability, and others block without depolarization.

### Local anesthetics

Local anesthetics are an incompletely defined group of compounds that can be used to produce sensory and motor paralysis locally in any part of the body. They anesthetize nerves because they block the sodium conductance changes of excitation. They do not depolarize. Shanes (1958, 1963) reviews many classical pharmacological studies that demonstrate (1) a summation of the effects of local anesthetics and treatments which decrease sodium currents: low external sodium, high external calcium, refractoriness, and depolarization by elevated external potassium or by applied electric currents; and (2) an antagonism between local anesthetics and treatments which enhance sodium currents: high external sodium, low external calcium, veratrine, and hyperpolarization by electric currents.

The actions of Xylocaine and procaine are similar (see structures in Figs. 12 and 29). Both abolish sodium currents at 3.5 mM concentrations as rapidly as the solutions can be applied (Fig. 30). In some experiments $\bar{g}_K$ is also depressed (e.g. in record 41) and in most cases the relationship between $\tau_n$ and potential is shifted in the direction of depolarization (e.g. slowing of the rise of the potassium currents in record 303). The reduction of $\bar{g}_K$ tends

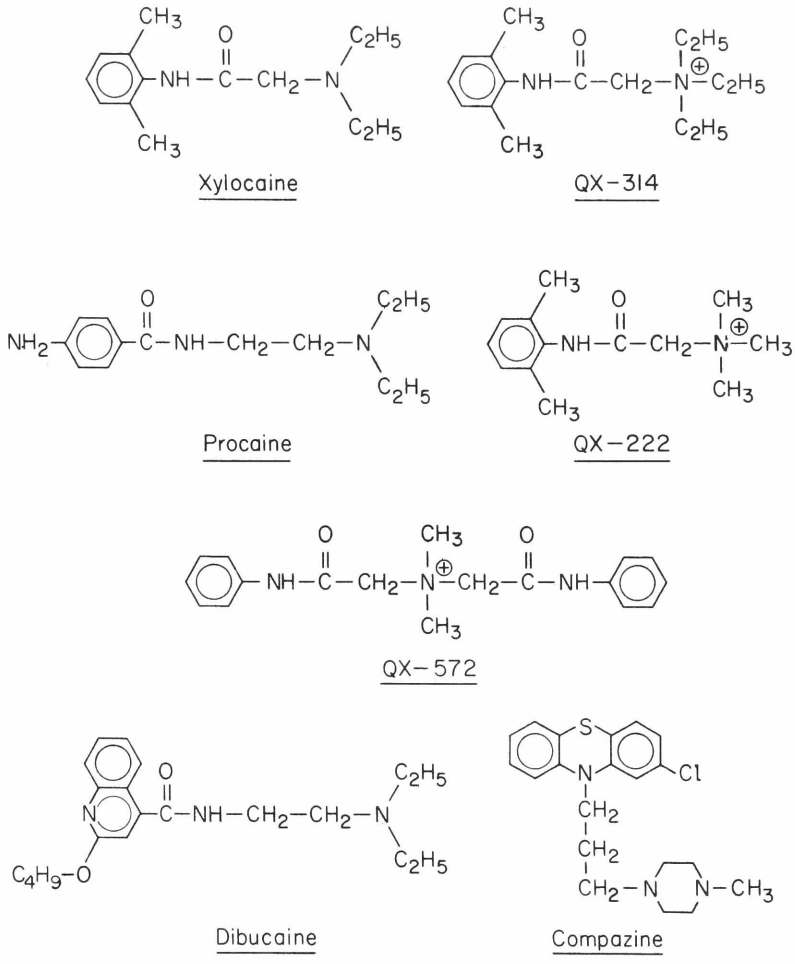


Figure 29. Some anesthetics and congeners. The structures of some local anesthetics and related compounds that were studied with the voltage clamp.

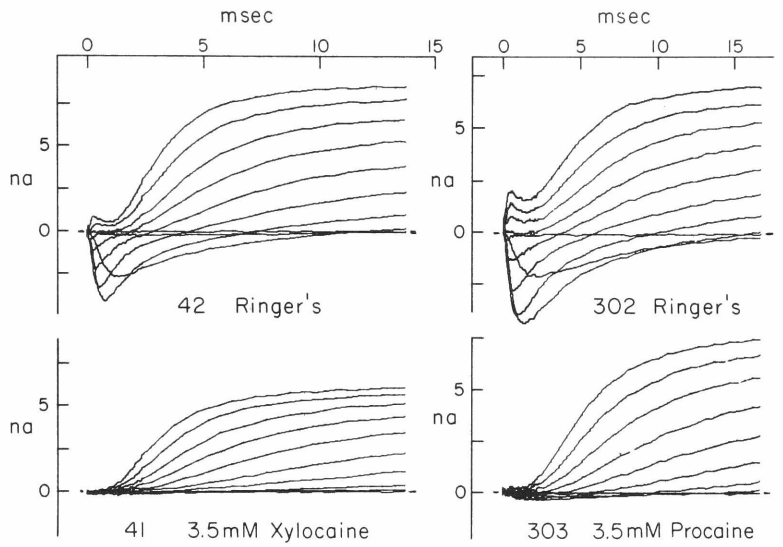


Figure 30. Xylocaine and procaine. The voltage clamp currents of two different nodes in Ringer's solution and in local anesthetic solutions. The greatest depolarization in records 41 and 42 is to +67.5 mv (T = 6° C), and in curves 302 and 303, to +80 mv (T = 3° C).

to increase with time. A five minute exposure to 3.5 mM procaine shifted the $\tau_n$ curve 15 to 18 mv in each of four experiments and caused a reduction of $\bar{g}_K$ by 0%, 9%, 10% and 40% in the four cases. The variable, time-dependent effects on the potassium currents were not studied in any detail, but they do seem readily dissociable from the "instantaneous" and reproducible abolition of sodium currents. Recovery of both the sodium and potassium currents is definitely slower than the recovery from the effects of TEA, for example. Several washes are required, yet frequently a certain fraction of the normal $\bar{g}_{Na}$ is restored as soon as washing begins.

When Xylocaine or procaine are used by the dentist, they are injected locally at 35 mM (1%) or 18 mM (0.5%) concentrations. Therefore my measurements probably account for the anesthesia seen under typical clinical conditions.

Experiments with low concentrations of local anesthetics show that they reduce the sodium currents by reducing $\bar{g}_{Na}$ and probably also shift the curves of the sodium parameters (peak conductance, $\tau_m$, and $\tau_h$) in the direction of depolarization. The measurement of the voltage shift is not reliable because the sodium currents are small (reduced $\bar{g}_{Na}$) and the shifts are small. For example, three nodes in 0.05 mM, 0.18 mM and 0.35 mM Xylocaine showed a reduction of $\bar{g}_{Na}$ to 80%, to 55%, and to 34% of normal, respectively, and a shift of the peak sodium conductance relation by 0 mv, by 2 mv, and by 6 mv, respectively. About 0.25 mM Xylocaine or 0.25 mM procaine reduces $\bar{g}_{Na}$ to 50% of normal. At these lower concentrations the anesthetic effects are more quickly and more completely reversed by washing.

The leakage conductance was not affected by the local anesthetics. Pooling fourteen measurements of $\bar{g}_L$ in Xylocaine and procaine solutions gives an average of 102% ± 7% (mean ± S.D.) compared with normal.

When 1.8 mM Xylocaine and 6 mM TEA are applied together, their effects are exactly additive: $\bar{g}_{Na}$ is reduced by 95% and $\bar{g}_K$ by 90%.

Also, as will be discussed later, 3.5 mM procaine abolishes all of the extra sodium currents appearing in veratrine solutions.

What properties of local anesthetic molecules contribute to their potency? Lipid solubility is an important factor. Local anesthetics that contain large aromatic regions or long alkyl chains are more lipid-soluble than Xylocaine, work at lower concentrations, and have an action that persists for a longer time even after repeated rinsing with anesthetic-free solutions. I have studied two of these lipophilic agents, the anesthetic Dibucaine and the tranquilizer Compazine (see structures in Fig. 29). Dibucaine blocks action potentials at 0.005 mM, and 3 mM is sufficient to lyse a node. Lysis is seen as a sudden and permanent loss of resistance of the node. The resistance falls at least one hundred fold. The lysis may be preceded by a prolytic phase in which there are temporary decreases of resistance following large imposed changes of potential or following the mechanical agitation of solution changes. Compazine reduces $\bar{g}_{Na}$ to 50% at 0.02 mM and to 5% at 0.05 mM without affecting $\bar{g}_{K}$. Compazine lyses nodes at 0.5 mM. Clearly, lipid solubility is a factor governing the anesthetic concentrations of these drugs, even when they act on naked nodes.

Another characteristic of local anesthetic molecules that has long been considered to be important is the presence or absence of a charge. Local anesthetics generally contain a tertiary nitrogen that is mostly protonated at pH 7.3. The $pK_a$ of Xylocaine is 7.85 and of procaine, 8.92. When applied to intact nerve trunks, these agents are found to act rapidly in alkaline solution, but it is recognized that the greater activity of the free base form in this case reflects the slower diffusion of the protonated form through the tissue layers surrounding the site of anesthesia (Ritchie, Ritchie and Greengard, 1965b). This problem of diffusion should not arise with naked nodes of Ranvier if the site of action is on the extracellular side of the membrane, and therefore a better measurement

of the relative activities of the cationic and of the free base form might be possible. Dettbarn (1962) showed that more acid solutions favored anesthesia in this case. Ritchie, Ritchie and Greengard (1965a and b) and Ritchie and Greengard (1966) have concluded that the cationic form is the active form from their very fine studies of the pH dependence of the anesthesia of sheathed and desheathed nerve trunks.

I have not tested the influence of pH on the anesthetic potency of the local anesthetics, but I have studied a related problem. The structures of three permanently ionized (quaternary) derivatives of Xylocaine are drawn in Fig. 29. I tested these compounds on the node expecting to observe a rapid and complete block of $\bar{g}_{Na}$; however, in my experiments there is no detectable effect of 4 mM QX-314 or of 3.5 mM QX-222 on the voltage clamp currents of the frog node. No change in $\bar{g}_K$ is found in 40 mM QX-314. On the other hand, the actions of QX-572 are similar to those of Xylocaine. A 0.13 mM solution of QX-572 reduces $\bar{g}_{Na}$ to 50% of normal and $\bar{g}_K$ to 85% of normal. The peak sodium conductance relation is shifted 7 mv in the direction of depolarization. The observations show that some local anesthetics can act as cations, although they do not prove that the cationic form is necessary or even preferable.

One significant difference between QX-572 with two aromatic groups and Xylocaine with one is that the effects of QX-572 are only slowly and poorly reversible, a persistence of action that is like that of Dibucaine. It was of interest therefore to know the relative lipid-solubility of the quaternary compounds and of Xylocaine. Dr. George Camougis and Dr. Bertil Takman, of Astra Pharmaceutical Products Inc., were kind enough to report to me some measurements of distribution coefficients (K) using oleyl alcohol as the "oil" phase and 0.25 M phosphate buffer as the water phase:

$$\text{Xylocaine:}\quad K = \frac{(\text{Base in oil})}{(\text{Base in water})} = 225 \pm 15$$

$$\text{QX-572:}\quad K = \frac{(QX^+ \text{ in oil})}{(QX^+ \text{ in water})} = 0.91 \pm 0.14$$

The values for QX-314 and for QX-222 are not known, but they have informed me that their lipid solubilities are less than that of QX-572. It is my feeling that these measurements may not provide the best basis for analysis of the problem for two reasons: 1) Nerve lipids contain many fixed anionic phosphate groups that might serve as counter-ions for the quaternary anesthetics. Such fixed counter-ions are not available in the oleyl alcohol. 2) The quaternary anesthetics will have some surface activity derived from a hydrophobic region at one end and a charge at the other, a kind of property that is not measured directly in a bulk-phase partition experiment. It may be that a "surface lipid solubility" or surface activity is the significant solubility parameter in local anesthesia. This question is raised again at the end of Chapter V.

Other anesthetic agents

Many of the anesthetics depolarize. I have not studied this aspect of their action, but it can be assumed that the agents mentioned in this section do depolarize. The experiments are, as before, carried out with a nerve maintained at -75 mv by the voltage clamp. The results are summarized in Table V in terms of the effects on $\bar{g}_{Na}$, $\bar{g}_{K}$, and $\bar{g}_{L}$. As these are from single experiments, the results are to be considered qualitative observations. The experiments with the gaseous anesthetic, nitrous oxide, were carried out in collaboration with Mr. Alan Steinbach using high pressure chambers that he designed and constructed.

About 1 M ethanol or 150 p.s.i. $N_2O$ block the conducted action potential of the sciatic nerve. These are much higher concentrations than are needed to anesthetize (or even to kill) a whole animal. Presumably in normal applications to anesthesia these agents act on sensitive structures in the central nervous system. All the agents listed in Table V reduce $\bar{g}_{Na}$ more than $\bar{g}_{K}$. Ethanol and $N_2O$ reduce $\bar{g}_{Na}$ with only small effects on $\bar{g}_{K}$, while dimethylsulfoxide (DMSO) and chloretone are less selective. $N_2O$ was certainly the most reversible, recovery taking only a few seconds either with isolated fibers or with whole nerve trunks.

Table V

LIPID-SOLUBLE COMPOUNDS WITH ANESTHETIC ACTION

| Compound | Node | $\bar{g}_{Na}$ | $\bar{g}_{K}$ | $\bar{g}_{L}$ |
|---|---|---|---|---|
| 190 p.s.i. $N_2O$ | p82B | 58% | 92% | 100% |
| 8% Ethanol (1.4M) | 63 | 56 | 89 | 92 |
| 10% DMSO* (1.4M) | 226 | 71 | 88 | 88 |
| 20% DMSO* (2.8M) | 227 | 57 | 79 | 81 |
| 2 mM Chloretone | 305 | 70 | 75 | 100 |
| 10 mM Chloretone | 307 | 15 | 55 | 85 |
| 20 mM Chloretone | 311 | 0 | 25 | 92 |

*DMSO: Dimethylsulfoxide

## Veratrine

The alkaloids in veratrine depolarize nerves (Shanes, 1958, 1963). The interesting experiments of other authors demonstrating that veratridine, one of the components of veratrine, acts by activating the sodium permeability mechanism will be discussed in Chapter V.

In my measurements at 15° C, $10^{-4}$ g/ml veratrine depolarizes a node by 20 to 40 mv in 5 min. The effect continues to intensify for at least 30 min and decreases slowly when the veratrine solution is washed away. In voltage clamp measurements unusual sodium currents appear. Even if the membrane potential is clamped at -75 mv there is a maintained small inward current (up to 0.6 na). In the usual kind of voltage clamp experiment with a hyperpolarizing prepulse, transient sodium currents and delayed potassium currents may be elicited. However, on repolarization there appears a large inward current (up to 5 na) that decays with a time constant between 200 and 600 msec. This inward current appears only if the previous depolarization is large enough and long enough to elicit a transient sodium current. Sodium-free media abolish this current. Thus the current is due to a persistence of the sodium permeability increase seen in the transient current. It seems that the early transient change is abnormal in the sense that it does not turn off (inactivate) completely. Both TTX and procaine abolish the depolarization, the persistent inward current at -75 mv, and the larger inward current that follows a depolarization in veratrine. The concentration of TTX or of procaine needed is the same as that required to block the normal transient sodium permeability change. In the experiment with both veratrine and procaine on the node, the delayed potassium currents appear normal and no sodium currents flow. The potassium currents in veratrine-treated nodes can be abolished with TEA. The high concentration of veratrine used in all of these experiments causes a constant deterioration of the membrane in that over a period of 30 min $\bar{g}_{Na}$ and $\bar{g}_{K}$ gradually fall to below half of their normal value.

In summary veratrine activates the sodium permeability mechanism without producing marked changes in the potassium permeability mechanism. The veratrine-induced sodium currents can be abolished by agents that abolish the normal transient sodium currents. The actions of veratrine are in some way associated with a depression of the sodium inactivation process.

# Chapter V

## DISCUSSION AND CONCLUSIONS

The first part of this chapter is a comparison of the published observations of other investigators with my results with special emphasis on experiments with the voltage clamp technique. It can be said that basically my results agree with theirs. The second and larger part of this chapter is devoted to a consideration of the conclusions that can be drawn concerning the ionic permeability mechanism from these and other experiments.

One point must be made before comparing results from isolated frog fibers with those from almost any other commonly used nerve preparation. Electron micrographs of frog nerves show a basement membrane and a loose collar of pseudopod-like processes from adjacent Schwann cells over the nodes of Ranvier. The cell membranes of the processes are not in contact with the nodal membrane (Robertson, 1960). In addition, as the dissection of the single frog fiber proceeds, it is not uncommon to see the nodal gap widening, probably because of the stresses of dissection. In nearly every other common nerve preparation a uniform closely adhering cellular layer bounded in turn by a basement membrane covers the nerve surface. These structural features make the nodal membrane of isolated fibers one of the most naked excitable membranes available for study. Thus, for example, conduction block in a sodium-free medium occurs in one second with isolated frog fibers but takes 1.5 min with cleaned squid giant axons (Hodgkin and Katz, 1949) and 8 hr with the whole sciatic nerve trunk still covered by the epineurium (Lorente de Nó, 1947; Gallego, 1951). Similary drugs applied to preparations with diffusion barriers tend to take longer to act, require higher concentrations in a short application, and are much more difficult to wash out than in a corresponding experiment with isolated myelinated fibers.

## Similar Experiments Reported in the Literature

### Tetrodotoxin

In an excellent review Kao (1966) traces the history of TTX starting with Chinese sources from before Christ. Some physiological studies were undertaken in America after TTX (once called tarichatoxin) was found in certain West Coast salamanders by Twitty (see for example Twitty, 1937), and at the same time TTX from puffer fish was studied in Japan. However, not until 1960, when Narahashi, et al. applied TTX to single frog muscle fibers, was the specificity of its action noted. They used two internal glass capillary microelectrodes, one for recording and one for polarizing, to show that the resting potential, the resting resistance, and the delayed rectification were unaffected by TTX while the action potential was abolished. This experiment was like the one illustrated in Fig. 18. Narahashi, et al. concluded that the sodium system had been blocked more or less selectively. Their experiment called the attention of many investigators to the useful properties of this compound.

Since 1960, many voltage clamp studies with TTX have appeared. The published results are virtually identical with mine except that other tissues were used. All studies have demonstrated a completely specific reduction of $\bar{g}_{Na}$. With the lobster giant axon it has been shown that 15 to 100 nM TTX selectively reduces $\bar{g}_{Na}$ without changing the kinetics of the sodium current and without a shift in the peak sodium conductance-potential relation or in the steady-state sodium inactivation ($1-h_\infty$) relation (Narahashi, Moore, and Scott, 1964; Takata, Moore, Kao, and Fuhrman, 1966). With the squid axon it has been shown that 150 nM TTX applied in the bathing medium selectively blocks sodium currents in 5 min (Nakamura, Nakajima, and Grundfest, 1965a), whereas a 1000 nM solution perfused internally through the axon for 30 min had no effect on sodium currents and a 10,000 nM solution perfused internally for 17 min had no effect on the action potential (Moore, 1965; Narahashi, Anderson, and Moore, 1966b). Inward lithium currents of squid axons are stopped by TTX

(Moore, Anderson, and Narahashi, 1966), and action potentials in sodium-free media containing ammonium, guanidinium, hydrazinium, or hydroxylammonium cations are blocked by TTX (Tasaki, Singer, and Watanabe, 1966). (See later in this chapter for more discussion of the cations that will substitute for the sodium ion.) The sodium currents of the electroplaques of Electrophorus electricus are selectively abolished by 150 nM TTX (Nakamura, et al. 1965b). In all the voltage clamp experiments, TTX has been found to affect exclusively the voltage-dependent permeability changes that are normally associated with the inward movements of sodium ions. No other investigators have reported voltage clamp experiments with vertebrate nerves, but my experiments agree fully with the reported experiments on invertebrate nerves.

A much larger number of studies with TTX have appeared that did not involve voltage clamp techniques (see Kao, 1966, for references). In every case action potentials that are normally dependent on inward sodium fluxes (i.e. "sodium spikes") are abolished, and all other kinds of electrical responses, including "calcium spikes, various "chloride -" or "potassium-rectifications" end plate potentials, synaptic potentials, and receptor potentials, are totally insensitive to TTX. It is important to note that although the last three kinds of "potentials" frequently involve sodium permeability changes, these changes are usually not as selective for sodium ions as are those underlying action potentials, and, perhaps more significantly, these changes are independent of the membrane potential.

The structural features of the TTX molecule that are important for its action have yet to be identified. Several derivatives have been synthesized involving the addition or deletion of various groups. In all cases the potency of the molecule is considerably reduced by the modification (Kao, 1966). Apparently the TTX-receptor complex has a very finely adjusted fit. Much work should be done with structure-activity relationships of TTX-like molecules, because of the possibility of finding out more about the receptor which is

intimately associated with the electrogenic mechanisms of the nerve membrane. Perhaps analogs of TTX will be found in animals closely related to the puffer fish or to the salamanders from which it is now extracted. It is a remarkable biological observation that the desheathed myelinated nerves of these puffer fish and salamanders are insensitive to high concentrations of TTX although the nerves are of the normal sodium-requiring type (Kao, 1966). It must be concluded that as these animals evolved the TTX molecule, the TTX receptor of their nerve fibers also changed to eliminate the close fit, thus protecting the animal from its own poison.

Tetraethylammonium ion and related ions

As was mentioned in Chapter IV, the effects of quaternary ammonium ions fall into at least two categories: interference with some aspect of chemical transmission and a direct modification of voltage-dependent permeability changes. We are concerned here with the latter kind of action. Unfortunately, the literature on the effects of TEA is not as easy to review as that for TTX, there being no recent general review article and no simple generalization of the observations. One can say that indirect evidence (the prolongation of action potentials) suggests that potassium currents are reduced by TEA in many kinds of excitable cells (see Schmidt, 1965) and that direct evidence from a few cases shows that each kind of cell responds to TEA in a different manner. A few of these specific cases will be discussed now. In all cases the effects of TEA on sodium currents, if they exist, are small.

The giant axon of the squid Loligo pealii is insensitive to 100 mM TEA in the bathing solution (for 30 min), but a 40 mM internal concentration produces an immediate, profound change in the potassium currents. In this condition the potassium conductance is normal for inward potassium currents and essentially nil for outward currents, a change that can be symbolized in the equivalent circuit of Fig. 1 by inserting a diode in series in the potassium branch of the circuit

(Armstrong and Binstock, 1965). The TEA-induced rectification is easily seen in high -potassium solutions in which inward and outward potassium currents can normally be large. If in a voltage clamp experiment the axon is depolarized beyond $E_K$, the expected delayed outward currents do not appear, although, on repolarization to the holding potential of -113 mv, a large "tail" of inward potassium current appears. The magnitude of the tail is small following short depolarizations and larger following long depolarizations. When they described these phenomena Armstrong and Binstock (1965) suggested that internal TEA might be swept into the membrane with outward potassium current, and hence block, and be flushed out again by inward current. As the experiment with "potassium tails" shows, the process represented by the parameter n seems to occur whether the passage of potassium ions is blocked by TEA or not. No changes in the sodium currents were reported. Armstrong (1966) has investigated the effects of lower internal concentrations of TEA, showing that about 0.8 mM TEA will reduce outward potassium currents by a half. At these low concentrations, however, the inhibition is not apparent when the depolarizing pulse is applied. Rather, the expected outward currents appear, and then over some fraction of a millisecond they decay away. Again the experiments suggest that TEA is swept into and out of the membrane. It seems that at low concentrations of TEA many potassium ions leave the cell before the accumulation of TEA in the membrane is large enough to block. Many more details of these fascinating phenomena are found in Armstrong's paper, but, because the action of TEA on the squid axon differs from its action on frog nodes of Ranvier in the induced rectification, in the dynamic nature of the inhibition, and in the intracellular site of action, the squid axon will not be discussed further. It should be pointed out that since 0.8 mM internal TEA has a profound effect and 100 mM outside has no effect in 30 min, the squid axon must be quite impermeable to TEA.

Certain cells of the central nervous system of a marine snail (Onchidium verruculatum, a mollusk like the squid) respond to TEA more as frog nodes do than as squid axons do. The normal voltage

clamp currents of the cell bodies of supra- and subesophageal ganglion cells of this snail closely resemble the currents of the standard type seen in giant axons and myelinated fibers (Hagiwara and Saito, 1959). The delayed rectification is reduced to one fourth of normal by 100 mM TEA applied extracellularly for 30 sec, whereas the transient sodium currents are only slightly reduced. The reduction in TEA is independent of whether the sodium current has been blocked by 2% urethane. Apparently even 125 mM TEA will not abolish the delayed rectification completely. Thus if TEA acts by binding in this case, either the dissociation constant is one hundred times larger than it is in my experiments or some fraction of the delayed rectification is insensitive to TEA. Unfortunately Hagiwara and Saito did not report dose-response studies. The rapidity of the inhibitory effect suggests an extracellular site of action.

TEA has also been applied to cell bodies in the vertebrate central nervous system. Voltage clamp experiments of Nakajima (1966) show that 200 mM external TEA reduces the potassium conductance to 72% of normal in supramedullary ganglion cells of the Atlantic puffer fish Spheroides maculatus. (This fish does not contain tetrodotoxin.) The low sensitivity to TEA cannot be attributed to an inability of ions to get to the cell surface because in the same experiments high-potassium solutions depolarized quickly and completely. In this preparation TEA did not induce the kind of rectification seen with the squid axon. No experiments have been reported in which TEA has been applied to cell bodies of motoneurons in the spinal cord. Such studies would be interesting because these cells give rise to the motor axons studied in my experiments.

Extensive studies of the effects of TEA on frog peripheral nerves have been carried out in the laboratory of Stämpfli using desheathed nerve bundles with the sucrose-gap technique (Schmidt, 1960 and 1965) and using single nerve fibers with the air-gap technique (Schmidt and Stämpfli, 1965) and with the Frankenhaeuser-Dodge voltage clamp technique (Koppenhöfer and Weyman, 1965;

Koppenhöfer, 1966 and 1967). Their observations on Rana esculenta and Xenopus laevis nerves agree among themselves but do not agree entirely with my experiments on Rana pipiens nerves. Most of their experiments employ 5 mM TEA in a Ringer's solution containing 1 mM calcium (I use 1.8 mM calcium). We agree that TEA strongly decreases outward and inward (in high-potassium solutions) potassium currents, doubles or triples the duration of the action potential, and does not affect $\bar{g}_{Na}$, $\bar{g}_{L}$, $\tau_{m}$, or $h_{\infty}$. In experiments with 0.3 mM and 5 mM TEA Koppenhöfer (1967) reports a reduction of the potassium permeability to 70% and to 16% of normal when measured in high depolarizations (to +40 mv or more). These values fall almost exactly on the dose-response curve that I have obtained (Fig. 24). Schmidt and Stämpfli's measurements of membrane potential changes using the sucrose-gap are far more reliable than mine. They report that 5 mM TEA depolarizes by 5 mv and that lowering the calcium level can more than double the depolarization in TEA. Presumably with the higher calcium concentration used in my experiments the depolarization in TEA would be very small. There are three points on which my experiments may differ from those of Stämpfli's group. Koppenhöfer (1967) reports that $\tau_{n}$ is increased 70% by 0.3 mM TEA, that $\tau_{h}$ is increased 40% by 5 mM TEA, and that the reduction of the potassium current in 5 mM TEA is 100% in a depolarization to -30 mv and 84% in a depolarization to +50 mv. In my experiments $\tau_{n}$ and $\tau_{h}$ are definitely insensitive to TEA in the same concentration range (see Figs. 20 and 22) to within the 5 to 10% reproducibility of the measurements. Isotonic TEA increased the value of $\tau_{h}$ at +67.5 mv by 9% (Fig. 23) but I do not feel that the change was significant. In that experiment it was not possible to use the value of $E_{Na}$ as a check against a small drift in the voltage measuring amplifier. In my experiments there may have been a greater reduction of potassium currents by TEA for small depolarizations than for large depolarizations (see Fig. 22), but the difference is not as great as that reported by Koppenhöfer. I believe that there may be two factors contributing to his differing observation, one that would lead to an underestimation of the potassium currents at

low depolarizations, namely the use of pulses that are too short to allow a steady state to be reached, and a second that would lead to an overestimation of the potassium currents at high depolarization, namely the rectification of nodes in the current measuring circuit as described in Appendix II.

There is only one experiment with peripheral nerves in which many quaternary ammonium ions related to TEA were used. Lorente de Nó (1949) studied the effects on bullfrog sciatic nerve trunks with the sheath intact of sodium-free isotonic solutions of 25 different quaternary ammonium ions containing methyl, ethyl, hydroxyethyl, propyl, butyl, and phenyl groups. In all cases the conduction of the fast fibers was lost in a few hours as would be expected in sodium-free solutions. Conduction returned when sodium ions were restored to the medium. Surprisingly, however, in eleven of the solutions a large class of slow fibers was not blocked although the conduction velocity was greatly reduced. The eleven solutions could restore activity to this special class of fibers after the conduction was blocked by one of the inactive solutions (e.g. tetramethylammonium ion). These fibers were dubbed the "Et" fibers because quaternary ions containing several ethyl groups supported their activity. It is not known to which fiber group(s) the Et fibers belong, either in the anatomical or in the functional sense, although it is certain that they do not comprise the large fibers that I study. Among the quaternary ions that restored conduction to the Et fibers were the ions that most strongly depressed $\bar{g}_K$ in my experiments. The four ions with apparent dissociation constants of their receptor complexes (see Table V) of 15 mM or less in my experiments were the best restoring agents in Lorente de Nó's experiments and those with apparent dissociation constants of 240 mM and greater did not restore. This is probably an example of a general phenomenon that will be discussed later in this chapter, namely that action potentials can be elicited in media containing very poor current carriers if the factors tending to prevent the rise of the action potential (e.g. potassium current

flow and leakage current flow) are diminished. It is not apparent whether in the case of Et fibers the quaternary ammonium ion or some other ion (calcium) is carrying the inward current during the excitation.

In an analogous case, long and slowly rising action potentials can be elicited in frog spinal ganglion cells (the cell bodies of the peripheral sensory axons) in sodium-free media containing TEA (Koketsu, Cerf, and Nishi, 1959). These potentials reflect, at least in part, divalent ion permeability changes (Nishi, Soeda, and Koketsu, 1965). They are insensitive to high concentrations of tetrodotoxin, although tetrodotoxin abolishes the action potential of the spinal ganglion cell in normal sodium Ringer's solution and in hydrazine Ringer's solution (Koketsu and Nishi, 1966).

In summary TEA has different effects on different cells even when animals from the same phylum (whether mollusks or vertebrates) are compared. Although it is hard to believe that nodes of Ranvier of various frogs including members of the same genus differ qualitatively in their esponse to TEA, there are reported differences between Rana pipiens on the one hand and R. esculenta and Xenopus laevis on the other. I hope that this difference will be resolved, perhaps as a difference in procedure and analysis. At present my experiments are the only ones in which it has been observed that millimolar concentrations of TEA reduce $\bar{g}_K$ nearly to zero without any other effect on the electrical properties of the membrane.

Calcium

As a component of the natural environment of living cells, calcium has been widely studied by biologists and medical doctors. It is generally agreed that the effects of elevated calcium levels on nerve cells are analogous to a hyperpolarization (see review by Brink, 1954; Shanes, 1958a and b). Numerous voltage clamp studies have been reported and the results agree quantitatively with mine. Table VI is a list of some of the voltage shifts reported for an e-fold

Table VI

EFFECTS OF e-FOLD INCREASES IN CALCIUM CONCENTRATION

| nerve (ref.) | voltages shifts (mv) (all positive) $h_\infty$ | $m_\infty$ | $n_\infty$ | conductance decrease (%) $\bar{g}_{Na}$ | $\bar{g}_K$ |
|---|---|---|---|---|---|
| squid (1) | 4.0 | 9.4 | 8.9 | 0 | 0 |
| lobster (2) | - | 6.3 | - | - | - |
| lobster (3) | - | 8.0 | - | 8 | 8 |
| lobster (4) | - | 5.5 | - | - | - |
| frog (5) | 6.0 | 8.5 | - | 0 | 0 |

references:

1) Frankenhaeuser and Hodgkin (1957)
2) Julian, Moore, and Goldman (1962b)
3) Blaustein and Goldman (1966)
4) Takata, Pickard, et al. (1966)
5) Hille (this thesis)

increase in the calcium concentration in published experiments and in my experiments. The values are given as millivolts of displacement of the curve of voltage dependence of the parameters $m_\infty$, $h_\infty$, and $n_\infty$ recalculated from an average of the observed shifts by assuming that the logarithmic relationship (see Chapter IV) can be used for interpolating between concentrations. All authors report a lengthening of the time constants $\tau_m$, $\tau_h$, $\tau_n$, where measured, in a manner suggesting a shift of their voltage-dependence. In my experiments $\tau_n$ is lengthened very little, and sometimes not at all, in contrast to the observations on squid and lobster. The magnitude of $\bar{g}_{Na}$ has been reported to be unchanged by a 25-fold change in calcium for the squid axon (Frankenhaeuser and Hodgkin, 1957) and to be reduced by 9% for a 4-fold increase of calcium for the lobster axon (Blaustein and Goldman, 1966).

Cases in which calcium serves as a current carrier will not be discussed in detail except to mention a shift that is relevant to this section. Hagiwara and Naka (1964) have shown that with very low internal calcium concentrations the barnacle muscle fiber will produce a "calcium spike" if there is calcium in the medium. In the voltage clamp there are transient inward calcium currents that behave much as the sodium currents of normal axons behave and apparently normal delayed potassium currents. Changes in the calcium concentration not only displace the calcium equilibrium potential 29 mv per ten-fold change but also shift the peak calcium conductance relation 12 mv per e-fold change (Hagiwara, 1966).

There are many current clamp studies of threshold shifts and sodium inactivation shifts on a wide range of axons. These all arrive at the same conclusions as the voltage clamp experiments. There is also another related class of experiments that I shall not review, in which divalent ions other than calcium, such as magnesium, strontium, barium, and nickel, and trivalent ions, such as aluminum, have been tested on axons (Dodge, 1961; Narahashi, 1966; Takata, Pickard, Lettvin, and Moore, 1966). Frequently it is found

that an equimolar substitution for calcium ion does not reproduce the normal state of the axon but seems to act more like excess calcium or low calcium. Changes in the concentration of these other metal ions cause shifts of the kind observed when the calcium concentration is changed.

Lipid-soluble anesthetic agents

When the ionic basis of the action potentials of squid axons was clarified by Hodgkin and Huxley, it was suspected that non-depolarizing anesthetics must reduce the transient inward sodium currents (see Shanes, 1958). In my experiments $\bar{g}_{Na}$ is reduced 100% in seconds by 3.5 mM Xylocaine or procaine, with much smaller effects on $\bar{g}_K$ developing only gradually. With several other lipid soluble anesthetics, however, doses that reduce sodium currents also reduce potassium currents significantly.

Voltage clamp experiments show that the sodium and the potassium conductances of invertebrate axons do not have the high differential sensitivity to local anesthetics that I found with the node of Ranvier. With 3 mM cocaine on the squid axon Shanes, et al. (1959) reported a reduction of $\bar{g}_{Na}$ to 35% of normal and of $\bar{g}_K$ to 43% of normal. Taylor (1959) has made a careful study of the effects of 3.5 mM procaine on the voltage clamp parameters of the squid axons, finding a reduction of $\bar{g}_{Na}$ to 37% of normal and of $\bar{g}_K$ to 70% of normal, and a shift of the curve relating peak sodium conductance (or $m_\infty$) to voltage by 6 mv in the direction of depolarization. The sodium inactivation ($1-h_\infty$) curve was not shifted on the voltage axis, nor was the resting potential affected. The same concentration of procaine applied for 2 or 3 min to the lobster axon reduced both $\bar{g}_{Na}$ and $\bar{g}_K$ to about 60% of normal and slowed the time course of the turning on of the sodium currents (Blaustein and Goldman, 1966; Goldman and Blaustein, 1966). The leakage conductance was not affected. Lowered calcium levels increased, and raised calcium levels decreased, the sensitivity of the sodium conductance of the lobster axon to procaine, suggesting a competition between calcium and local anesthetics. Another local

anesthetic, tropine-p-tolyl acetate, at 2.5 mM concentration reduced $\bar{g}_{Na}$ and $\bar{g}_{K}$ to 50% of normal (Goldman and Blaustein, 1966).

Two different results have been reported for alcohols applied to the squid giant axon. Armstrong and Binstock (1964) found that $\bar{g}_{Na}$ is more sensitive to alcohols than $\bar{g}_{K}$. In two cases about 0.5 M (=3%) ethanol applied for 8 min reduced $\bar{g}_{Na}$ to 50% and 30% of normal and $\bar{g}_{K}$ to 98% and 92% of normal. Only 0.13 mM octyl alcohol is needed to produce the same depression of the conductances. On the other hand Moore, Ulbricht, and Takata (1964) observed that in 3% and 6% ethanol $\bar{g}_{Na}$ is reduced to 82% and 59% of normal and $\bar{g}_{K}$ is reduced to 80% and 69% of normal. They found no change in $\tau_{n}$ and $\tau_{m}$ and no shift of the peak sodium conductance relation or the sodium inactivation relation.

Hagiwara and Saito (1959) observed that 2% urethane blocked the sodium currents of the Onchidium ganglion cells with little effect on the potassium currents.

In summary, none of the lipid-soluble anesthetics is a completely selective inhibitor of $\bar{g}_{Na}$, although all depress $\bar{g}_{Na}$ at least as much as $\bar{g}_{K}$. With frog nodes some of the anesthetics exert such complete and immediate depression of $\bar{g}_{Na}$ without very much change in $\bar{g}_{K}$, that it is plausible to speak of two independent effects having different time courses. In most invertebrate preparations this kind of evidence for two effects does not exist. The effects on $\bar{g}_{Na}$ and $\bar{g}_{K}$ seem to go hand in hand. I believe that there may still be independent effects on the two permeabilities even in invertebrate axons, but that an overlap in the time courses and in the concentration dependences of the inhibitions makes them difficult to separate.

This concludes the description of the pharmacological experiments. In this review I have emphasized the phenomenological properties of nerves treated with drugs without discussing the possible mode of action of the drugs. The next three sections of this chapter consider some conclusions about the structure of the axon membrane that are

suggested by the phenomena I have described, and the last section in the chapter returns to the drugs and how they might act. What follows may be considered a statement of a point of view concerning membrane function. I hope that these considerations will be helpful in generating a new program of experiments.

## The Heterogeneity of the Membrane

The results of my experiments and of other similar published experiments have a direct bearing on a problem of considerable interest, namely, do the sodium and the potassium ions pass through the same or through different parts of the membrane? In the literature the alternatives have been called the homogeneous membrane and the heterogeneous or mosaic membrane. There is no consensus on which choice is correct.

Lacking an anatomical visualization of the passage of ions through membranes the physiologist must resort to indirect experiments. Experiments demonstrating that the movements of sodium and potassium are linked or coupled in any manner can be used to argue the homogeneous case, and experiments demonstrating that sodium and potassium movements are independent can be used to argue the heterogeneous case. In the paragraphs that follow I shall consider some of the kinds of observations that can be used to help decide this point.

### Kinetic and electrochemical measurements

Hodgkin, Huxley, and Katz (1952) and Hodgkin and Huxley (1952a, b, c and d) were able to write the empirical formulae for the sodium and potassium components of the current as independent kinetic equations (see Fig. 3 for the equations), the only common factors found in the expressions for $I_{Na}$ and for $I_K$ being time and potential. They also demonstrated that changes in the sodium concentration changed $E_{Na}$ and $\bar{g}_{Na}$ more or less as predicted by the Nernst equation and the "independence principle" without affecting $E_K$ or $g_K$. The

independence principle is an electrochemical theory that they developed from the assumption that "the chance that any given ion will cross the membrane in a specified interval of time is independent of other ions which are present." Finkelstein and Mauro (1962) have pointed out that this type of behavior is not found in an ionic diffusion regime in which several different salts are dissolved in the solution. Most of the conclusions of these classical experiments suggest independence of the sodium and potassium movements and hence heterogeneity of the membrane. The same kind of kinetic and electrochemical independence has been demonstrated in nodes of Ranvier of Rana pipiens by Dodge (1963).

On the other hand, there are two observations that suggest an interdependence between $I_{Na}$ and $I_K$. The first is that in individual fresh squid axons $\bar{g}_{Na}$ and $\bar{g}_K$ are equal, although their value may vary by a factor of six among different axons (Cole and Moore, 1960). The second is that during any depolarization $g_{Na}$ increases transiently first and then $g_K$ increases in a manner that suggests a precursor-product relationship between the two conductances. For example, it could be thought that the sodium inactivation process is a necessary antecedant of the potassium activation. This sequence is preserved at all potentials because, as the model describes it, the time constants $\tau_m$, $\tau_h$, and $\tau_n$ all change with potential in a similar, although by no means identical manner. The sequence also obtains at all temperatures from 0° C to 27° C, i.e. the temperature coefficients of the three rate processes are similar. The most careful measurements of the temperature coefficient ($Q_{10}$) have been made on Xenopus nodes with the following results (Frankenhaeuser and Moore, 1963a):

$\tau_m$ : 1.8 $\qquad$ $\bar{g}_{Na}$ : 1.3

$\tau_h$ : 2.9 $\qquad$ $\bar{g}_K$ : 1.2

$\tau_n$ : 3.0

As an aside to the precursor-product question, please observe that the rates of change of the conductances are very sensitive to the

temperature whereas the magnitudes of the conductances are relatively independent of temperature. I refer to these temperature studies again later in this chapter. Returning to the possible sequential dependence of the potassium conductance changes on the sodium conductance changes, I repeat that Hodgkin and Huxley did not find it necessary to invoke such a relationship. Pharmacological studies (see below) also seem to rule out the hypothesis.

Pharmacological measurements

Until recently most of the pharmacological studies with voltage clamped axons suggested that if the sodium movements were affected, the potassium movements would be also. This is true of all of the experiments with alcohols, including mine, and of all of the experiments with calcium ion changes and with local anesthetics, except mine. On several occasions these observations have been used to support the hypothesis of homogeneity of the membrane. However, in the last few years, especially after the introduction of tetrodotoxin, many experiments have demonstrated that sodium movements and potassium movements can be modified independently by applied drugs. The first of these was Hagiwara and Saito's (1959) study of Onchidium ganglion cells bathed in 2% urethane and 100 mM TEA. Only in 1965 and 1966 did many new studies with TTX and with TEA demonstrate the pharmacological independence of the components of current. This aspect has been emphasized in the presentation of my experiments in Chapter IV and in the discussion of similar experiments earlier in this chapter.

In my experiments it has been possible to demonstrate that the currents that are blocked independently by TTX and by TEA correspond exactly to the components of current that have been demonstrated to be kinetically and electrochemically independent in the same kind of nerve by Dodge (1963). I conclude that this is a strong confirmation of the hypothesis of heterogeneity. In the experiment of Fig. 23 in which the membrane is disturbed by a strong electric shock, $\bar{g}_K$ is irreversibly reduced to zero although $\bar{g}_{Na}$ seems normal after a few seconds. In all of these experiments the drug or other treatment can

abolish one of the conductances.

My experiments on calcium changes and on veratrine are of a different character. Calcium concentration changes shift the curves of $\tau_m$ and $\tau_h$ along the voltage axis without affecting the curve of $\tau_n$ in many cases, again a differential effect on the sodium and on the potassium systems. In effect the time constant of turning off of the sodium current ($\tau_h$) at some potentials (-45 to -15 mv) can be varied 4 to 5-fold by calcium changes and still the potassium current turns on at the normal time. Extremes of slowing of the sodium inactivation can be obtained with veratrine treatments. The sodium conductance can be activated by the drug without any apparent disturbance of the normal turn-on and turn-off of the potassium currents. This case is very interesting because it offers the opportunity to demonstrate that both conductances can be fully activated simultaneously, an observation that would rule out a precursor-product relationship between $g_{Na}$ and $g_K$. More quantitative study of the effects of the veratrine alkaloids will be needed.

## Conclusion

In summary, a large body of voltage clamp data has been gathered by several workers using electrochemical, kinetic, and pharmacological methods. All the observations are consistent with the idea that the nerve cell membrane is a heterogeneous structure in the sense that sodium and potassium ions move through different places, and many of the observations would be extremely difficult to incorporate into a model based on a homogeneous membrane. Therefore from this point on I shall consider the hypothesis of a heterogeneous membrane to be established by experiment. The regions through which sodium ions flow will be called the sodium channels and the regions through which the potassium ions flow will be called the potassium channels. In all experiments with drugs the leakage conductance is a constant. Thus there must also be leakage channels.

## Properties of the Ionic Channels

I shall assume that the different kinds of ionic channels are formed by molecules or collections of molecules that are specialized for the task they perform. In other words, I shall speak of the channels as one might of enzymes or other parts of the cell that have clearly defined functions. Their structure has been carefully perfected by natural selection specifically to pass certain ions in a temporal pattern appropriate to effective nervous signalling. Since they are material entities it will be meaningful to speak of their composition, synthesis, dispersal, and destruction and of their development, evolution, genetics, and pathology. The different channels may not resemble each other more than different enzyme molecules resemble each other, so each kind should be treated separately, much as the individual enzymes must be treated separately.

### The kinds of channels

In addition to the sodium, potassium, and leakage channels, how many other kinds of specialized channels contribute to normal electrical responses? At the present time it would be impossible to guess, as the majority of membranes have yet to be studied. Sea water and the blood of most marine invertebrates contain six ions in greater than 10 mM concentration: sodium, potassium, calcium, magnesium, chloride, and sulfate. Of these only three are found in concentrations greater than 100 mM in the intracellular or the extracellular fluids of all animals, and, indeed, these three ions, sodium, potassium, and chloride account for most of the electrical responses that can be observed under physiological conditions.

Grundfest (1961 and 1966), long a proponent of the heterogeneous membrane and of the wide diversity of ionic channels, has reviewed the literature on nerve and muscle fibers and on electroplaques, including discussions of specific voltage-dependent sodium, potassium, chloride, and calcium channels. His point of view is in most respects

identical with that expressed here and played a formative role in the development of my ideas. Eccles (1966) has reviewed the literature on the ionic mechanisms of excitatory and inhibitory post-synaptic and endplate potentials showing that the transmitter agent produces various combinations of sodium and potassium conductance increases or of potassium and chloride conductance increases in different cases. These conductance changes at junctions and those underlying the transduction processes of primary sense receptors are generally voltage-independent and are not known to exhibit the high ionic specificity of the channels associated with the propagated action potential. Quantitative studies of the ionic basis of most junctional and receptor potentials remain to be carried out. In addition to the ionic channels associated with the various excitability phenomena, there are certain properties such as the extraordinarily high chloride permeability and low cation permeability of mammalian red blood cells that suggest specific ionic channels with physiological importance (here to mediate the "chloride shift") in many cells. Thus the range of possibilities is large.

Any one of these kinds of channels including those in "inexcitable" cells may provide the key to a new understanding of the nature of ionic channels. In the rest of this thesis, however, I shall restrict myself to the voltage-sensitive ionic channels of nerves and muscles, and more specifically to the sodium and potassium channels. Potentially the chloride, calcium, and leakage channels may be more interesting, but they simply are not as well known today.

## The ionic specificities of the channels

A quantitative knowledge of the ionic selectivity of the ionic channels will probably play an important role in the future theories that are designed to explain the nature of the channels. While there is no fundamental physical theory that serves as a basis for assigning values to the ionic specificities of a channel, it is simple and appropriate to assign a value of 12:1, for example, to the relative permeability ratio of the permeabilities to sodium and potassium when,

in an experiment, 120 mM K is approximately equivalent to 10 mM Na. This procedure is in common use. On this basis Chandler and Meves (1965) have found relative permeabilities of the sodium channel for Li:Na:k:Rb:Cs of 1.1:1:1/12:1/40:1/61 using perfused squid giant axons. It is also known that the sodium channel of the squid axon is permeable to ammonium, guanidinium, hydrazinium, and hydroxylammonium cations (Tasaki, Singer, and Watanabe, 1966). The permeability ratio for $Na:NH_4$ is about 1:1/3 (Binstock and Lecar, 1967). No quantitative studies have been performed to determine the relative permeabilities for organic ions other than ammonium. Probably divalent ions are also permeant, as under extreme conditions TTX-sensitive action potentials can be elicited in 200 mM Ba, Ca, or Sr media with no other external cations (Watanabe, et al., 1967). Hodgkin and Keynes (1957) found an extra calcium influx on stimulation in a 112 mM Ca solution amounting to 0.08 pmole/$cm^2$ per impulse compared to 12 pmole/$cm^2$ per impulse of sodium influx from a 450 mM Na solution. Assuming a linear relation between flux and concentration and neglecting electrical forces, one can assign a tentative value of 1:1/37 for the relative permeabilities Na:Ca.

The sodium channel of the frog node of Ranvier is similar to the squid axon's. The ratio for Na:K is 1:1/20 (Frankenhaeuser and Moore, 1963b) for Na:Li it is 1:0.8 (single observation, this thesis) for $Na:NH_4$ it is 1:1/5 (Dodge, 1963), and for Na:guanidinium it is 1:1/10 (Luttgau, 1958). Simple experiments with impulse propagation show that the sodium channel is also permeable to hydrazinium and hydroxylammonium cations (Lorente de No', Larramendi, and Vidal, 1957).

The potassium channel of the node has not been studied from the point of view of specificity except for one report that the rubidium permeability is comparable to the potassium permeability (Müller-Mohnsen and Balk, 1966). In the case of the squid giant axon the relative permeabilities for K:Rb:Cs of the potassium channel are approximately 1:0.8:0 (Pickard, et al., 1964). Furthermore internally (but not externally) applied cesium is a reversible and

selective inhibitor of the potassium channel in the squid axon (Chandler and Meves, 1965). Internal rubidium may have a similar effect although the effect is not so large. Thus many recent experiments using axons perfused with cesium salts are abnormal in the sense that the potassium channels are eliminated by the procedure. Cesium and rubidium ions are selective inhibitors of the potassium channels of eel electroplaques (Nakamura, et al., 1965b). In the squid axon ammonium passes through the potassium channel more readily than through the sodium channel, the permeability ratio $K:NH_4$ being about 1:1/2 for the potassium channel (Binstock and Lecar, 1967).

One factor that is usually considered to play a role in the determination of specificity is the radius of the ion. For many years the discussions of radius have foundered on the difficult question whether one should speak of the crystal radius, of the hydrated radius, or of some other radius. If one assumes that size is important, then it seems that the question can now be answered to the extent of ruling out the crystal radius. At the same time the hydrated radius alone is not a sufficient criterion for permeation. The basis of these statements is found in Table VII. The three columns of numbers are the Stokes-Einstein radii ($R_s$) estimated from the limiting equivalent conductivities, the corrected (see below) Stokes-Einstein radii ($R_s'$), and the crystallographic radii ($R_c$) of the listed ions. The ions are grouped into three categories: those that pass through the potassium channel (1), those that pass through the sodium channel (2), and those that pass through neither or whose properties are not yet known (3). The correction factor for the radii is discussed in Chapter VI of Robinson and Stokes (1965). It compensates for the underestimation of the radii of particles with a radius smaller than 5 Å, using symmetrical quaternary ammonium ions (TMA, TEA, etc.) as a standard. In other words, while the column $R_s$ reflects the probable rank order of the hydrated radii, the column $R_s'$ is intended to suggest a more accurate picture of the actual dimensions. The values in parentheses are again corrected values using a more or less arbitrary extrapolation of the correction curve. In any case it is well to bear in mind that the numbers in the second column are the

Table VII

APPROXIMATE RADII OF IONS

| | Ion | $R_S$ | $R'_S$ | $R_C$ (in Å) |
|---|---|---|---|---|
| 1) | Rb | 1.18 | (2.4) | 1.48 |
| | K | 1.25 | (2.5) | 1.33 |
| | $NH_4$ | 1.25 | (2.5) | 1.48 |
| 2) | $NH_4$ | 1.25 | (2.5) | 1.48 |
| | Na | 1.84 | 3.3 | 0.97 |
| | Li | 2.38 | 3.7 | 0.60 |
| | Guan. | - | - | 2.70* |
| | $NH_3OH$ | - | - | 2.20* |
| | Hyz. | - | - | 2.20* |
| | Ca | 3.10 | 4.2 | 0.99 |
| 3) | Cs | 1.19 | (2.4) | 1.69 |
| | Ag | 1.30 | (2.6) | 1.26 |
| | TMA | 2.05 | 3.47 | 3.47 |
| | TEA | 2.82 | 4.00 | 4.00 |
| | TBA | 3.92 | 4.52 | 4.52 |

abbreviations:

| | |
|---|---|
| $R_S$ | Stokes-Einstein radius |
| $R'_S$ | Corrected value of $R_S$ (see text) |
| $R_C$ | Crystallographic radius |
| Guan. | Guanidinium |
| Hyz. | Hydrazinium |
| * | Geometric mean of the radii estimated from bond lengths, my calculation |

references: The radii are derived using the following formulae, tables, and appendix in Robinson and Stokes (1965)

| | |
|---|---|
| $R_S$ | Appendix 6.2 and formula 2.49a |
| $R'_S$ | Tables 6.2 and 6.3 and Figure 6.1 |
| $R_C$ | Appendix 3.1 |

prediction of a hypothesis. Our idea of the sizes of hydrated ions might change at any time in response to the experiments and theories of electrochemists.

The point to be made from Table VII is that on the basis of their crystal radii some of the ions that pass through the sodium channel are much smaller and others are much larger than those that pass through the potassium channel, while on the basis of hydrated radii they are uniformly larger. Thus the hydrated radius is of greater predictive value. Note that the ammonium ion, which passes through both sodium and potassium channels in the squid axon, occupies an intermediate position between the ions that pass through the sodium or potassium channels alone on the scale of hydrated radii. On the other hand, the hydrated radii of the impermeant class of ions fall in the same range as those of the permeant ions showing that there must be other factors involved in the selectivity of ionic channels as well. I believe the evidence suggests that ions cross the membrane in the hydrated form rather than in the unhydrated form. More evidence related to this point appears in the section entitled "The ionic movements and aqueous diffusion."

Although there are numerous theoretical discussions of how ionic specificity arises in various physico-chemical systems, there is as yet no experimental demonstration that one kind of theory is to be favored for nerve membranes. I shall not attempt to discuss this further and only reiterate that somewhere in the channel there is a device that can tell certain classes of ions from others. The multiplicity of channel types shows that these selection devices take various forms. It may be unwise to formulate a general theory to account for all kinds of devices inasmuch as their modes of action may differ. Some clues may come from studies of other biological examples of ionic specificity. Perhaps the "ion pumps" or the ion-activated enzymes will provide a key. Another very promising approach is the study of the ionic permeabilities induced in artificial bimolecular lipid films by various natural products.

Substances are known that make these films as permselective as nerve membranes and other substances produce voltage-dependent permeabilities that can lead to "action potential" phenomena (Mueller and Rudin, 1967a and b).

The voltage-dependent permeabilities

Early studies of the rectifying properties of squid giant axons (e.g. Cole and Curtis, 1941) led naturally to the proposal that the rectification might be the same as that found in permselective membranes with unequal concentrations of the diffusing ions on the two sides (Goldman, 1943). This proposal had to be abandoned for various electrochemical reasons such as its inability to account for the very large observed rectification ratios for small voltage changes (see Cole, 1965), but also it had to be abandoned for strong biological reasons.

The biological reasons were revealed with the voltage clamp method and with the comparative approach. Perhaps the most striking example is that in the squid axon and the frog node the potassium conductance increases on depolarization, as expected from the simple diffusion theory, whereas in the eel electroplaque the potassium conductance decreases on depolarization, an example of so-called anomalous rectification (Nakamura, et al., 1965b). Although the distribution of potassium and chloride ions is about the same for all cells, the potassium and chloride channels may separately exhibit an increase or a decrease of conductance on depolarization, depending on the particular tissue being studied (see Grundfest, 1966, for a review). A second observation from the voltage clamp experiments is that, the potassium conductance of nerves increases on depolarization regardless of whether the higher concentration of potassium ions is on the inside, as it normally is, or on the outside. The delayed rectification also occurs with equal potassium concentrations inside and outside. Thus, in general, the conductance changes cannot be explained on the basis of the properties of simple permselective

diffusion systems (see Cole, 1965, for a review of arguments leading to this conclusion). The rectifying mechanism must be part of the structure of the channels themselves. It must in some way affect the mobilities of the ions in the channel.

It is now widely assumed that some gate is associated with each channel that, in the simplest hypothesis, can "open" the channel or "close" it in response to the local electric field. It is convenient to imagine that the gate is in series with the device conferring ionic selectivity. This is a kind of all-or-none hypothesis at the molecular level, with the total conductance of the membrane increasing in units or "quanta" of the size of the conductance of one channel. The gates must respond to field changes in a few tens of microseconds, but that is not faster than some of the rapid conformational changes that have been described for macromolecules. The measured $Q_{10}$'s of the rates of opening and closing of the channels are between 1.8 and 3, as discussed earlier in this chapter. Such temperature coefficients are compatible with the idea of conformational changes.

Certain voltage-dependent properties of the channels have been examined only in the last few years. These are changes that have time constants longer than 100 msec. When an axon is depolarized by applied current or by elevated potassium concentrations, the potassium conductance increases in a few milliseconds as described by the Hodgkin-Huxley model, but if the depolarization is maintained, the conductance decreases again considerably (see for example Frankenhaeuser, 1963, or Ehrenstein and Gilbert, 1966). Frankenhaeuser (1963) proposed a parameter called k to describe this slow inactivation of potassium permeability. In the squid axon the time constants $\tau_k$ are of the order of ten seconds both for the inactivation at low potentials and for the loss of inactivation at high potentials (Ehrenstein and Gilbert, 1966). In addition to the fast sodium inactivation described by the parameter h, a slow inactivation of the sodium permeability mechanism also occurs in my experience

with frog nodes and has been reported with lobster axons (Narahashi, 1964). Sometimes the frog node has to be repolarized for several minutes before the sodium currents regain their full size. For this reason the reproducibility of measurements can be improved by clamping the nerve at the normal resting potential even when measurements are not being made. I follow this procedure in my experiments. It is not clear that the slow potassium and sodium inactivations are as simple as the closing of a normal gate. They may constitute a more extensive disarrangement of the channels.

## The ionic movements and aqueous diffusion

There are many properties of the ionic fluxes through channels that suggest that the ions move by aqueous diffusion. Some evidence for the hydration of the ions has already been discussed in the section "The ionic specificities of the channels." That evidence is at best indirect and, strictly, relates only to the processes determining selectivity. I have also mentioned that the $Q_{10}$'s of the maximum conductances are about 1.3, which is the same as the $Q_{10}$ of the conductance of an aqueous solution. In this section I shall show that the involvement of metabolism and of carriers can be ruled out for the channels.

There are many older studies that have been reviewed elsewhere showing that metabolic inhibitors and anoxia stop nervous conduction because, in the absence of a renewed supply of ATP, the sodium pumping mechanism slows and the ionic gradients cannot be maintained. The major new experimental approach in this area is the internally perfused squid axon. After 95% of the axoplasm is removed and replaced by a constantly flowing potassium sulfate solution, an axon can remain excitable for five hours and may conduct $3 \times 10^5$ impulses (Baker, Hodgkin, and Shaw, 1962). Axons survive four hours on internal perfusion with potassium chloride buffered with phosphate and cooled to 0° (Chandler and Meves, 1965), and they survive at least an hour when perfused with 50 mM cesium fluoride in 12 volumes

per cent glycerol at 23° C (Tasaki, Singer, and Takenaka, 1965). In Tasaki's experiments pronase or some other proteolytic enzyme is included in the perfusion medium for a minute or two to loosen up cytoplasmic components. In all of these experiments the ionic gradients are being maintained by perfusion and all metabolic events must have ceased by virtue of the (supposed) removal of all small molecules and most proteins and because of the adverse ionic and thermal conditions. Nevertheless, the channels behave normally showing that their function does not depend directly on metabolism. Doubtless metabolism is required in the long run to maintain some of the structural feature of the channels.

One of the best documented features of the ionic movements through channels is that an individual ionic current always flows in the direction of lower electrochemical potential, or, stated another way, an individual ionic current reverses its sign at the theoretical equilibrium potential for the ion in question. Hodgkin and Huxley (1952a) demonstrated this for the movements of sodium ions using different external sodium concentrations, and now it has been shown for internal sodium changes as well (e.g. Chandler and Meves, 1965). My experiment in Fig. 23 also relates to this point. In the published experiments $E_{Na}$ has been varied from +50 mv to about -50 mv. Frankenhaeuser (1962a) has given the most complete demonstration of the changes in the potassium currents with external changes of potassium concentration varying $E_K$ from about -80 mv to 0 mv. Other interesting measurements can be found in Moore, Anderson, Blaustein, et al. (1966). In all cases the observations agree that the direction of movement of ions through the channels is determined by the electrochemical potential grandient alone, in complete analogy with aqueous diffusion. Thus there is no thermodynamic evidence that the ionic fluxes are coupled to a source of free energy other than their own electrochemical activity differences.

Many of the transport processes in cell membranes are thought to involve carriers. The carrier hypothesis is usually proposed when

the relationship between the flux of a molecule and its concentration is a rectangular hyperbola instead of a straight line, i.e., when "saturation kinetics" are found. The concentration dependence of the transport can then be specified by a maximum velocity and an apparent dissociation constant K equal to the concentration of the transported substance that gives half of the maximum velocity. In general the value of K is within the range of physiologically encountered concentrations so that the carrier mechanism operates near its maximum velocity in some physiological conditions. Such phenomena have been extensively described in many cells, and elaborate kinetic schemes have been formulated that fit the data extremely well. An example of a well known system is the hexose carrier of the human erythrocyte with an apparent dissociation constant of 7 mM for D-glucose (LeFevre, 1962). There is no question that the mechanism is a membrane phenomenon as it can be demonstrated in erythrocyte ghosts (LeFevre, 1961). Another, more complicated carrier system is the "Na-K pump" of mammalian erythrocytes. The substrates of the pump are external potassium and internal sodium, ATP, and magnesium, all of these being needed simultaneously. The sodium and potassium ions can be transported against their electrochemical gradients by the pump. In almost physiological conditions the apparent dissociation constant of the carrier complex for sodium is about 40 mM and for potassium it is about 2 mM (Glynn, 1956; Post and Jolly, 1957). The cation pump can also be demonstrated in erythrocyte ghosts (Hoffman, 1962). Similar ionic pumps are found in all cell membranes including axon membranes. It should be remembered that the pump is not the same as the ionic channels.

There is no evidence for a carrier mechanism in the operation of the ionic channels of nerves. Consider, for a moment, that there is a carrier. Then we would expect 1) a maximum possible velocity (flux) near the highest velocity actually encountered in physiological conditions, and 2) a non-linear relation between ionic concentrations and ionic fluxes. What value should be chosen for the physiologically

maximum flux? The peak currents during the action potential are a reasonable choice. In the Rana node of Ranvier these currents are on the order of 3 na/node (or about 10 ma/$cm^2$ assuming a nodal area of 30 $\mu^2$) (Dodge, 1963), in Xenopus about 5 ma/$cm^2$ (Frankenhaeuser and Huxley, 1963), and in the squid giant axon about 0.8 ma/$cm^2$ (Hodgkin and Huxley, 1952d). Nevertheless in this thesis I have reported inward sodium currents of 20 na (or about 66 ma/$cm^2$) and outward potassium currents of 20 na in Rana. Frankenhaeuser (1962b) has reported inward potassium currents of 30 ma/$cm^2$ in Xenopus (in 120 mM KCl), and for the squid axon inward sodium currents of 5 ma/$cm^2$ and outward potassium currents of 10 ma/$cm^2$ are commonly reported (Cole and Moore, 1960). Thus, unlike typical carriers, the sodium and potassium channels can operate ten to twenty times faster than is required in physiological situations, and there is every indication from the nearly linear relationship between flux and potential that had large currents been the aim in these experiments, one would have needed only to increase the applied voltage to obtain currents of twice the observed value. The second property of carriers, the non-linear concentration dependence, has not been tested in sodium and potassium concentrations that exceed isotonic concentrations. The experiment should be done. It is well known that in the concentration range below isotonic, the sodium conductance is approximately proportional to the sodium concentration.

In summary, no evidence can be found for the direct involvement of metabolism or of carriers in the operation of the ionic channels. This is not because it would have been impossible to develop specific ionic carriers from the available biochemicals, for such an ion carrier (pump) mechanism does exist in membranes. It is specialized, however, for the recovery and the maintainance of the ionic gradients that the channels need for normal function. The channels, when open, behave in every respect, except for their great specificity, like open aqueous diffusion paths.

The number of channels at a node

In discussing the mechanism of channel function it would be helpful to know how many channels there are for this would indicate whether, for example, 1 or $10^6$ ions pass through a channel in an impulse. In the future it should be possible to count channels by some chemical labelling technique, perhaps with a derivative of TTX, but there are no such experiments at present. There is, however, one reported study in which the adsorption of TTX by a nerve was measured by a bioassay technique (Moore, Narahashi, and Shaw, 1967). A nerve trunk from the lobster walking leg was dipped into 50 μl of a 300 nM TTX solution until its conducted compound action potential failed. The blocked nerve was removed, and a fresh one was dipped into the same solution until it blocked. Although the process was repeated with seven nerve trunks, the bioassay showed the the TTX concentration was still more than 100 nM. Moore, et al. then estimated the extracellular space of the seven trunks and the total surface area of axonal membranes and concluded that fewer than 13 molecules of TTX were bound per square micron of axon surface in the blocked nerve. They suggested therefore that there are no more than 13 sodium channels per square micron in the lobster nerve.

The number of sodium channels per node of Ranvier may be estimated from this experiment with the lobster nerve by making two assumptions: 1) The conductance of a single sodium channel is the same in the node as in the lobster axons. 2) The average value of $\bar{g}_{Na}$ is the same in the lobster walking leg axons as it is in the lobster circumesophageal giant axon. The maximum sodium conductance of the node is 0.75 μmho (see Fig. 3) and that of the lobster giant axon is about 0.53 mho $cm^{-2}$ or 0.0053 μmho $\mu^{-2}$. This value for the lobster is twice the mean value of the 23 measurements reported in Table I of Narahashi, et al. (1964), doubled because it is apparent from their definition of maximum sodium conductance that they are actually reporting the value of the peak sodium conductance, which, as explained before, is only about half as great as $\bar{g}_{Na}$. With these

values the number of sodium channels at a node can be estimated:

$$13 \times 0.75/0.0053 = 1850 \text{ channels per node}$$

I have not tried an adsorption measurement on myelinated nerves. My simple equilibrium experiments give no information, as 1 ml of 1 nM TTX solution contains 1 pmole or almost $10^{12}$ molecules of TTX. The next few paragraphs present calculations based on simple physical chemical principles that suggest a lower limit to the number of ionic channels. This theoretical lower limit is a few thousand sodium channels per node, nearly the same as the upper limit estimated from the experiment of Moore, et al. The next few paragraphs present calculations based on simple physical chemical principles that suggest a lower limit to the number of ionic channels.

I recognize that in treating structures with dimensions of the order of atomic diameters, macroscopic phenomenological laws that are based on the properties of a continuum may have very little meaning. Nevertheless, I think it is instructive to carry through the calculations from our macroscopic point of view to get a sense of the order of magnitude of the events involved. At some time, probably far in the future, it may become possible to take explicit account in these calculations of the effects of water structure and of pore structure.

I assume that there is a single cylindrical aqueous pore in an infinite dielectric membrane. The radius (r) of the pore is 3 Å, in the range of the size of the ions of interest. A much wider pore seems unlikely because I assume that ionic specificity can arise only in confined spaces. The length (L) of the pore is 5 Å, a low value chosen because the part of the pore that is assumed to confer specificity need not be narrow for a distance of more than a few atomic diameters. The rest of membrane thickness might contain a wide funnel-like structure that connects the short pore to the surrounding fluids. The resistivity ($\rho$) of the aqueous medium is chosen to be 100 ohm cm, and the concentration (n) and diffusion constant (D) of the electrolyte are $10^{-4}$ moles $cm^{-3}$ and $10^{-5}$ $cm^2 sec^{-1}$, respectively. These values are appropriate for Ringer's solution.

1) The resistance of the pore: The resistance (R) of a conducting structure is equal to the integral of the resistance along the paths (L) of current flow:

$$R = \rho \int_0^L \frac{1}{A} \, dL \qquad (5.1)$$

where A is the area normal to the current flow. For our cylindrical pore the result is

$$R_{pore} = \rho \frac{L}{A} = \frac{100 \times 5 \times 10^{-8}}{\pi \times (3 \times 10^{-8})^2} = 2 \times 10^9 \text{ ohms}$$

In addition to the pore resistance, any macroscopic measurement would also include the access resistance, the resistance from the narrow pore to the bulk medium. The access resistance is easily approximated by integrating equation 5.1 assuming spherical symmetry from infinity to a hemispherical shell of radius 3 Å. The calculated value is then doubled to include the contribution from each end of the pore.

$$R_{access} = 2 \times \frac{\rho}{2\pi r} = \frac{100}{\pi \times 3 \times 10^{-8}} = 10^9 \text{ ohms}$$

The total observed resistance of the hypothetical pore would be

$$R = R_{pore} + R_{access} = 2 \times 10^9 + 10^9 = 3 \times 10^9 \text{ ohms}$$

This calculation can be used to estimate the number of ionic channels at a node of Ranvier on the assumption that a channel corresponds in a general way to the pore used here. The total resistances (the reciprocals of the maximum conductances) of the sodium, potassium, and leakage channels are 1.5, 8, and 40 megohms, respectively, suggesting that there are a minimum of 2000, 375, and 75, respectively, of the three kinds of ionic channels.

In the calculation one third of the total resistance is attributed to access resistance. This portion of the resistance should therefore increase with increases in the viscosity of the medium although the pore resistance might remain constant if the pore excluded the molecule used to increase the viscosity. Frankenhaeuser and Moore (1963b) increased the viscosity of the Ringer's solution many-fold by adding the salts to 0.5 M sucrose. In this experiment the total resistance to inward movements of sodium increased about 9%. Their experiment suggests that the access resistance is relatively much smaller for a real channel than for the hypothetical pore. Therefore, there may be many more than 2000 sodium channels with a resistance higher than $3 \times 10^9$ ohms per channel.

2) The diffusion-limited velocity: It is possible to estimate the rate of arrival of new ions at the mouth of a pore from Fick's law of diffusion. The flux through a channel cannot be larger than this rate.

The problem is exactly analogous to the problem of calculating the rate of encounter-controlled (diffusion-limited) chemical reactions. The simplest method is to use a solution of the diffusion equation for a spherical sink of radius r in an infinite medium of molecules at concentration n (first done by Smoluchowski). The desired quantity is the flux $\phi$ of molecules into the sink. It is easiest to consider the boundary condition n = 0 on the surface of the sphere. The time-dependent solution for the flux into the sink is (Frost and Pearson, 1961)

$$\phi_{sink} = 4 \pi r D n [ 1 + r (\pi Dt)^{-1/2} ] \qquad (5.2)$$

After about $10^{-7}$ sec the molecules near a sink of radius 3 Å have entered the sink and the flux is within 1% of the steady-state value:

$$\phi_{sink} = 4 \pi r D n \qquad (5.3)$$

The derivation and limitations of equations 5.2 and 5.3 have been discussed in many places in the literature of chemical kinetics. Some of these papers consider the effects of water structure, of crowding of the sinks, and of attractive and repulsive forces between the particles (see, for example, Noyes, 1960).

Formula 5.3 can be used for the pore model with the assumption that there is a hemispherical sink at one end of the pore. The arrival of new ions at the sink covering the pore is

$$\begin{aligned}\Phi_{pore} &= 2\pi r\, D\, n = 2\pi \times 3 \times 10^{-8} \times 10^{-5} \times 10^{-4} \\ &= 2 \times 10^{-16} \text{ moles sec}^{-1} \\ &= 1.3 \times 10^{8} \text{ ions sec}^{-1} \\ &= 20 \text{ pa}\end{aligned}$$

In the last line the flux is expressed as an electric current for direct comparison with the available data. If the sink has a single negative charge then the limiting flux of univalent positive ions is approximately doubled (Frost and Pearson, 1961), so I take 40 pa as the limiting current. Extrapolating to about twice the normally observed values, I estimate the maximum sodium, potassium, and leakage currents to be greater than 40, 40, and 5 na, respectively, giving a minimum of 1000, 1000, and 125, respectively, of the three kinds of ionic channels.

Thus two different calculations suggest a minimum of a few thousand sodium and potassium channels and a hundred leakage channels at one node of Ranvier. This number is very close to the estimated maximum number calculated from the entirely independent experiment of Moore, et al. (1967). Let us assume that there actually are $10^4$ sodium channels and calculate some parameters of their operation.

What is the surface density of channels? A node that is a 1μ gap between Schwann cells on a 10 μ axon has an area of about 30 $\mu^2$.

The actual dimensions of a node are still uncertain. There would be 300 channels per $\mu^2$, or, with the channels on a square lattice, each channel would be 600 Å from the next.

How rapidly do ions enter the channels? The conductance of a single sodium channel would be $10^4$ times smaller than the maximum sodium conductance of a node, or about $8 \times 10^{-11}$ mho (see Fig. 3), and the net flux of sodium ions through the sodium channel is proportional to the difference between the membrane potential and the sodium equilibrium potential. At the resting potential the driving force for sodium ions is about 125 mv, so the resulting current in one channel would be 10 pa or 60 ions $\mu sec^{-1}$. During a normal action potential the "standard node" model exhibits a net influx of $2 \times 10^{-17}$ moles of sodium or $1.3 \times 10^7$ sodium ions (Dodge, 1963). About 50% of the sodium channels are unavailable because of steady-state inactivation. The remainder pass an average of $2.5 \times 10^3$ sodium ions in one impulse.

How many sodium channels are open at the resting potential, and how many are open near the threshold firing potential? At -75 mv the value of $m_\infty^3 h_\infty$ is about 0.0001 (Table I) which means that each channel is open about $10^{-4}$ of the time or that at any particular time only one channel is open on the average! The firing threshold of typical frog nodes is -50 mv, i.e., 25 mv of depolarization. At threshold the inward current through the sodium channels just balances the outward current through leakage channels and therefore it is easy to calculate the value of $m^3h$ at threshold by setting the total ionic current (formula 1 in Fig. 3) equal to zero:

$$I_i = 0 = \bar{g}_L(E-E_L) + m^3h\left(1-\frac{E}{183}\right)\bar{g}_{Na,0\ mv}(E-E_{Na})$$

$$= 0.025 \times 25 + m^3h \times 1.3 \times 0.750 \times (-98)$$

$$= 0.63 - m^3h \times 96$$

$$m^3h = 0.0066$$

In other words, only about 70 sodium channels need to be activated to allow the node to fire. This small number suggests that it should be experimentally possible to see a "graininess" in the threshold and subthreshold responses of a node. Just such a phenomenon has been reported by del Castillo and Suckling (1957). From their studies of the fluctuation of the subthreshold response of nodes of Ranvier of Rana temporaria nerve fibers, they have suggested that "the subthreshold response is made up by the addition of a variable number of unit potential changes (equal to 1/100 - 1/200 of the action potential)." With their preparation (described in del Castillo and Stark, 1952) the average threshold depolarization is one quarter of the average spike height, and so the subthreshold response seems to be composed of 25 to 50 unitary events, in fair agreement with the prediction of the theories presented in the last few pages.

A reservation should be made before leaving this subject. I have treated the node of Ranvier as though it is a structure of constant properties. Of course, nodes differ greatly between fibers of different diameters and probably differ on individual fibers, especially near terminations or branches where extra demands are made. Specifically the numbers I have used in the preceeding discussion are for the standard node whose electrical properties are listed in Fig. 3. The estimated area of such a node is about 30 $\mu^2$. This value leads to an estimated capacitance of 6 $\mu F/cm^2$ (from 2 pF/node) and an estimated specific resistance of 12 ohm $cm^2$ (from 40 megohm/node).

## A View of the Axon Membrane

A very particular hypothesis of the permeability mechanisms of nerve membranes has been developed in the last two sections. In this section the hypothesis is summarized and restated in terms of a picture of the axon membrane. The final section of this chapter is a brief discussion of possible mechanisms of action of the drugs that I have studied.

Many of the components of axon membranes are revealed only by their physiological properties, and they are defined by operational definitions. In this sense we have no idea what the components look like and it will be the goal of future research to describe their physical structure. Nevertheless, I have drawn a schematic picture of the membrane (Fig. 31) that includes some of the operationally defined components. This drawing is the focus of the discussion that follows. It must be emphasized that the Fig. 31 is little more than an operational diagram of a square section of membrane. No particular scale has been used, but it might be useful to remember a few approximate dimensions: carbon-to-carbon bond, 1.5Å; diameter of hydrated sodium ion, 7Å; thickness of the unit membrane, 70Å; and estimated separation of sodium channels, 600Å.

The cell membrane is largely a flexible dielectric film that is permeable to oil- or lipid-soluble molecules and impermeable to most other molecules. It includes a bimolecular sheet of lipids whose hydrocarbon "tails" are in a quasi-liquid state in the center of the membrane and whose polar heads, bearing in general a net negative charge, lie near the surface of the membrane. The lipid layer probably accounts for the dielectric and permeability properties just mentioned. The surface regions and probably part of the central region include protein and polysaccharide molecules. The polysaccharides confer many antigenic properties on cell membrane and their sialic acid groups contribute negative charges. The proteins, and possibly the lipids as well, may account for most of the specialized transport and enzymatic functions associated with cell membranes.

The enzymatic functions of cell surface membranes are contributed by hydrolytic enzymes of which the ATPases, phosphotases, and cholinesterases have been most widely studied. In general the enzymes seem oriented to hydrolyze substrates on one particular side of the membrane only. Thus, for example, the ATPase associated with the ion pump requires intracellular ATP.

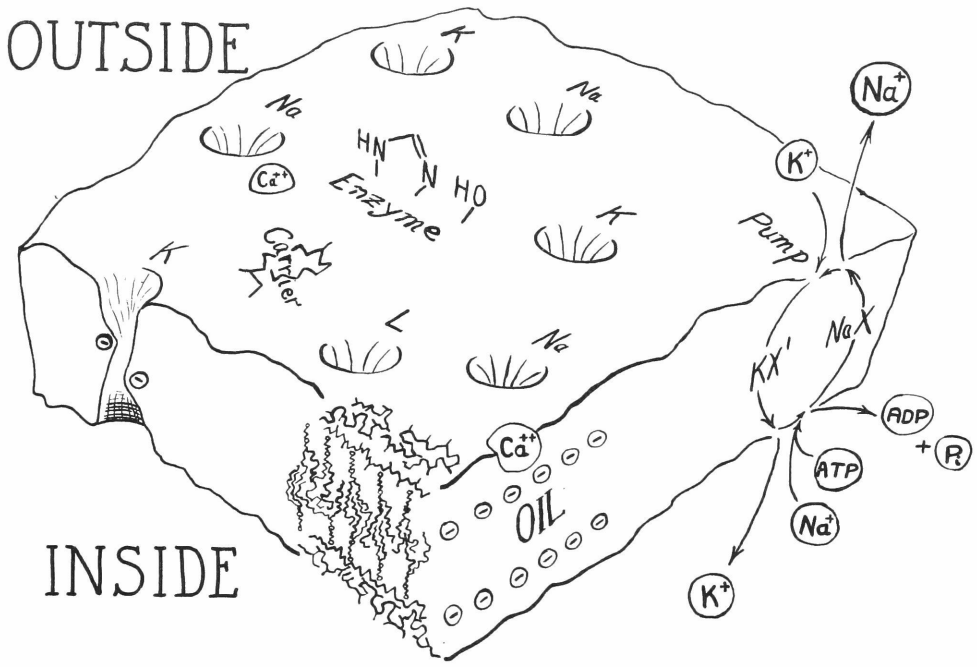


Figure 31. A view of the membrane. A schematic diagram of a square area of axon membrane showing physiological components that are known only in an operational sense. The components are not meant to be drawn to any particular scale. See text for a description of this hypothetical view.

The transport functions of the membrane are contributed by the ion pump just mentioned, various carriers for sugars and other metabolites, and the ionic channels. Each of these must be specialized structures somehow embedded in and penetrating the lipid layer of the membrane. As I have outlined in the previous two sections, the ionic channels seem to be ion-specific diffusion paths that open or close rapidly in response to the local electric field. In the picture the channels are represented as pores with a short constriction in conformance with the considerations discussed earlier. These few statements and the discussions in the other sections of this chapter summarize what can be said about the observable properties of the ionic channels. There is no chemical compound or group that has been demonstrated to be a part of or associated with the ionic channels. Much work remains to be done in this area.

## On the Mode of Action of the Drugs

There is a large literature that discusses the mode of action of some of the drugs I have studied. Many hypotheses have been advanced, but few firm conclusions can be reached. One of the most comprehensive reviews of drug action on excitable cell membranes is by Shanes (1958). He divided the drugs broadly into two categories, stabilizers and labilizers, defined by whether the drug action opposed changes in the membrane potential or enhanced them. Local anesthetics, high calcium, and TEA were called stabilizers, and veratrine was called a labilizer. It is clear now that voltage clamp measurements permit a much more complete characterization of drug effects than was possible at the time that Shanes wrote his review and that the stabilizer and labilizer categories are no longer as useful as they were then. Because in many cases, like that just mentioned, recent findings necessitate a revision of older ideas, I shall not review the older hypotheses. Nevertheless, any point of view that could be presented today would still be hypothetical, and what I say below should be considered to be a selection of some current speculations rather than an original contribution.

## Tetrodotoxin, Tetraethylammonium, and Calcium

Consider the ionic drugs TTX, TEA, and calcium. They act rapidly and reversibly when applied to the outside of the node. In each case fairly strong arguments can be advanced for an extracellular site of action on the frog node. Their actions are extremely specific, and concentrations much higher than those needed to produce measurable effects do not seem in any sense to be deleterious in my experiments, i.e., to produce lysis or mechanical fragility or similar, irreversible effects. It seems unlikely that these drugs enter into any chemical reaction that involves breaking or making a covalent bond, and I have presented evidence that each of them complexes reversibly with some specific receptor substance. The receptor for TEA is different from the receptors for TTX and for calcium. I have not been able to determine experimentally whether the receptors for TTX and for calcium are themselves different. There is associated with every sodium channel one TTX receptor and possibly several calcium receptors (see below) and with every potassium channel one TEA receptor.

In the simplest hypothesis the TTX and the TEA receptors would be the ionic channels themselves with the TTX and the TEA molecules partially entering the channels and obstructing the diffusion paths for the sodium and the potassium ions. Equally possible is the binding of the inhibiting molecule to a receptor that is adjacent to the channel. The formation of the complex would close the channel in some indirect fashion. In this hypothesis it is assumed that a single inhibitor molecule will completely inhibit a single channel without any effect on those channels lacking inhibitor complexes.

The above reasoning does not readily describe the action of high or low calcium concentrations. If it did, the sodium currents should be mathematically resolvable into two components, one of which would be the response of sodium channels lacking a bound calcium and

the other, the response of those with a bound calcium. One should be able to match all the sodium currents at all concentrations of calcium by adding together varying proportions of the two mathematical components. This cannot be done. Several explanations can be suggested. 1) There may be a single receptor as in the theory above but with the calcium complex forming and dissociating many times during one millisecond. In this case the probabilities of the opening and the closing of a sodium channel will be a complex time sequence compounded from the brief times when a calcium ion is bound and the intervening times when a calcium ion is not bound. 2) There may be several binding sites per channel with each having a particular degree of influence. 3) The channel may be affected by some property of the membrane that responds gradually to an increasing density of bound calcium. In the next few paragraphs I discuss a theory of calcium action that is a combination of the last two types of explanations.

Huxley (cited in Frankenhaeuser and Hodgkin, 1957) proposed a plausible theory of the action of calcium starting from the observation that a treatment with high calcium is analogous to a hyperpolarization in the squid giant axon. He suggested that the divalent cation binds to the outer surface membrane in sufficient concentration to cause a local increase in the outer surface potential, a change that can be shown to be analogous to a hyperpolarization. A schematic picture might be drawn as follows:

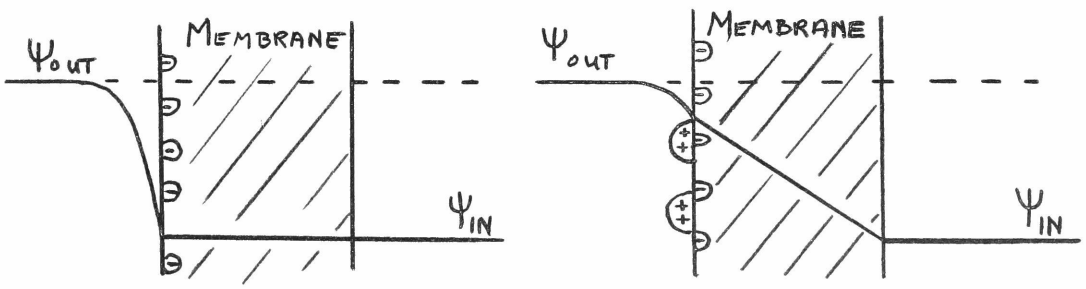

The diagram on the left represents a microscopic view of the membrane with negative charges on the outside and shows the hypothetical potential profile ($\Psi$) through the membrane with a large local potential drop outside (a surface potential) associated with the fixed charges. On the right some of the fixed charges have been neutralized by bound divalent ions and most of the potential drop now occurs inside the membrane. If the potential-measuring component of the permeability gate in an ionic channel is somewhere within the membrane, the change of the local electric field with the binding of calcium should be indistinguishable from the change that would occur in a true hyperpolarization. Notice that the actual membrane potential difference (measured in the bulk solutions) has been assumed to remain constant.

To adapt this theory to fit my observations on frog nodes, it is necessary to assume that the fixed negative charges (the calcium receptors) have a higher surface density near the sodium channels than near the potassium channels (or, more exactly, a higher density near the voltage-sensing device of the sodium channels). Then an increase in the calcium concentration would lead to a selective and gradual (as opposed to all or none) alteration of the kinetics of the sodium permeability changes. All of the voltage-dependent sodium parameters would be equally affected. One question remains. Does this explain the logarithmic relationship between calcium concentration and the observed voltage shifts and does this explain the value of the observed slope? A logarithmic relation is familiar for the Nernst membrane potential, and an approximately logarithmic relationship can be derived for the Gouy, the Donnan, and the Stern surface potentials (see equations 2.31, 2.42, and 2.45 in Davies and Rideal, 1963). The Stern theory seems suitable in the case of calcium effects because specific adsorption is taking place. It permits slopes up to 12.5 mv per e-fold change in a divalent ion to be compared with the observed 8.5 mv. At the present time there are enough unknown quantities to prevent a satisfactory test of a theory like Stern's; however, I

feel that Huxley's suggestion is an extremely valuable hypothesis that ties up the facts neatly and that someone may soon find a way to test it critically. Two important parameters to determine are the number of sites and the dissociation constant of the complex.

Some calcium ions have been included in the schematic drawing of the membrane (Fig. 31). They are assumed to be associated with some of the negative charges in the membrane near the sodium channels. Notice that if Huxley's hypothesis is correct, then the receptors for TTX and the receptors for calcium are proably different structures. Undoubtedly the other multivalent cations that have calcium-like actions exert theri effects by binding to the calcium receptors. The experimental observations suggest that the complexes formed by these cations have different dissociation constants from that of the calcium complex.

Lipid-soluble agents

Although the pharmacology of lipid-soluble anesthetics has been studied extensively, the mechanism of action of these drugs is considerably less well understood than that of drugs such as TTX, TEA, and calcium. One property of lipid-soluble drugs that has prevented a quick understanding of their mode of action is the diversity of molecules with anesthetic properties. The receptor hypothesis that is so fruitful in other areas of pharmacology begins to fall to pieces if local anesthetics, tranquilizers, alcohols, noble and "unreactive gases", and steroids (and possibly TTX) are said to share one receptor where they exert their major anesthetic effects. It is apparent that anesthetic action is not usually dependent on very precise steric relationships between the anesthetics and the receptors, if there are receptors.

Another difficulty in drawing firm conclusions springs from the lipid solubility of these molecules, which allows them to penetrate cells rapidly and to accumulate in all membrane-containing organelles. By permeating rapidly, the drugs frustrate attempts to

localize their site of action to the outside surfaces of the cell membrane. It has been shown, for example, that procaine is approximately as effective on the squid axon when applied internally by internal perfusion as when applied externally in the bathing medium (Narahashi, Anderson, and Moore, 1966a).

By accumulating in all membranes the lipid-soluble molecules necessarily produce many "non-specific" effects (including deleterious ones such as lysis) that are irreversible or at least slow to reverse. Adsorption studies have shown that about $10^8$ molecules of the phenothiazine tranquilizers (e.g., Compazine) are removed from the bathing medium by a single human red blood cell suspended in a 3 to $6 \times 10^{-5}$ M solution of the agent (Seeman and Weinstein, 1966). This adsorption corresponds approximately to one phenothiazine molecule bound per 100 $\mathring{A}^2$ of cell surface. In a $1.4 \times 10^{-5}$ M Compazine solution the area of the red cell surface, as estimated from electronmicroscopy, is 20% larger than normal without an appreciable increase in the membrane thickness (Seeman, 1966b). The extra area probably is contributed by tranquilizer molecules in the membrane and corresponds in amount to the expected area of the adsorbed molecules. At these low concentrations, phenothiazines stabilize the cell against lysis, presumably because the added membrane surface allows the cell to assume a larger final volume before the membrane is stretched. Ten times higher concentrations cause lysis of the red blood cell. Recall that in my experiments $2 \times 10^{-5}$ M Compazine selectively reduces $\bar{g}_{Na}$ by 50% and that $5 \times 10^{-4}$ M Compazine lyses the node. Seeman (1966a and b) has evidence for a similar degree of accumulation of alcohols, steroids, and local anesthetics in the red blood cell membrane at concentrations that are close to those that anesthetize nerves.

It is probable that the lipid-soluble agents accumulate in axonal (and other) membranes about as much as they do in erythrocyte membranes. Skou (1954) has studied the penetration of anesthetics into monolayers of lipids extracted from the sciatic nerves of frogs.

Five local anesthetics ranging from procaine to Dibucaine (a 1000-fold range of potency) accumulated in the monolayer at a surface densities varying from 0.4 to 1.0 molecules per 100 $\mathring{A}^2$ when they were applied in the aqueous phase at their "minimum blocking concentrations". Butyl alcohol at its minimum blocking concentration (68 mM) produced a surface density of 1.5 molecules per 100 $\mathring{A}^2$. To estimate the actual accumulation in the nerve membrane, these numbers should be divided by two. This divisor is derived as follows: the minimum blocking concentration is about four times higher in Skou's measurements on sciatic nerves with the sheath intact than in measurements with single fibers (i.e., divide by four) and further the nerve surface is a bimolecular layer of lipids rather than a monolayer (i.e., multiply by two). In any event, at anesthetic concentrations the drugs contribute significantly to the composition and volume of the membrane. Probably the mole fraction of drug in the membrane reaches 0.2 in some cases and the volume fraction may be 0.2 as well, as Seeman found for the erythrocyte. It is easy to see that such a drastic modification of the membrane could lead to many changes that are not directly related to the anesthetic action.

With this unpromising introduction to the difficulties inherent in studies with lipid-soluble agents, let us consider what statements can be made regarding their mode of action, with special reference to local anesthetics. Within the series of alcohols, of noble and "unreactive" gases, or of local anesthetics it is the lipid solubility (and related properties) that correlates most closely with the measured anesthetic potencies (Brink and Posternak, 1948; Carpenter, 1954; Miller, 1961; Löfgren, 1948; Skou, 1954). This sweeping correlation suggests that the molecules that exert the anesthetic action are mostly, if not entirely, within a region of lipid or hydrophobic character. Furthermore this region can become spacious enough to accomodate such large groups as the phenothiazine ring. Almost any part of the axolemma would be a good candidate for such a region.

At the same time, as was discussed in Chapter IV, there is considerable good evidence from studies of the pH dependence of the action of Xylocaine, Dibucaine, and Compazine that the active molecules are in the cationic form (Ritchie, et al., 1965a; Ritchie and Greengard, 1966). In these experiments on various desheathed nerves, a low pH favored anesthesia, a fact that stands in marked contrast to Skou's (1954) demonstration that a high pH in the underlying solution increased the equilibrium amount of anesthetic in a monolayer of nerve lipids. Seeman (1966b) also showed that high external pH favored the accumulation of local anesthetics and phenothiazines in the red blood cell membrane (as judged by stabilization against lysis). For example, the concentration of Dibucaine that gave the maximum stabilization was about $10^{-4}$ M at pH 8, $10^{-3}$ M at pH 7, and $10^{-2}$ M at pH 6. Considering the various experiments, one can see that a suitable increase of the pH of the anesthetizing solution might increase the quantity of anesthetic in the membrane by a factor of ten and yet relieve the conduction block. Thus accumulation per se does not produce the anesthetic action (however, Seeman's (1966b) experiments suggest that it does produce lysis).

The discussion of the preceding paragraphs leads naturally to the conclusion that only a few of the anesthetic molecules in the membrane actually contribute to the anesthesia. Let me call these molecules the "active molecules" and the remainder the "inactive molecules". The published experiments suggest that the hydrophilic nitrogens of active molecules are protonated and that the hydrophobic parts are surrounded by hydrophobic groups of the membrane.

Consider the hypothesis that only one active molecule is needed to block one ionic channel as is the case with TEA. In my experiments the sodium channels are fairly selectively inactivated by procaine, Xylocaine, and Compazine. As discussed earlier there may be one anesthetic molecule per 100 $\text{Å}^2$ of the membrane at the blocking concentration. This is a surface density 3600 times greater than the estimated surface density of sodium channels, so the ratio of active

molecules to inactive molecules would be 1:3600. It would be desirable to increase this ratio to nearly 1:1 to test the hypothesis of one active molecule per channel.

The active fraction probably increases significantly as the pH is lowered below pH 7.3 (the value used in my experiments). Indeed both Skou (1954) and Seeman (1966b) saw large decreases in accumulation on lowering the pH from 7 to 6. Experiments with isolated nerves should therefore be tried at low pH because of the theoretical interest in the minimum number of adsorbed molecules needed for anesthesia and because there may be fewer deleterious and irreversible side effects of accumulation. Possibly the depression of $\bar{g}_K$ and the small shifts of the voltage-dependent parameters produced by procaine and Xylocaine are caused by some of the molecules that I have called "inactive". In that case pH changes could also make it possible to separate the blockage of sodium channels from these other effects. If experimental conditions are found that permit a clear separation of the effects on $\bar{g}_{Na}$ from all other effects it will be reasonable to suppose that TTX and local anesthetics act on the same receptors.

A different approach to the investigation of the active molecules is the use of permanently quaternary derivatives of the local anesthetics. There has been almost no research in this area either with model systems such as red blood cells or monolayers of lipids or with single nerve fibers. In Chapter IV I discussed a few experiments with three quaternary derivatives of Xylocaine: QX-314, QX-222, and QX-572. It was a great surprise to find that QX-314 and QX-222 are not only non-toxic but also without any detectable actions even at concentrations as high as 40 mM. Only QX-572 has typical local anesthetic activity. This substance has the interesting properties of being 250 times less soluble in oleyl alcohol than Xylocaine, yet active at the same concentrations as Xylocaine and far more difficult to wash away (like the very much more lipid-soluble Dibucaine in this respect). Clearly these properties are due to the

permanent charge combined with a duplication of the hydrophobic end of the molecule; however, until model studies are done with this and other quaternary molecules, it will be difficult to interpret my experiments in the framework of the preceding discussion. There is room for much additional work in this area.

Even less is known about the mode of action of lipid-soluble agents other than local anesthetics. I will not attempt to discuss this difficult area further. It seems that some new experimental design or some new hypotheses on the molecular action of these compounds will be needed before we can increase our understanding significantly.

# Appendix I

## THE LEAKAGE AND THE CAPACITY CURRENTS

This appendix concerns a determination, from leakage current measurements, of some of the resistances in the equivalent circuit of the mounted nerve and a discussion of an extra capacity current that appears in nerves several hours after they are dissected.

### The Leakage Current

In the experiments described in this thesis the membrane currents are calibrated by using the assumption that the leakage resistance is 40 megohms, the value determined by Tasaki (1953 and 1955). Other authors, for example Schmidt and Stämpfli (1966), calibrate the currents in a different way. They assume that the resistance in the current path from pool E to point D (refer to Fig. 33 of Appendix II) is 37.5 megohms for Xenopus and thus they can calculate the current flowing from E to D from the measured potential in pool E by Ohm's law. Since in my measurements I also have a record of the potential in pool E, it is possible both to compare the calibration methods for consistancy and to determine the ratio of the resistance from E to D to the leakage resistance of the node $N_o$ ($R_{ED}$:$R_N$).

Table VIII is a list of the observed values of this ratio arranged as a histogram. The numbers in each column are the identifying numbers (in octal) of the first record taken on each of the 25 nodes studied in my experiments with the computer. The numbers are not scattered widely, which shows that $R_{ED}$:$R_N$ is fairly constant in my experiments and justifies the independent procedures for calibrating the current. The mean value of the ratio is about 0.75, meaning that a 75 mv potential applied to pool E will polarize the node $N_o$ by 100 mv. If the leakage resistance is 40 megohms, then $R_{ED}$ is about 30 megohms for these nerves.

Tasaki (1953) measured the cable properties of single toad nerve fibers. He found that a small steady voltage signal applied at

Table VIII

A HISTOGRAM OF THE RATIOS OF THE TWO RESISTANCES $R_{ED}:R_N$

| Ratio of resistances ($R_{ED}:R_N$) | | | | |
|---|---|---|---|---|
| .58-.67 | .68-.77 | .78-.87 | .88-.97 | .98-1.07 |
| 1 | 7 | 12 | 34 | 62 |
| 210 | 25 | 22 | 360 | 231 |
| 313 | 40 | 52 | 366 | 235 |
| 327 | 246 | 200 | | |
| 374 | 331 | 266 | | |
| 407 | 343 | | | |
| | 437 | | | |
| | 461 | | | |

Each number listed is the identifying number of the first measurement on a node.

one node spreads electrotonically down the fiber, attenuated by a factor of two at successive nodes. This would correspond to a space constant of about 3 mm for the largest fibers with 2 mm between nodes. The D.C. cable properties of a fiber can be represented by the following equivalent circuit:

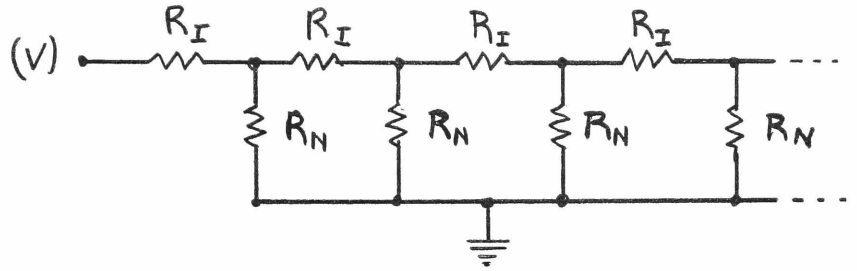


where $R_I$ stands for the internodal resistance and $R_N$ for the nodal resistance. It turns out that any cable with the ratio of $R_I$:$R_N$ equal to 1:2 will have the property that Tasaki observed of attenuating a steady voltage V by a factor of two at each node. Therefore if $R_N$ of a normal fiber is 40 megohms, then $R_I$ is 20 megohms. This value for $R_I$ has been used in other parts of this thesis.

Now we can calculate the value of $R_N$ of the nodes that are depolarized by KCl in pool E. Because of the depolarization, the resistance of these nodes is expected to be lower than 40 megohms. Consider that the point labelled (V) in the above diagram is point D and that the grounded part of the circuit is pool E. The values of $R_I$ and $R_{ED}$ are 20 and 30 megohms, respectively. A simple calculation shows that 16 megohms is the value of $R_N$ for the nodes in pool E. In other words, prolonged depolarization in KCl lowers the resistance of a node 2.5 times - from 40 to 16 megohms - and, as can easily be shown, the decrement of potential per node in such a cable would be 3-fold instead of 2-fold. Frankenhaeuser and Waltman (1959) showed that the space constant of Xenopus fibers falls by a factor of two and that the nodal resistance falls by a factor of four on KCl depolarization. They were surprised to find that the resistance only fell 4-fold inasmuch as voltage clamp measurements give much larger resistance changes with short depolarizations. Their observation led

them to propose a slow potassium inactivation that is now well established (see Chapter V). My measurement shows that there is a slow potassium inactivation in Rana fibers also, for if there were no potassium inactivation the resistance of Rana nodes would be expected to fall more than 6-fold in KCl (the ratio of $\bar{g}_K$ to $\bar{g}_L$).

## The Capacity Current

The elimination of the capacity current is a trivial problem when the circuit of Fig. 1 is a truly equivalent representation of the electrical behavior of the preparation. In an ideal voltage clamp a delta function of current would flow into the capacitor charging it instantly to its new voltage. In practice the maximum current available is finite and therefore the capacity current flows for a finite time. If the maximum voltage swing of the clamping amplifier is small, the maximum current through the preparation will be small, and the flow of capacity current will persist long enough to obscure the early time courses of the ionic currents. When the amplifiers used in these experiments are used to clamp a simple electrical equivalent circuit of the preparation with the node represented by a 40 megohm resistor and a 2 pF capacitor in parallel, the capacitative transient is finished after 40 μsec.

In recent years a new kind of equivalent circuit has appeared that seems to apply to the membranes of most muscle fibers (Falk and Fatt, 1964). The new feature is that in addition to purely resistive or purely capacitative branches in the circuit there is at least one branch with a resitor and a capacitor in series, e.g. the left hand branch of Fig. 32. In muscle fibers this branch can be identified anatomically with a specialized internal extension of the cell membrane, the transverse tubular system (Peachey, 1965). The capacitance represents the dielectric of the membrane in the tubule, and the resistance represents the narrow lumen of the tubule through which applied current must flow to reach the membrane. Special problems arise when one attempts to apply a voltage clamp to such a

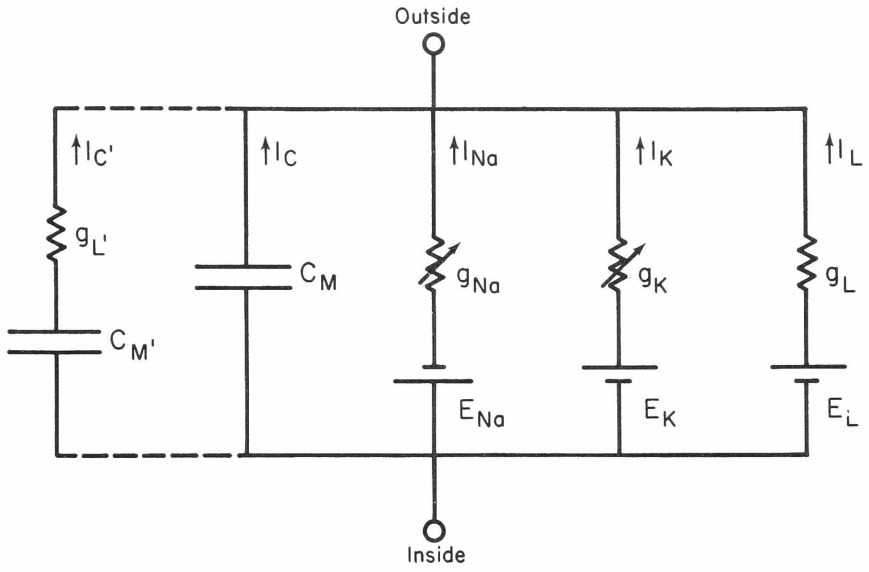


Figure 32. Equivalent circuit with an extra series R-C branch. An equivalent circuit consisting of the circuit originally proposed by Hodgkin and Huxley for the squid axon (see Fig. 1) plus an extra branch containing a series resistance and capacitance (connected by dashed lines). Sometimes this circuit is a better representation of the nodal membrane than the circuit in Fig. 1 (see text).

system. The voltage clamp will measure potential and supply current between the inside of the fiber and the bath, but the membrane within the tubule will remain partially uncoupled from the feedback system to a degree that depends on the resistance of the tubule. Thus when the "ordinary" capacitance ($C_M$) of the membrane is charged in a step change of voltage, the potential across the extra capacitance in the tubule ($C'_M$) will approach the desired voltage with an exponential time course having a time constant given by the product $R'_L \times C'_M$ of the resistance and capacitance in that branch of the circuit. This time constant is frequently on the order of milliseconds, and thus the delay in the voltage clamp of muscle fibers is much more than can be tolerated in many experiments. In this discussion I have tacitly assumed that the membrane in the tubule does not itself undergo any electrical excitation. Another consequence of this additional branch in the equivalent circuit is that the capacity current is prolonged. This is to say that ideally in the circuit of Fig. 32 there is a delta function of current corresponding to charging of the "ordinary" capacity, followed by an exponentially decaying extra-capacity. The time constant of the extra-capacity current is identical with the time constant of the charging. The extra-capacity current has to be subtracted from the voltage clamp currents before the analysis of the ionic currents can proceed.

In my experiments with the node of Ranvier, I observe a component of current that behaves like an extra-capacity current and that is apparent after a poor dissection or appears several hours after a good dissection. The magnitude of the current increases gradually with time and the time constant of the decay increases gradually to as long as one millisecond. This is probably the same as the "capacitative artifact" seen by Dodge and Frankenhaeuser (1959) in Xenopus nodes. The amplitude of the current is always proportional to the change of the membrane potential in a step displacement in either direction, and the amplitude and time constant are insensitive to drugs, to changes in the ionic content of the medium, and to

changes in the frequency response of the voltage clamping amplifier. If the standard parallel 40 megohm leakage resistance and 2 pF capacitance of the nodal equivalent circuit are supplemented by another branch, as in Fig. 32, containing a 20 megohm resistance and 15 pF capacitance in series, the observed currents of a typical case can be imitated. This gives an extra-capacity current whose initial amplitude is half as large as the leakage current and whose time constant of decay is 0.3 msec. In fact, the decay of the extra-capacity current is not strictly exponential. It is more closely imitated by the sum of several exponentially falling curves. My interpretation of these phenomena is that the myelin on either side of the node gradually lifts away from the axon over a longitudinal distance of several microns, thus exposing a new large area of axon membrane that contributes the extra capacitance. The series resistance would then be the resistance of the newly formed external crack between the myelin and the exposed membrane. If this new membrane were electrically excitable it would lead to instability in the voltage clamp because of the large decoupling resistance. As instability appeared only rarely and not always in association with extra-capacity currents, I conclude that the axon membrane that is normally covered by myelin is electrically inexcitable.

If these interpretations are correct, then the gradual appearance of extra membrane during an experiment will not affect the accuracy of the voltage clamp measurements so long as the extra-capacity current is subtracted from the records.

The phenomenology of this extra-capacity current was first called to my attention by Dr. J. W. Moore who has observed similar currents with the lobster giant axon using the sucrose-gap technique (Takata, Pickard, Lettvin, and Moore, 1966). In the case of the lobster axon this extra current has been considered to be part of a time-dependent leakage current. It would be interesting to attempt to test the hypothesis of extra capacitance by an electron microscopic study of nodes of Ranvier that do and those that do not exhibit this extra current component.

# Appendix II

## SOME ERRORS IN THE MEASUREMENTS

Some of the errors of the voltage clamp procedure of Frankenhaeuser and Dodge are discussed in their original papers (1958, 1959) and by Dodge (1963). In this appendix, I discuss two errors which they did not consider in detail.

### An Error in the Potential Measurement

This discussion is based on the equivalent circuit in Fig. 9 of Chapter III and on the expanded circuit of Fig. 33 in this appendix. Figure 33 includes the cable properties of the myelinated nerve with successive nodes and internodes, the stray capacitances from the internodes to pools B and E, the potentials at calomel cells C and B and at the liquid junction C-B in the seal, and the stabilizing chopper amplifier (3). I assume that the reader understands the operation of the method and the meaning of Figs. 9 and 33. This section concerns the calomel and liquid junction potentials and the properties of amplifiers 1 and 3 as they influence the recorded membrane potential.

#### The origin of the error in principle and in practice

Ignore for a moment amplifier 3 and recall that amplifier 1 operates with negative feedback that keeps its summing point (the input) at zero potential. Because, ideally, no current flows in this condition, point D is also at zero potential. What happens if the D.C. balance of amplifier 1 is in error by 1 mv (always referred to the input of the amplifier)? Then point C is held 1 mv off ground and a current of 0.5 na ($10^{-3}$ volts/$2\times10^{6}$ ohms) flows from C to B and also, of necessity, from D to C. The resistance from D to C is approximately 40 megohms (see Appendix I) so point D is polarized 20 mv off ground (0.5 na $\times$ 40 $\times$ $10^{6}$ ohms) by the current flow. Furthermore, more than half of the current flowing in the circuit

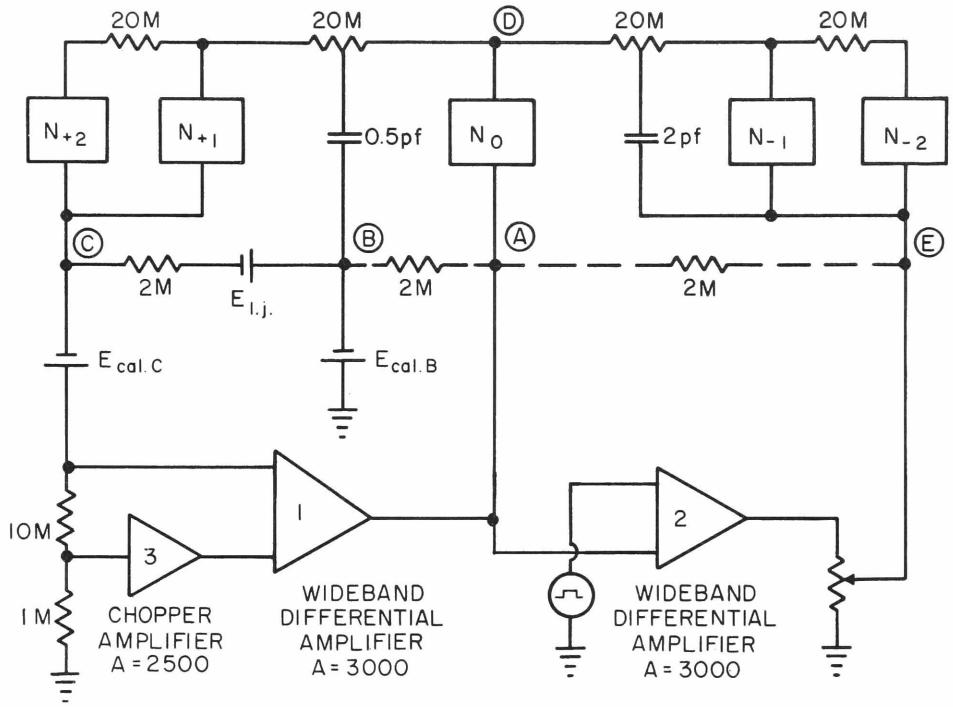


Figure 33. Equivalent circuit of the voltage clamp. The electrical equivalent circuit of the preparation with the associated amplifiers drawn to suggest some of the errors in the method. Compare this circuit with Fig. 9. The point D is inside the node under investigation and C, B, A, and E are in the electrolyte solutions of the lucite chamber. The circuit includes the resistance of the internodal axoplasm (20 M), the impedances of the nodes (labelled N), the "seal" resistance from pool to pool (2 M), some stray capacitance from pools to internodes (0.5 pF and 2 pF), and the potentials at calomel cells ($E_{cal}$) and at one liquid junction ($E_{l.j.}$).

D-C-B will flow through $N_o$ (the rest of it comes through the branch E-D), and this will polarize the node by perhaps 10 mv. Thus in an experiment to measure the resting potential of a node, a 1 mv unbalance in amplifier 1 can cause a 30 mv error (the sum of the errors above) in the measurement as well as a potentially deleterious polarization of the node.

In the above example the unbalance is assumed to arise in the amplifier itself but similar arguments show that errors of the same magnitude arise if the amplifier is well balanced but has a 0.5 na grid current and also if the potential $E_{l.j.}$ or the difference in the calomel cell potentials $E_{cal.C}$ and $E_{cal.B}$ amounts to 1 mv.

In practice all of these conditions are encountered during an experiment. The amplifier drifts 1 mv in less than an hour and can be displaced more than this instantly by a mechanical shock. Bad 5879 tubes used for the input cathode followers can exhibit 0.5 na grid currents. Old calomel cells of the small size used to reduce stray capacitance may differ by 1 mv especially when their temperature is lowered by 15° at the beginning of an experiment. The liquid junction potential between the Ringer's solution in pool B and the KCl in pool C can be several millivolts. As it is not convenient to monitor these factors during the course of an experiment, it must be considered that the value of the resting potential or even the value of the membrane potential in this voltage clamp is not known.

The following procedure is useful for standardizing experiments. Successive records with the same node can be compared by first matching the value of $E_{Na}$, a stable reference point (see Chapter III). Also at the beginning of the experiment the holding potential of the voltage clamp is adjusted until the value of the resting sodium inactivation ($1-h_\infty$) is between 0.4 and 0.5 as judged visually from the relative amplitude of the sodium currents. In normal fibers this potential is thought to be approximately -75 mv (Dodge and Frankenhaeuser, 1958; Dodge, 1963). During an experiment it occasionally is clear that there has been a large drift from this setting, and

the system is then rebalanced. In general, the deviations are attributable to a drift of the balance of amplifier 1. All the figures in this thesis have a voltage calibration that depends on this method of estimating the absolute potential at the beginning of the experiment. The usefulness of the method is indicated by the close correspondence between the "standard" node, adapted from Dodge (1963), and the various nodes described in this thesis (after adjustment is made for the difference in temperature between the preparation and the standard). Figure 27 illustrates how similar some of my observations are to Dodge's. Indeed it was a surprise to me to find a very high degree of similarity in the details of the empirical rate constants among the great majority of the nodes that I studied.

The chopper amplifier

Dr. J. W. Moore recommended chopper stabilization of amplifier 1, a convenient method of automatic compensation for the D.C. drift of wide-band amplifiers. The basic principle of a chopper amplifier is to convert a D.C. signal to an A.C. signal that can then be amplified readily and rectified to give the amplified D.C. signal. The chopping procedure results in unusual D.C. stability in chopper amplifiers. Amplifier 3 in Fig. 33 is an A.C. amplifier with a gain of $10^4$ (modelled after Moore and Gebhart, 1962) preceded by a 94 cps chopper and succeeded by another 94 cps chopper and a long time constant filter, attenuator, and balance network. The overall gain for a D.C. signal at the input is about -2500 with a D.C. stability on the order of 1 μv over a several day period. The input of amplifier 3 is connected by a ten-to-one divider (10M:1M) to the in-phase input of amplifier 1, and the output of 3 is connected directly to the out-of-phase input of 1. When both amplifiers are in operation in the feedback loop A-B-C, the overall drift is such that pool C may vary by 10 μv in a day and the measured membrane potential (at A) may vary by 0.3 mv in the same period. Thus the chopper amplifier effectively removes the drift due to changes in the balance of amplifier 1, although it does not correct for grid

current or for potentials in calomel cells or at liquid junctions. Amplifier 3 was built after experiment 355 was completed and was used consistently from experiment 360 on. The need for correcting records by matching $E_{Na}$ was nearly eliminated by its use.

## An Error in the Current Measurement

In most of my experiments and in most of Dodge's (1963) the measured time courses of the potassium currents at the highest depolarizations cannot be matched by the mathematical expression for potassium currents that appears in the model for voltage clamp current (see Fig. 9). The deviation from the theoretical expression can readily be seen in some of the records in this thesis as a maintained slow increase of the potassium currents instead of the expected asymtotic approach to a steady state. For example, compare the theoretical curves in Fig. 4 and the "normal" curves in Figs. 14 and 21 with the "abnormal" curves in Figs. 13, 17, and 30. See also the last few points at high depolarization in Fig. 2.13 of Dodge (1963). In this section I show that these abnormalities in the measured currents arise from an artifact in the method of measurement and that the actual currents probably have a time course that conforms to theoretical expectation. The artifact comes from a rectification in the current measuring circuit.

The currents are normally taken to be proportional to the voltage applied to pool E in the chamber, because the resistance from pool E to point D ($R_{ED}$) is assumed to be constant. It will now be helpful to refer to the equivalent circuit of Fig. 33 and to recall the contents of the first part of Appendix I. Appendix I shows that $R_{ED}$ is about 30 megohms (M), the total resistance of the following equivalent circuit:

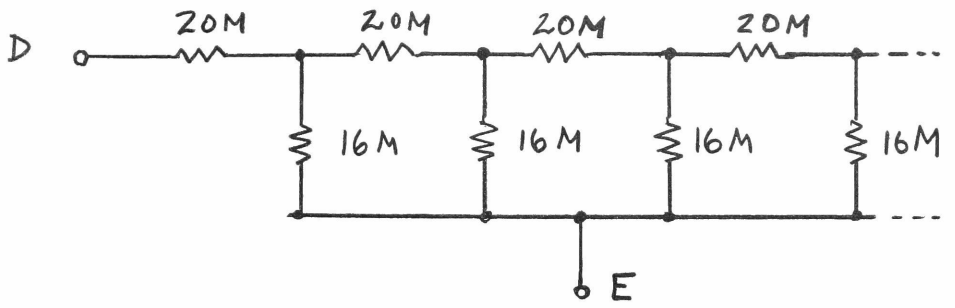


When an outward (depolarizing) current flows through the node under investigation ($N_o$), the same total current will flow inward (hyperpolarizing) through the nodes in pool E in a distributed fashion. About 2/3 of the current flowing from E to D will enter at the first node ($N_{-1}$), 2/3 of the remaining 1/3 will enter at the second node ($N_{-2}$), etc.

Consider, for example, a voltage clamp to +75 mv. The total outward current through $N_o$ might be 15 na in the steady state. Of this, 10 na is entering through $N_{-1}$, polarizing it to -160 mv (10 na $\times$ 16M) from its resting state of 0 mv. The nodes in pool E have a lower resistance than a restingnode because they are depolarized in KCl. Hyperpolarization always turns off the low resistance potassium channels and leaves only the leakage resistance (about 30 M in KCl-treated nodes). Thus during a voltage clamp to +75 mv some of the nodes in pool E will be repolarized enough to make them revert slowly towards their high resistance state. Replacing the value 16M by 30 M in node $N_{-1}$ of the cable above increases the value of $R_{ED}$ from 30 M to 35 M, showing that a 15% slow increase in the resistance $R_{ED}$ can be expected when large outward currents are made to flow through $N_o$. The increase may be slightly larger (to a limit of 36.5 M) if several nodes revert to high resistance. This resistance increase will cause an increase in the recorded voltage in pool E even though the current through $N_o$ may have reached a steady state. These factors account well for the slow apparent increase in the potassium current after a steady state should have been reached.

The rectification at the nodes in pool E is especially clearly seen in steady-state current-voltage measurements made with depolarizations lasting many seconds instead of the 25 msec used in all my other experiments. I have made such longer time measurements by connecting an X-Y recorder directly to the current and voltage signals of the voltage clamp. The clamp voltage is then varied continuously by turning a potentiometer from -75 mv to -120 mv, then from -120 mv to +70, and finally from +70 mv back to -75 mv at a rate of about 2 mv/sec. Several of these records are superimposed on each other in Fig. 34. Arrows indicate the direction in which the lines were traced out. Line 1 shows the current-voltage relation obtained with a normal fiber. In the hyperpolarizing direction the relation is a straight line with a slope that is used to obtain the current calibration. In the depolarizing direction the expected potassium conductance increase of the node in pool A appears as a non-linearity starting at -43 mv. The change is small because of potassium inactivation with these long depolarizations. As the clamp voltage increases further, there are at least two more regions of rectification (at +6 mv and at +33 mv). These do not appear in the more rapid measurements elsewhere in the thesis (e.g., Figs. 20, 22 and 28) and probably represent rectification (increase of resistance) in the individual nodes in pool E. These artifacts first appear when the current is strong enough to repolarize the first node in pool E. Because of the rectification, the current calibration becomes incorrect. After reaching +70 mv the voltage is slowly decreased again. The currents now seem high because of the high resistance in the current measuring circuit. The "current" decreases gradually as the voltage decreases until suddenly the current record falls sharply by 8% in one step at +25 mv and again by 20% at +11 mv. The steps in the record represent the sudden decreases of resistance of the nodes in pool E as the polarizing current through them falls. In effect these nodes produce a "potassium spike" caused by long anodal polarization followed by a depolarization. After this measurement the nodes in pool E are treated for 30 sec with 1%

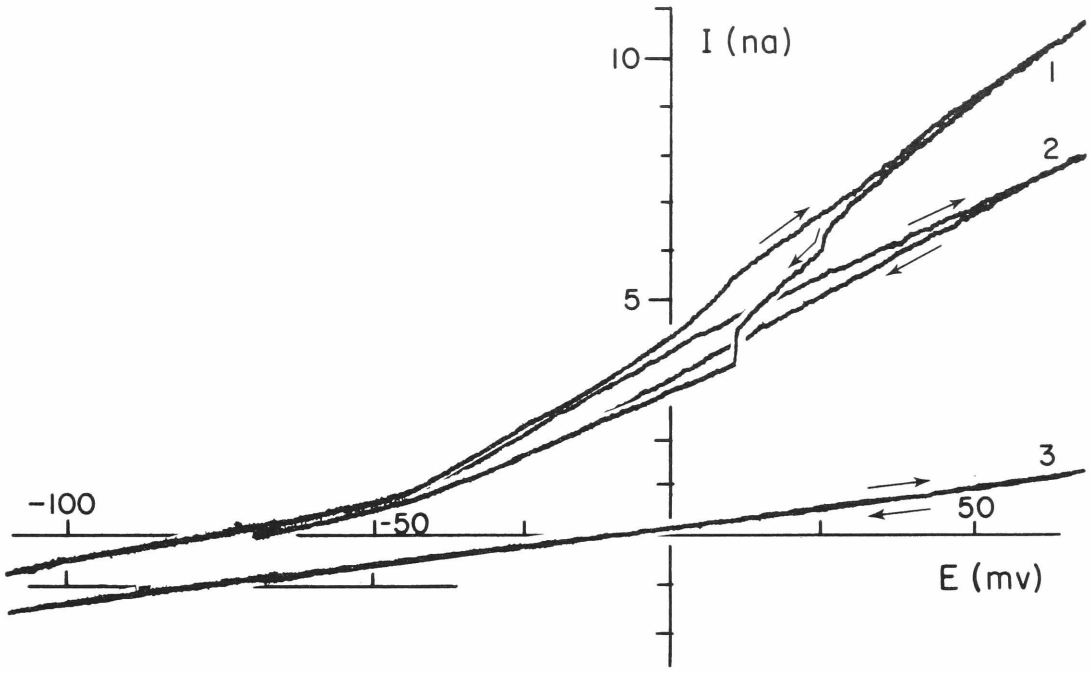


Figure 34. Demonstration of rectification of the nodes in pool E. Three superimposed records of the current-voltage relations of the same node of Ranvier. The current scale is calibrated using the initial slope of line 1 but, as explained in the text, is inaccurate over much of the recorded range. 1) Ringer's solution in pool A. 2) As before but KCl in pool E briefly replaced by 1% formaldehyde. 3) 115 mM TEA Ringer's in pool A. This last line is displaced by -1 na for clarity. The current-voltage relations were traced out on an X-Y recorder in the direction indicated by the arrows at a rate of 2 mv/sec. (T = 20° C)

formaldehyde and the record of line 2 is taken. Only part of the record is shown. The brief formaldehyde treatment removes most of the resistance changes in pool E and the measured current probably is a more faithful record of the actual current. The remaining hysteresis may be attributable to potassium inactivation in the node in pool A. Finally the Ringer's solution in pool A is replaced by isotonic TEA, and the record of line 3 is taken. The record is displaced by -1 na on the current axis for clarity. Notice that $\bar{g}_L$ has been decreased to 65% of normal in isotonic TEA, as reported earlier, and that the current-voltage relation of the leakage channels is perfectly linear (ohmic).

The rectification in the current path that occurs in the 25 msec of my standard test pulse makes it necessary to estimate the value of the steady-state current (for current-voltage relations) from the part of the record that precedes the rectification. This is achieved in the procedure described in the Methods by matching the master template for the time course of the potassium current to all but the latest part of the log-log plot of currents. The record and the template usually match at least to the point where the theoretical curve has reached 95% of its final amplitude. From this point on the measured curve, as drawn in the log-log plot, may continue to rise along a straight line of very shallow slope instead of levelling off to a steady state. This artifactual rise of current usually occurs to a significant degree in 25 msec only for the largest depolarizations used (to above +30 mv).

# Appendix III

## COMPUTER TECHNIQUES

This appendix is a technical statement of some of the techniques used in gathering and analysing the voltage clamp records. It contains little of general usefulness to those who are not interested in using this apparatus or in imitating it. It is assumed that the reader is familiar with computers and with programming, and that he understands the methods as outlined in Chapter III.

A block diagram of the flow of information in the peripheral equipment is shown in Fig. 35. The boxes in the left side of the figure are the standard components of any voltage clamp experiment: a repetition rate generator (PRF) that triggers a sequence of three pulse generators (S1, S2, and S3) whose outputs can be varied in amplitude and duration; voltage clamp amplifiers; the nerve preparation; and an oscilloscope (OSC).

The remaining boxes in the figures serve in the analog-to-digital conversion of the current and voltage signals from the nerve. The period during which digital samples are to be recorded is determined by the sample length gate generator that gates the primary 10 μsec crystal clock. The gated 10 μsec clock triggers a time scaling circuit to produce a stable 50 μsec timing clock that starts sometime within 10 μsec of the rise of the sample length gate. The master control switch controls a gate that gates the 50 μsec clock signal. Thus the line labelled "sample clock" has a 50 μsec clock signal that lasts as long as the sample gate and that appears only if the master control switch is set to on. This timing clock signal activates the digital conversion circuits. The master control switch is mounted with the controls of the voltage clamp circuits and allows the experimenter to start and stop the recording process without leaving the experiment.

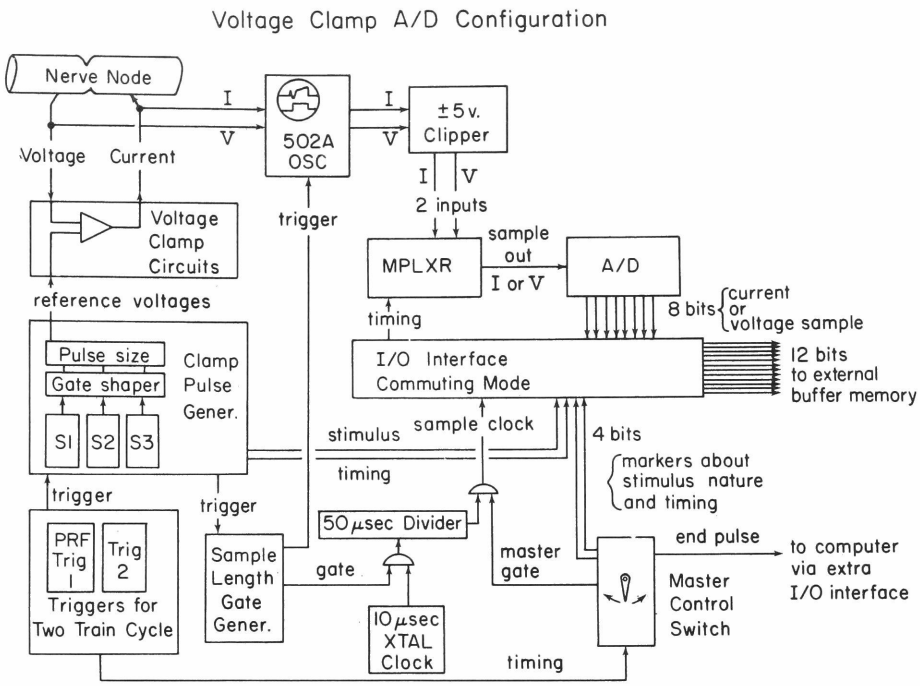


Figure 35. Block diagram of the analog to digital conversion. A schematic diagram of the flow of information from the nerve to the computer memory showing the voltage clamp apparatus (left), the clock circuits (lower center), and the interface with associated multiplexer and analog to digital converter (center and right). See text for explanation.

The amplified current and voltage signals are taken from cathode followers in the oscilloscope, through a circuit that attenuates the signal 2:1 and limits the voltage swing to the useable range of ±5 volts, and to the multiplexer (MPLXR, Adcom model 401). The multiplexer is initially set to follow the current channel. The 50 μsec timing pulses activate the following sequence. On the arrival of the timing pulse the multiplexer "hold" circuit operates until the analog-to-digital converter (A/D, Adcom model 208C) has generated an 8 bit word representing the current. The 8 bit number plus four more bits of information (see below) are sent to the computer memory about 14 μsec after the beginning of the sequence. Then the multiplexer switches automatically (commuting mode) to the voltage signal, following and holding until a second 8 bit word has been generated and sent to the computer. The multiplexer is then switched back to the current channel, and the sequence is terminated about 30 μsec after its beginning. I have used this apparatus successfully with a 40 μsec clock instead of the 50 μsec clock normally used. It would not be possible, however, to obtain a current and voltage sample every 30 μsec.

The extra four bits that go to the computer can be used for any information that is useful in the analysis of the record. I use them to mark the beginning and end of the voltage clamp test pulse, to mark the beginning of a record i.e. the first word to go in at the beginning of the sample gate, and to denote whether the amplifiers are in the current clamp mode or in the voltage clamp mode.

Dr. Hartline's CDC 160-A computer has four 4096-word memory banks. The digital sampling, the preliminary analysis, and the output to the magnetic tape are controlled by a machine language program that occupies half of one bank. The program activates one bank as an external buffered memory to store the incoming digital samples and then waits for a signal (end pulse) to appear on an auxilliary input-output interface that signifies the end of the buffered input. The end pulse is generated by the voltage clamp circuits a few milliseconds

after the sample length gate has risen and fallen for the second time. (Recall from Chapter III that two lists of digital samples are stored in memory in quick succession before any analysis is performed.) When the end pulse arrives, the program disconnects the input buffer and searches the new data lists for the bit that marks the beginning of the second list. With the lists identified, the rest of the operation is handled by standard machine language techniques. Chapter III describes the steps in sufficient detail.

After the magnetic tape record of the condensed data has been made, one character is put out on the computer's typewriter and the input buffer is initiated again for input from the analog-to-digital conversion circuits. The output of one character on the typewriter serves to record the progress of the experiment both because it makes a typed count of the number of the records that have been made and because the typewriter makes enough noise for the experimenter to hear that the sampling and analysis cycles are taking place.

After the experiments are finished, the magnetic tape record is analysed by a Fortran program. This program is 500 Fortran statements in length and uses standard techniques throughout. Only one point deserves mention. The data are taped in a machine language format, which is at least three times more condensed than the standard Fortran format. The condensed format saves time in the later analysis because it shortens the length of tape to be searched for the desired record. (All the experiments in this thesis are recorded in a total of about a million 12 bit words.) Because of the machine language tape format, I have combined a machine language program for magnetic tape input with the Fortran program for analysis.

An additional Fortran program was used to calculate nodal action potentials and other responses to applied currents from the Hodgkin-Huxley equations with empirical rate constants appropriate to the node of Ranvier. This mathematical model of the node is discussed in Chapter II and is illustrated in Fig. 3 and in Table I. The empirical formulae from which the curves of Fig. 3 and the numbers in Table I

were calculated are listed below. These formulae are adapted with small changes from Dodge's (1963) description of his "node 7".

(m): $$\alpha_m = \frac{1.6\,\phi}{\exp\phi - 1} + \frac{6.0}{1+\left(\frac{E+25}{18}\right)^2}; \quad \phi = \frac{-37.5-E}{3.8}$$

$$\beta_m = \frac{4.05\,\phi}{\exp\phi - 1} \quad ; \quad \phi = \frac{37.5 + E}{13.2}$$

(h): $$\alpha_h = \frac{0.14\,\phi}{\exp(0.8\phi) - 1} \quad ; \quad \phi = \frac{79 + E}{5.9}$$

$$\beta_h = \frac{4.0}{\exp\phi + 1} \quad ; \quad \phi = \frac{-17 - E}{14.5}$$

(n): $$\alpha_n = \frac{0.34\,\phi}{\exp\phi - 1} + 0.1 \quad ; \quad \phi = \frac{-15 - E}{15.9}$$

$$\beta_n = \frac{0.085\,\phi}{\exp\phi - 1} \quad ; \quad \phi = \frac{37.5 + E}{12.2}$$

The program for calculating action potentials uses a modified Euler method to integrate the simultaneous non-linear equations of the complete model (e.g. equations of the form of equation 2.10). One of these calculations is shown in this thesis in Fig. 18. The time increment between successive approximations of the integrals was set a 4 μsec for this calculation. A time increment of 1 μsec is suitable for accurate calculations of normal action potentials. The calculation in Fig. 18 could be done by a coarser "integration interval" because the rapidly changing sodium permeability was assumed to be absent.

# BIBLIOGRAPHY

Armstrong, C. M. (1966). Interference of injected tetra-n-propyl ammonium bromide with outward sodium ion current in squid giant axons. Nature, 211, 322-323.

Armstrong, C. M. and Binstock, L. (1964). The effects of several alcohols on the properties of the squid giant axons. J. Gen. Physiol. 48, 265-277.

Armstrong, C. M. and Binstock, L. (1965). Anomalous rectification in the squid giant axon injected with tetraethylammonium chloride. J. Gen. Physiol. 48, 859-872.

Askari, A. (1966). Uptake of some quaternary ammonium ions by human erythrocytes. J. Gen. Physiol. 49, 1147-1160.

Baker, P. F., Hodgkin, A. L., and Shaw, T. I. (1962). Replacement of the axoplasm of giant nerve fibres with artificial solutions. J. Physiol. 164, 330-354.

Bard, P. (1961). Medical physiology. 11th ed., St. Louis, C. V. Mosby Co.

Binstock, L. and Lecar, H. (1967). Ammonium ion substitutions in the voltage clamped squid giant axon. Abstr. 11th Meet. Biophys. Soc. 19.

Blaustein, M. P. and Goldman, D. E. (1966). Competitive action of calcium and procaine on lobster axon. A study of the mechanism of action of certain local anesthetics. J. Gen. Physiol. 49, 1043-1064.

Brink, F. (1954). The role of calcium ions in neural processes. Pharm. Rev. 6, 243-298.

Brink, F. and Posternak, J. M. (1948). Thermodynamic analysis of the relative effectiveness of narcotics. J. Cell. and Comp. Physiol. 32, 211-234.

Carpenter, F. G. (1954). Anesthetic action of inert and unreactive gases on intact animals and isolated tissues. Am. J. Physiol. 178, 505-509.

Castillo, J. del and Stark, L. (1952). Local responses in single medullated nerve fibers. J. Physiol. 118, 207-215.

Castillo, J. del and Suckling, E. E. (1957). Possible quantal nature of subthreshold responses at single nodes of Ranvier. Fed. Proc. 16, 29.

Chandler, W. K., Hodgkin, A. L. and Meves, H. (1965). The effect of changing the internal solution on sodium inactivation and related phenomena in giant axons. J. Physiol. 180, 821-836.

Chandler, W. K. and Meves, H. (1965). Voltage clamp experiments on internally perfused giant axons. J. Physiol. 180, 788-820.

Cole, K. S. (1965). Electrodiffusion models for the membrane of squid giant axons. Physiol. Rev. 45, 340-379.

Cole, K. S. and Curtis, H. J. (1941). Membrane potential of the squid giant axon during current flow. J. Gen. Physiol. 24, 551-563.

Cole, K. S. and Moore, J. W. (1960). Ionic current measurements in the squid giant axon membrane. J. Gen. Physiol. 44, 123-167.

Cowan, S. L. and Ing, H. R. (1935). Quaternary ammonium salts and the action currents in nerve. J. Physiol. 84, 90-110.

Cowan, S. L. and Walter, W. G. (1937). The effects of tetraethyl-ammonium iodide on the electrical response and the accommodation of nerve. J. Physiol. 91, 101-126.

Davies, J. T. and Rideal, E. K. (1963). Interfacial Phenomena. 2nd ed., New York and London. Academic Press.

Dettbarn, W. D. (1962). The active form of local anesthetics. Biochim. Biophys. Acta. 57, 73-76.

Dodge, F. A. (1961). Ionic permeability changes underlying nerve excitation. In Biophysics of Physiological and Pharmacological actions. AAAS, Washington, D.C.

Dodge, F. A. (1963). A study of ionic permeability changes underlying excitation in myelinated nerve fibers of the frog. Thesis, The Rockefeller University.

Dodge F. A. and Frankenhaeuser, B. (1958). Membrane currents in isolated frog nerve fibre under voltage clamp conditions. J. Physiol. 143, 76-90.

Dodge, F. A. and Frankenhaeuser, B. (1959). Sodium currents in the myelinated nerve fibre of Xenopus laevis investigated by the voltage clamp technique. J. Physiol. 148, 188-200.

Eccles, J. C. (1966). The ionic mechanisms of excitatory and inhibitory synaptic action. Ann. N. Y. Acad. Sci. 137, 473-494.

Ehrenstein, G. and Gilbert, D. L. (1966). Slow changes of potassium permeability in the squid giant axon. Biophysical J. 6, 553-566.

Falk, G. and Fatt, P. (1964). Linear electrical properties of striated muscle fibers observed with intracellular electrodes. Proc. Roy. Soc. B. 160, 69-123.

Finkelstein, A. and Mauro A. (1963). Equivalent circuits as related to ionic systems. Biophys. J. 3, 215-237.

Frankenhaeuser, B. (1957). A method for recording resting and action potentials in the isolated myelinated frog nerve fibre. J. Physiol. 135, 550-559.

Frankenhaeuser, B. (1962a). Delayed currents in myelinated nerve fibers of Xenopus laevis investigated with voltage clamp technique. J. Physiol. 160, 40-45.

Frankenhaeuser, B. (1962b). Potassium permeability in myelinated nerve fibres of Xenopus laevis. J. Physiol. 160, 54-61.

Frankenhaeuser, B. and Hodgkin, A. L. (1957). The action of calcium on the electrical properties of squid axons. J. Physiol. 137, 217-243.

Frankenhaeuser, B. and Huxley, A. F. (1964). The action potential in the myelinated nerve fibre of Xenopus laevis as computed on the basis of voltage clamp data. J. Physiol. 171, 302-315.

Frankenhaeuser, B. and Moore, L. E. (1963a). The effect of temperature on the sodium and potassium permeability changes in myelinated nerve fibres of Xenopus laevis. J. Physiol. 169, 431-437.

Frankenhaeuser, B. and Moore, L. E. (1963b). The specificity of the initial current in myelinated nerve fibres of Xenopus laevis. J. Physiol. 169, 438-444.

Frankenhaeuser, B. and Waltman, B. (1959). Membrane resistance and conduction velocity of large myelinated nerve fibers from Xenopus laevis. J. Physiol. 148, 677-682.

Frost, A. A. and Pearson, R. G. (1961). Kinetics and mechanism. 2nd ed., N.Y., John Wiley and Sons, Inc.

Gallego, A. (1951). Loss and recovery of excitability by normal and by degenerating nerves deprived of sodium. J. Gen. Physiol. 35, 129-144.

Gallego, A. and Lorente de Nó, R. (1951). On the effect of ammonium and lithium ions upon frog nerve deprived of sodium. J. Gen. Physiol. 35, 227-244.

Glynn, I. M. (1956). Sodium and potassium movements in human red cells. J. Physiol. 134, 278-310.

Goldman, D. E. (1943). Potential, impedance, and rectification in membranes. J. Gen. Physiol. 27, 37-60.

Goldman, D. E. and Blaustein, M. P. (1966). Ions, drugs, and the axon membrane. Ann. N. Y. Acad. Sci. 137, 967-981.

Goto, T., Kishi, Y., Takahashi, S. and Hirata, Y. (1965). Tetrodotoxin. Tetrahedron. 21, 2059-2088.

Grundfest, H. (1961). Ionic mechanisms in electrogenesis. Ann. N. Y. Acad. Sci. 94, 405-457.

Grundfest, H. (1966). Heterogeneity of excitable membrane: electrophysiological and pharmacological evidence and some consequences. Ann. N. Y. Acad. Sci. 137, 901-949.

Hagiwara, S. (1966). Membrane properties of the barnacle muscle fiber. Ann. N. Y. Acad. Sci. 137, 1015-1024.

Hagiwara, S. and Naka, K. (1964). The initiation of spike potential in barnacle muscle fibers under low intracellular $Ca^{++}$. J. Gen. Physiol. 48, 141-162.

Hagiwara, S. and Saito, N. (1959). Voltage-current relations in nerve cell membrane of Onchidium verruculatum. J. Physiol. 148, 161-179.

Hille, B. (1966a). Selective inhibition of ionic channels in nerve. Abstr. 10th Meet. Biophys. Soc. 142.

Hille, B. (1966b). The common mode of action of three agents that decrease the transient change in sodium permeability in nerves. Nature, 210, 1220-1222.

Hille, B. (1967a). Quaternary ammonium ions that block the potassium channel of nerves. Abstr. 11th Meet. Biophys. Soc., 19.

Hille, B. (1967b). The selective inhibition of delayed potassium currents in nerve by tetraethylammonium ion. J. Gen. Physiol. in press.

Hodgkin, A. L. and Huxley, A. F. (1952a). Currents carried by sodium and potassium ions through the membrane of the giant axon of Loligo. J. Physiol. 116, 449-472.

Hodgkin, A. L. and Huxley, A. F. (1952b). The components of membrane conductance in the giant axon of Loligo. J. Physiol. 116, 473-496.

Hodgkin, A. L. and Huxley, A. F. (1952c). The dual effect of membrane potential on sodium conductance in the giant axon of Loligo. J. Physiol. 116, 496-506.

Hodgkin, A. L. and Huxley, A. F. (1952d). A quantitative description of membrane current and its application to conduction and excitation in nerve. J. Physiol. 117, 500-544.

Hodgkin, A. L., Huxley, A. F. and Katz, B. (1952). Measurement of current-voltage relations in the membrane of the giant axon of Loligo. J. Physiol. 116, 424-448.

Hodgkin, A. L. and Keynes, R. D. (1957). Movements of labelled calcium in squid giant axons. J. Physiol. 138, 253-281.

Hoffman, J. F. (1962). The active transport of sodium by ghosts of human red blood cells. J. Gen. Physiol. 45, 837-859.

Huxley, A. F. and Stämpfli, R. (1951a). Direct determination of membrane resting potential and action potential in single myelinated nerve fibres. J. Physiol. 112, 476-495.

Huxley, A. F. and Stämpfli, R. (1951b). Effect of potassium and sodium on resting and action potentials of single myelinated nerve fibres. J. Physiol. 112, 496-508.

Ing, H. R. (1936). The curariform action of onium salts. Physiol. Rev. 16, 527-544.

Julian, F. J., Moore, J. W. and Goldman, D. E. (1962). Current-voltage relations in the lobster giant axon membrane under voltage clamp conditions. J. Gen. Physiol. 45, 1217-1238.

Kao, C. Y. (1966). Tetrodotoxin, saxitoxin and their significance in the study of excitation phenomena. Pharm. Rev. 18, 997-1049.

Kato, G. (1936). On the excitation, conduction, and narcotisation of single nerve fibres. Cold Spring Harbor Symp. Quant. Biol. 4, 202-213.

Khodorov, B. I. and Belyaev, V. I. (1964). Generation of A.P. in single nodes of R. of isolated frog nerve fibers under the influence of Ni and Cd ions. Bull. Exp. Biol. Med. 75, 379.

Koketsu, K., Cerf, J.A. and Nishi, S. (1959). Effect of quaternary ammonium ions on electrical activity of spinal ganglion cells in frog. J. Neurophysiol. 22, 177-194.

Koketsu, K. and Nishi, S. (1966). Effects of tetrodotoxin on the action potential in Na-free media. Life Sciences, 5, 2341-2346.

Koppenhöfer, E. (1966). TEA - Wirkung auf die Ionenströme markhaltiger Nervenfasern von Xenopus laevis. Arch. Ges. Physiol. 289, R9.

Koppenhöfer, E. (1967). Die Wirkung von Tetraäthylammoniumchlorid auf die Membranströme Ranvierscher Schnurringe von Xenopus laevis. Arch. ges. Physiol. 293, 34-55.

Koppenhöfer, E. and Weymann, D. (1965). Voltage clamp am bespülten Ranvierschen Schnürring. Arch. Ges. Physiol. 283, R7.

LeFevre, P. G. (1961). Persistence in erythrocyte ghosts of mediated sugar transport. Nature, 191, 970-972.

LeFevre, P. G. (1962). Rate and "affinity" in human red blood cell sugar transport. Am. J. Physiol. 203, 286.

Loeb, J. and Ewald, W. F. (1916). Chemical stimulation of nerves. J. Biol. Chem. 25, 377-390.

Löfgren, N. (1948). Studies on local anesthetics. Xylocaine, a new synthetic drug. Stockholm. Ivar Haeggströms Boktryckeri.

Lorente de Nó, R. (1947). A study of nerve physiology. Studies Rockefeller Inst. Med. Rev. 131 and 132.

Lorente de Nó, R. (1949). On the effect of certain quaternary ammonium ions upon frog nerve. J. Cell. Comp. Physiol. 33, Suppl., 1-231.

Lorente de Nó, R., Vidal, F., and Larramendi, L.M.H. (1957). Restoration of sodium-deficient frog nerve fibres by onium ions. Nature, 179, 737-738.

Lüttgau, H-C. (1958). Die Wirkung von Guanidinhydrochlorid auf die Erregunsprozesse in isolierten markhaltigen Nervenfasern. Arch. Ges. Physiol. 267, 331-348.

Mauro, A. (1961). Anomalous impedence, a phenomenological property of time-variant resistance. Biophys. J., 1, 353-372.

Miller, S. M. (1961). A theory of gaseous anesthetics. Proc. Nat. Acad. Sci. 47, 1515-1524.

Moore, J. W. (1965). Voltage clamp studies on internally perfused axons. J. Gen. Physiol. 48, No. 5 pt. 2, 11-17.

Moore, J. W. and Adelman, W. J., Jr. (1961). Electronic measurement of the intracellular concentration and net flux of sodium in the squid axon. J. Gen. Physiol. 45, 77-92.

Moore, J. W., Anderson, N., Blaustein, M., Takata, M., Lettvin, J. Y., Pickard, W. F., Bernstein, T. and Pooler, J. (1966). Alkali cation specificity of squid axon membrane. Ann. N. Y. Acad. Sci. 137, 818-829.

Moore, J. W., Anderson, N. and Narahashi, T. (1966). Tetrodotoxin blocking: early conductance channel or sodium? Fed. Proc. 25, 569.

Moore, J. W. and Gebhart, J. H. (1962). Stabilized wide-band potentiometric preamplifiers. Proc. I. R. E. 50, 1928-1941.

Moore, J. W., Narahashi, T. and Shaw, T. I. (1967). An upper limit to the number of sodium channels in nerve membrane? J. Physiol. 188, 99-105.

Moore, J. W., Ulbricht, W. and Takata, M. (1964). Effect of ethanol on the sodium and potassium conductances of the squid axon membrane. J. Gen. Physiol. 48, 279-295.

Mosher, H. S., Fuhrman, F. A., Buchwald, H. D. and Fischer, H. G. (1964). Tarichatoxin-tetrodotoxin: a potent neurotoxin. Science, 144, 1100-1110.

Mueller, P. and Rudin, D. O. (1967a). Development of $K^+$-$Na^+$ discrimination in experimental bimolecular lipid membrane by macrocyclic antibiotics. Biophys. Biochem. Res. Comm. 26, 398-404.

Mueller, P. and Rudin, D. O. (1967b). Action potential phenomena in experimental bimolecular lipid films. Nature, 213, 603-604.

Müller-Mohnssen, H. and Balk, O. (1966). Stationäre elektrische Eigenschaften des Ranvierschen Schnürrings während der Rb-Depolarisation. Arch. Ges. Physiol. 289, R8.

Nakamura, Y., Nakajima, S. and Grundfest, H. (1964). Eel electroplaques: spike electrogenesis without potassium activation. Science, 146, 266-268.

Nakamura, Y., Nakajima, S. and Grundfest, H. (1965a). The action of tetrodotoxin on electrogenic components of the squid axon. J. Gen. Physiol. 48, 985-996.

Nakamura, Y., Nakajima, S. and Grundfest, H. (1965b). Analysis of spike electrogenesis and depolarizing K inactivation in electroplaques of Electrophorus electricus, L. J. Gen. Physiol. 49, 321-349.

Narahashi, T. (1964). Restoration of action potential by anodal polarization in lobster giant axons. J. Cell. Comp. Physiol. 64, 73-96.

Narahashi, T. (1966). Dependence of excitability of cockroach giant axons on external divalent cations. Comp. Biochem. Physiol. 19, 759-774.

Narahashi, R., Anderson, N. C. and Moore, J. W. (1966b). Tetrodotoxin does not block excitation from inside the nerve membrane. Science, 153, 765-767.

Narahashi, T., Deguchi, R., Urakawa, N. and Ohkubo, Y. (1960). Stabilization and rectification of muscle fiber membrane by tetrodotoxin. Am. J. Physiology, 198, 934-938.

Narahashi, T., Moore, J. W. and Scott, W. R. (1964). Tetrodotoxin blockage of sodium conductance increase in lobster giant axons. J. Gen. Physiol., 47, 965-974.

Nishi, S., Soeda, H. and Koketsu, K. (1965). Effect of alkali-earth cations frog spinal ganglion cells. J. Neurophysiol., 28, 457-472.

Noyes, R. M. (1960). Effects of diffusion rates on chemical kinetics. Prog. Reaction Kinetics. 1, 129-160.

Peachey, L. D. (1965). The sarcoplasmic reticulum and transverse tubules of the frog's sartorius. J. Cell. Biol. 25, 209-232.

Pickard, W. F., Lettvin, J. Y., Moore, J. W., Takata, M., Pooler, J. and Bernstein, T. (1964). Caesium ions do not pass the membrane of the giant axon. Proc. Nat. Acad. Sci. 52, 1177-1183.

Post, R. L. and Jolly, P. C. (1957). The linkage of sodium, potassium, and ammonia active transport across the human erythrocyte membrane. Biochim. Biophys. Acta. 25, 118-128.

Raventós, J. (1937). Pharmacological actions of quaternary ammonium salts. Quart. J. Exp. Physiol. 26, 361-374.

Ritchie, J. M. and Greengard, P. (1966). On the mode of action of local anesthetics. Ann. Rev. Pharm. 6, 405-430.

Ritchie, J. M., Ritchie, B. and Greengard, P. (1965a). The active structure of local anesthetics. J. Pharm. Exp. Ther. 150, 152-159.

Ritchie, J. M., Ritchie, B. and Greengard, P. (1965b). The effect of the nerve sheath on the action of local anesthetics. J. Pharm. Exp. Ther. 150, 160-164.

Robertson, J. D. (1960). The molecular structure and contact relationship of cell membranes. Prog. Biophys. Biophys. Chem. 10, 344-418.

Robinson, R. A. and Stokes, R. H. (1965). Electrolyte solutions. 2nd ed. revised. London. Butterworths.

Schmidt, H. (1960). Die Wirkung von Calcium-Ionen auf das Membranpotential markhaltiger Nervenfasern. Arch. Ges. Physiol. 271, 634-654.

Schmidt, H. (1965). Die Wirkung von Tetraäthylammoniumchlorid auf das Membranpotential und den Membranwiderstand von Bündeln markhaltiger Nervenfasern. Arch. Ges. Physiol. 282, 351-361.

Schmidt, H. and Stämpfli, R. (1966). Die Wirkung von Tetraäthylammoniumchlorid auf den einzelnen Ranvierschen Schnürring. Arch. Ges. Physiol. 287, 311-325.

Seeman, P. (1966a). Erythrocyte membrane stabilization by steroids and alcohols; a possible model for anesthesia. Biochem. Pharmacol. 15, 1632-1637.

Seeman, P. (1966b). II. Erythrocyte membrane stabilization by local anesthetics and tranquilizers. Biochem. Pharmacol. 15, 1753-1766.

Seeman, P. and Weinstein, J. (1966). I. Erythrocyte membrane stabilization by tranquilizers and antihistamines. Biochem. Pharmacol. 15, 1737-1752.

Shanes, A. M. (1958). Electrochemical aspects of physiological and pharmacological action in excitable cells. Pharmacol. Rev. 10, 59-164, 165-274.

Shanes, A. M. (1963). Drugs and nerve conduction. Ann. Rev. Pharmacol. 3, 185-204.

Shanes, A. M., Freygang, W. H., Grundfest, H. and Amatniek, E. (1959). Anesthetic and calcium action in the voltage clamped squid giant axon. J. Gen. Physiol. 40, 859-879.

Skou, J. C. (1954). Local anaesthetics VI Relation between blocking potency and penetration of a monomolecular layer of lipoids from nerves. Acta. Pharmacol. et Toxicol. 10, 325-337.

Takata, M., Moore, J. W., Kao, C. Y. and Fuhrman, F. A. (1966). Blockage of sodium conductance increase in lobster giant axon by tarichatoxin (tetrodotoxin). J. Gen. Physiol. 49, 977-988.

Takata, M., Pickard, W. F., Lettvin, J. Y. and Moore, J. W. (1966). Ionic conductance changes in lobster axon membranes when lanthanum is substituted for calcium. J. Gen. Physiol. 50, 461-472.

Tasaki, I. (1953). Nervous transmission. Springfield. Charles C. Thomas.

Tasaki, I. (1955). New measurements of the capacity and the resistance of the myelin sheath and the nodal membrane of the isolated frog nerve fiber. Am. J. Physiol. 181, 639-650.

Tasaki, I. (1959). Demonstration of two stable states of the nerve membrane in K-rich media. J. Physiol. 148, 306-331.

Tasaki, I., Singer, I. and Takenaka, T. (1965). Effects of internal and external ionic environment on excitability of squid giant axon. J. Gen. Physiol. 48, 1095-1123.

Tasaki, I., Singer, I. and Watanabe, A. (1966). Excitation of squid giant axons in sodium-free external media. Am. J. Physiol. 211, 746-754.

Taylor, R. E (1959). Effect of procaine on electrical properties of squid axon membrane. Am. J. Physiol. 196, 1071-1078.

Twitty, V. C. (1937). Experiments on the phenomenon of paralysis produced by a toxin contained in Triturus embryos. J. Exp. Zool. 76, 67-104.

Ulbrich, W. (1966). Die Na-Permeabilität der veratrinisierten Schnürringsmembran. Arch. Ges. Physiol. 289, R9.

Watanabe, A., Tasaki, I., Singer, I. and Lerman, L. (1967). Effects of tetrodotoxin on excitability of squid giant axon in sodium-free media. Science, 155, 95-96.

Woodward, R. B. (1964). Structure of tetrodotoxin. Pure Appl. Chem. 9, 49-74.